Dissection of Clathrin Function Using the Small Molecule Inhibitor Pitstop®-2

Inaugural-Dissertation

to obtain the academic degree
Doctor rerum naturalium (Dr. rer.nat.)

submitted to the Department of Biology, Chemistry and Pharmacy
of Freie Universität Berlin

by

WIEBKE STAHLSCHMIDT

from

Pfaffenhofen a. d. Ilm

April 2014

Die vorliegende Arbeit wurde in der Zeit vom Januar 2008 bis April 2014 unter Anleitung von Prof. Dr. Volker Haucke am Institut für Chemie und Biochemie der Freien Universität Berlin im Fachbereich Biologie, Chemie, Pharmazie und am Leibniz-Institut für Molekulare Pharmakologie (FMP) im Fachbereich Molekulare Pharmakologie und Zellbiologie durchgeführt.

1. Gutachter: Prof. Dr. Volker Haucke

2. Gutachter: Prof. Dr. Christian Hackenberger

Datum der Verteidigung: 24.07.2014

Affidavit

I declare that my PhD thesis entitled “Dissection of Clathrin Function Using the Small Molecule Inhibitor Pitstop®-2” has been written independently and with no other sources and aids than quoted.

Berlin, 08.04.14 Wiebke Stahlschmidt

Acknowledgements

I would like to express my gratitude to all the people who have supported and inspired me during my doctoral studies.

First of all, I owe special thanks my supervisor Prof. Dr. Volker Haucke for the opportunity of performing my PhD work in his lab. Thank you for your guidance and excellent support throughout my project. Your enthusiasm for science and your encouragement have been a constant source of motivation.

I would like express my gratitude to all the collaborators who contributed to this project. Thank you to the groups of Adam McCluskey and Phil Robinson for your commitment to the synthesis and improvement of Pitstops. Thank you, also, to my collaborators on the peptide side of the project, Nicole Nischan, Prof. Dr. Christan Hackenberger, Franziska Diezmann and Prof. Dr. Oliver Seitz for the opportunity to work together and for giving me insights into a chemists mind. I would also like to thank Prof. Dr. Christian Hackenberger for evaluating my thesis.

Furthermore, I want to thank all the current and former members of the Haucke group for creating such a unique atmosphere. Working with all of you in this collaborative and inspiring environment was a great pleasure. Without your advice, the fruitful scientific and sometimes not so scientific discussions as well as the good times we have shared I would not have made it that far. Special thanks, also, to all of you who worked with me on the Pitstop-project, Lisa von Kleist, who initiated the project, Kira Gromova, and Dmytro Puchkov.

Last, but not least I owe my deepest thanks to my friends, near or far, my family, and especially Stefan. Thank you for your constant support and for always being by my side.

Directory

1 Abstract

The coat protein clathrin plays important roles in intracellular membrane traffic including endocytosis of plasma membrane proteins and receptors as well as protein sorting between the trans-Golgi network (TGN) and endosomes. In this study, the small molecule inhibitor Pitstop®-2 was used to acutely and pharmacologically inhibit clathrin terminal domain (TD) interactions and investigate the inhibitory effects on intracellular membrane traffic. Pitstop®-2 interferes with clathrin-mediated endocytosis (CME) of cargo such as the transferrin receptor. Additionally, we report the inhibition of major histocompatibility complex class I (MHCI) internalization in presence of Pitstop®-2, indicating that MHCI endocytosis occurs via a clathrin- and AP-2-dependent pathway. Inhibition of CME is accompanied by a dramatic increase in the lifetime of clathrin-coated pit (CCP) components such as clathrin itself and, amongst others, the adaptor protein complex 2 (AP-2) suggesting a role for the clathrin TD in regulating coated pit dynamics but not in the de novo formation of CCPs. Similar to AP-2-containing CCPs at the plasma membrane, Pitstop®-2 also impaired the dynamics of intracellular AP-1- and GGA- (Golgi-localized, gamma-ear containing, ADP- ribosylation factor- binding proteins) coated structures, revealing a requirement for functional clathrin TD interactions in TGN/ endosomal traffic. Impairment of clathrin function by Pitstop®-2 caused the peripheral dispersion of mannose 6-phosphate receptors (MPRs), a known cargo protein for clathrin- and AP-1-dependent-sorting at the TGN, indicating a role for clathrin in retrieval of cargo to the TGN. By contrast, secretory traffic of vesicular stomatitis virus G protein (VSVG), recycling of internalized transferrin from endosomes, or degradation of epidermal growth factor receptor (EGFR) as well as fluorescently labelled EGF proceed unperturbed in cells with impaired clathrin TD function. The data presented here extend our knowledge about the roles of the clathrin TD in endocytosis and in intracellular trafficking, indicating a role in the regulation of CCP maturation rather than in recruitment of adaptors and accessory proteins to the nascent CCP. Additionally, they demonstrate that Pitstop®-2 and future derivatives thereof provide useful tools to acutely perturb clathrin TD domain function with potential use as antibacterial, antiviral, or antimitotic agents.

2 Zusammenfassung

Das Hüllprotein Clathrin spielt bedeutende Rollen bei zellulären Transportvorgängen wie der Clathrin vermittelten Endozytose (clathrin-mediated endocytosis, CME) von Membranproteinen und Rezeptoren sowie beim intrazellulären Vesikeltransport zwischen dem Trans-Golgi-Netzwerk (TGN) und Endosomen. Im Rahmen dieser Arbeit haben wurde der „small molecule“ Inhibitor Pitstop®-2 benutzt, um Interaktionen der terminalen Domäne Clathrins pharmakologisch und akut zu inhibieren und die inhibitorischen Effekte auf den intrazellulären Transport zu untersuchen. Pitstop®-2 hemmt die CME von Liganden wie beispielsweise dem Transferrin Rezeptor. Zusätzlich konnte gezeigt werden, dass Pitstop®-2 die Internalisierung des Membranproteins MHCI (major histocompability complex class I) hemmt, ein Hinweis auf Clathrin und Adaptor-Proteinkomplex 2 (AP-2) abhängige Endozytose. Die Inhibition der CME geht mit einem dramatischen Anstieg der Lebensdauer von Komponenten Clathrin umhüllter Grübchen einher. Dies betrifft Clathrin selbst sowie unter anderem AP-2 und legt eine Rolle für die terminale Domäne (TD) von Clathrin bei der Regulation der CCP-Dynamik, jedoch nicht deren Neuentstehung, nahe. Auf vergleichbare Weise wie bei AP-2 enthaltenden CCPs an der Plasmamembran beeinträchtigt Pitstop®-2 die Dynamik intrazellulärer AP-1- (Adaptor-Proteinkomplex 1) und GGA- (Golgi-localized, gamma-ear containing, ADP- ribosylation factor- binding proteins) umhüllter Strukturen. Damit wird die Notwendigkeit funktionaler Clathrin TD Interaktionen für TGN / endosomalen Transport verdeutlicht. Die Störung der Funktion von Clathrin durch Pitstop®-2 führt zu einer Verteilung des Mannose-6-Phosphat Rezeptors (MPR), einem gut untersuchten Cargo-Molekül für Clathrin- und AP-1-abhängigen Sortierung am TGN. Dies deutet auf eine Rolle von Clathrin bei der retrograden Rückführung von Proteinen zum TGN hin. Im Gegensatz dazu konnte in Zellen mit beeinträchtigter Clathrin TD Funktion kein Effekt auf die Sekretion des Vesicular Stomatitis Virus G Proteins (VSVG), auf das Recycling von Transferrin aus Endosomen oder auf den Abbau des Epidermalen Wachstumsfaktor Rezeptors (epidermal growth factor receptor, EGFR) sowie fluoreszent markiertertes EGF festgestellt werden. Die hier präsentierten Daten erweitern das Wissen über die Rolle der Clathrin terminalen Domäne bei der Endozytose und beim intrazellulären Transport. Dabei scheint diese eher für die Regulation der Reifung von CCPs als für die Rekrutierung von Adaptoren und akzessorischen Proteinen erforderlich zu sein. Außerdem demonstrieren sie, dass Pitstop®-2 und zukünftige Derivate davon ein wertvolles Werkzeug sind, um akut die Funktion der Clathrin terminalen Domäne in Zellen in Hinblick auf antibakterielle, antivirale oder antimitotische Wirkung zu untersuchen.

3 Introduction

3.1 Cellular Trafficking Pathways

Cellular homeostasis requires the synthesis and degradation of proteins and membrane. This necessitates the constant shuttling of transport vesicles or tubules between different cellular organelles (Figure 3.1).

Proteins and membrane are synthesized in the endoplasmic reticulum (ER) from where they may be transported to various intracellular compartments or to the plasma membrane. After exiting the ER they pass through the Golgi complex, where they undergo posttranslational modifications. Afterwards, they leave from the trans-Golgi network (TGN) in vesicles and tubules for further transport to the cell surface or endosomes. In parallel, endocytosis of cargo molecules from the plasma membrane takes place to enable nutrient uptake, response to extracellular stimuli and the modulation of surface levels of plasma membrane components. Internalized material is sorted in early endosomes for recycling back to the plasma membrane or lysosomal degradation via late endosomes or multivesicular bodies. To retrieve the transport machinery from the acceptor compartments and recycle it back to the donor compartments, retrograde transport is required (Bonifacino and Glick, 2004).

Vesicular transport necessitates selective protein sorting to incorporate cargo into the nascent vesicle while retaining resident proteins in the donor compartment. Furthermore, membrane at the donor compartment has to be deformed to enable bud formation and fission of vesicles. Specific targeting of the vesicle to the destined compartment is required to ensure vesicle fusion with the correct compartment (Bonifacino and Glick, 2004). This is achieved by protein coats. These coats form supramolecular assemblies of proteins which are recruited from the cytosol to the nascent vesicle. In conjunction with accessory proteins, they deform flat membrane patches and enable specific cargo selection by recognition of sorting signals (Bonifacino and Lippincott-Schwartz, 2003; Kirchhausen, 2000).

Vesicle budding and cargo selection at different compartments are mediated by different coats and sorting signals. Coat protein complex II (COPII) enables export from the ER to the ER-Golgi intermediate compartment (ERGIC) or to the Golgi complex (Barlowe et al., 1994). The COPI complex is required for intra-Golgi transport and retrograde traffic from the Golgi back to the ER (Letourneur et al., 1994). However, the best characterized coat protein in cellular trafficking is Clathrin (see also 3.2). It is

restricted to post-Golgi sorting, being involved in endocytosis and transport from the TGN and endosomes (Brodsky, 2012). Yet, there are still open questions about its precise mechanisms of action in endocytosis and intracellular trafficking which have to be elucidated.

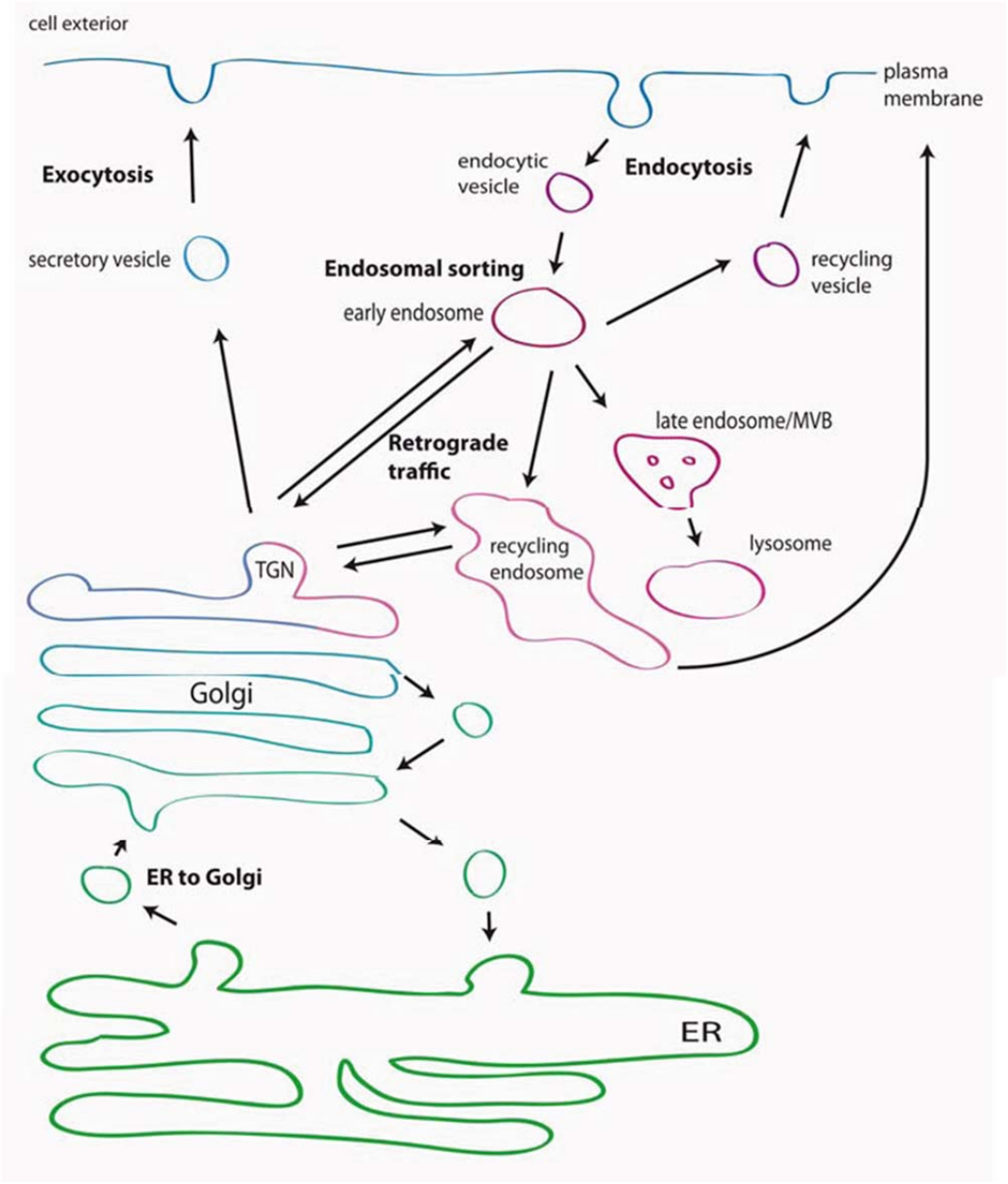

Figure 3.1 Overview of the cellular trafficking pathways. Membrane and secretory proteins are synthesized in the endoplasmic reticulum (ER). From there, they pass through the Golgi complex for subsequent exocytosis in secretory vesicles or tubules derived from the trans-Golgi network (TGN). After endocytosis, cargo molecules are sorted in endosomes for recycling or lysosomal degradation (figure with courtesy of Lisa von Kleist).

3.2 Clathrin, a key player in cellular traffic

Clathrin is a protein comprised of three identical clathrin heavy chains (CHC) and three clathrin light chains (CLC) forming an extended three legged structure, a triskelion (Brodsky, 2012).

In humans, there are two isoforms of the CHC, named for their encoding chromosomes. The ubiquitously expressed CHC17 is involved in endocytosis and intracellular transport from the TGN and endosomes (Brodsky, 2012). The CHC22 isoform, with 85% identity to CHC17, is less well characterized. It is required for a defined step in retrograde transport from endosomes to the TGN. Its highest expression is in muscle and fat, where CHC22 is involved in the regulation of the glucose transporter GLUT4 (Brodsky, 2012; Esk et al., 2010).

The CHC is the central building block of clathrin triskelia. It consists of a long α-solenoid region and a single β-propeller at the N-terminus. The α-solenoid comprises eight CHC repeats (CHCR) which form the ankle, the distal leg, and the proximal leg of the CHC. The trimerization domain is located at the vertex of the C-terminus to form the triskelion (Liu et al., 1995; Ybe et al., 1999). The N-terminal domain (TD) at the distal end of the leg, a 7-bladed β-propeller, is formed by seven WD40 repeats folding into four-stranded β–sheets.

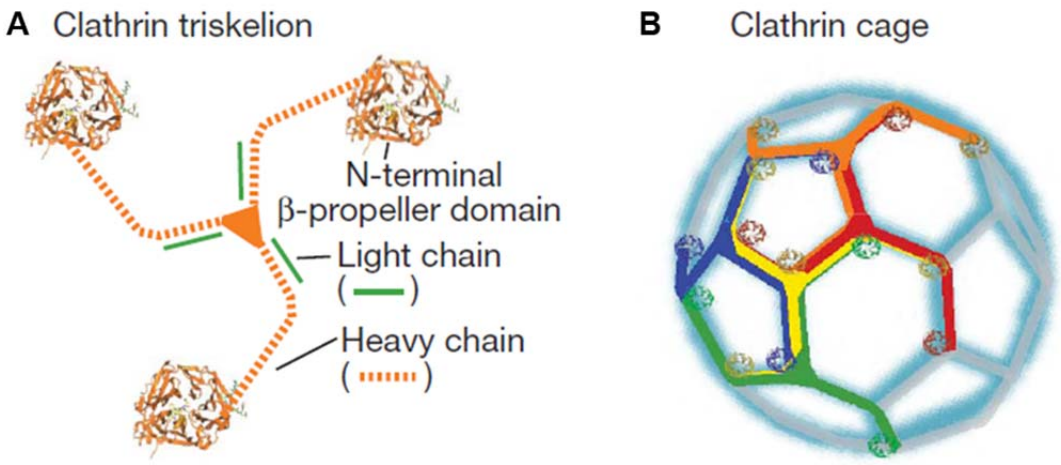

Figure 3.2 The protein structure of clathrin and its assembly into clathrin coats. (A) Scheme of a clathrin triskelion comprised of three heavy chains and three light chains. (B) Schematic representation of a clathrin cage. Individual triskelia are highlighted in different colors (Schmid and McMahon, 2007).

The clathrin β–propeller has been proposed to harbor four interaction sites for accessory proteins (Figure 3.3), three of which have been molecularly defined. The clathrin box motif (CBM) LΦXΦ[DE] (Φ is a bulky hydrophobic residue, X is any amino acid but often polar) binds to the β–propeller in a groove between blade one and two (ter Haar et al., 2000). It can be found in a variety of proteins such as the adaptor protein complexes AP-1, AP-2, and AP-3, the monomeric Golgi-localized, gamma-ear containing, ADP-ribosylation factor-binding proteins (GGAs), accessory proteins like EGFR pathway substrate 15 (Eps15), epsin, amphiphysin and many more (Brodsky, 2012; McMahon and Boucrot, 2012; Owen et al., 2004; ter Haar et al., 2000; Wieffer et al., 2009). The second clathrin binding motif is the so-called W-box motif PWXXW which is found in amphiphysin with a binding site located at the top of the CHC β-propeller (Miele et al., 2004). The third interaction site on the clathrin TD, the a2L site, binds to an 8-amino acid splice loop found solely in the long isoform of arrestin2 (arrestin2L), an adaptor for G-protein coupled receptors, and is situated between blades 4 and 5 on the CHC TD (Kang et al., 2009). Recently, a fourth interaction site on the CHC TD was suggested to be located between blades 6 and 7 that might bind short peptide motifs of currently unknown identity (Willox and Royle, 2012).

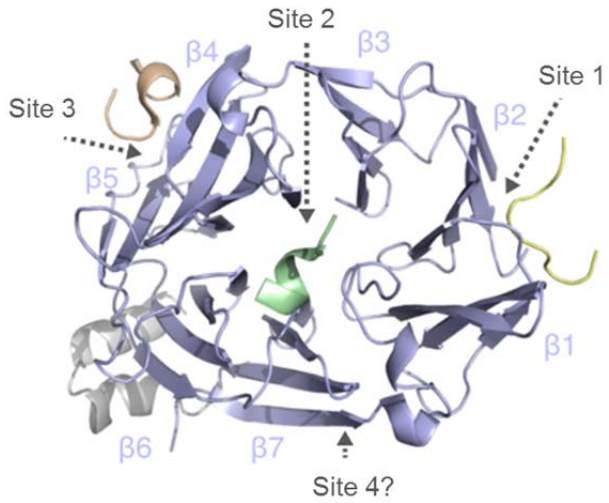

Figure 3.3 Scheme of the clathrin terminal domain and its interaction sites. (A) Position of the four interaction sites on a ribbon diagram of the clathrin terminal domain with their respective ligands (modified from Willox & Royle, 2014).

Clathrin triskelia form polyhedral lattices, also called clathrin coats, which cover the cytoplasmic face of cellular membranes (Figure 3.2) (Brodsky, 2012). The clathrin coat has been postulated to serve at least two major functions in endocytosis and intracellular trafficking: stabilizing deformed membrane domains (Hinrichsen et al., 2006) and providing an interaction hub for the recruitment of accessory proteins that regulate the progression of clathrin coated vesicle formation (Schmid and McMahon, 2007).

3.3 Clathrin-Mediated Endocytosis

Clathrin-mediated endocytosis (CME) is the best defined function of clathrin. It regulates cell surface levels and endocytic uptake of plasma membrane proteins, such as nutrient and growth factor receptors, transporters, ion channels, adhesion proteins and synaptic vesicle (SV) proteins in the brain (Brodsky, 2012; Ferguson and De Camilli, 2012; McMahon and Boucrot, 2011; Wieffer et al., 2009). But the CME machinery is also hijacked by pathogens such as bacteria and viruses to enter cells (see 3.7).

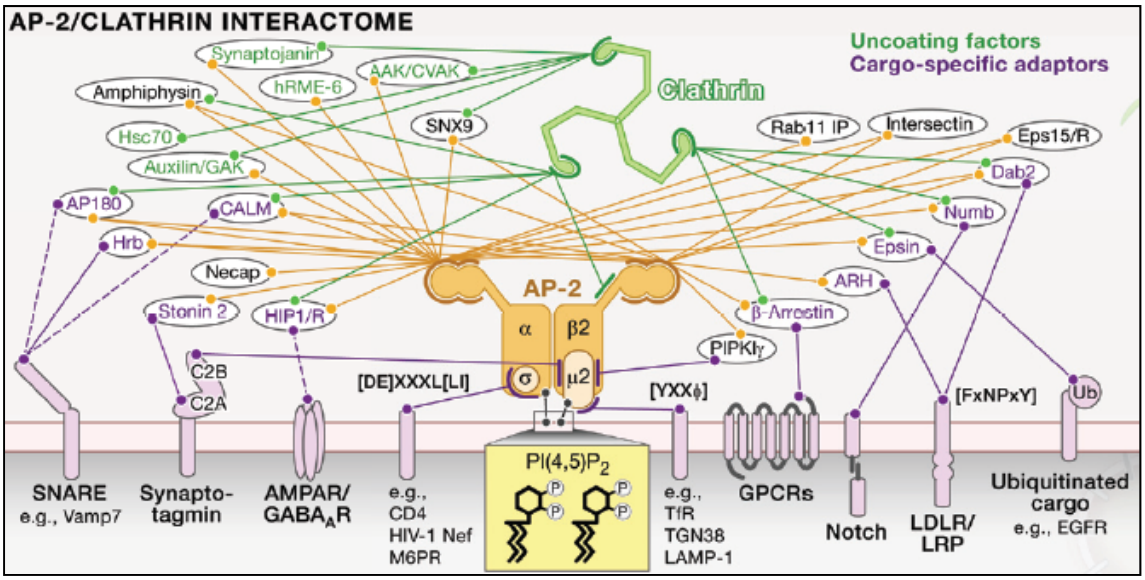

Figure 3.4 The AP-2 / clathrin interactome. The scheme displays the interactions between clathrin, AP-2 and accessory proteins involved in CME. (Wieffer et al., 2009)

CME is enabled by a complex interaction network with clathrin and the adaptor protein complex 2 (AP-2) as central interaction hubs. Numerous proteins temporarily associate with the forming clathrin coated pit (CCP) to generate a clathrin coated vesicle (CCV) (Figure 3.4) (Wieffer et al., 2009). AP-2 is a stable heterotetrameric complex comprised of two large subunits, the 100 kDa α-subunit, and the 100 kDa β2-subunit, one medium 50 kDa μ2-subunit, and one small 17 kDa σ2-subunit. Together they form a trunk-like structure from which, linked via unstructured hinge regions, the appendage domains of α- and β2-subunit extend (Collins et al., 2002; Edeling et al., 2006). The clathrin TD interacts with AP-2 by binding to the β2-hinge as well as to the β2-appendage (Knuehl et al., 2006; ter Haar et al., 2000). Additionally AP-2 binds to the plasma membrane via interaction with $PI(4,5)P_2$ and to cargo via tyrosine- or dileucine-based motifs (see also 3.3.2). The appendage domains recognize short peptide ligands in a plethora of endocytic proteins such as clathrin associated sorting proteins (CLASPs) and regulatory proteins. Altogether, this interactome consisting of clathrin and AP-2 as central hubs comprises the complex protein network required for endocytosis (Figure 3.4) (Wieffer et al., 2009).

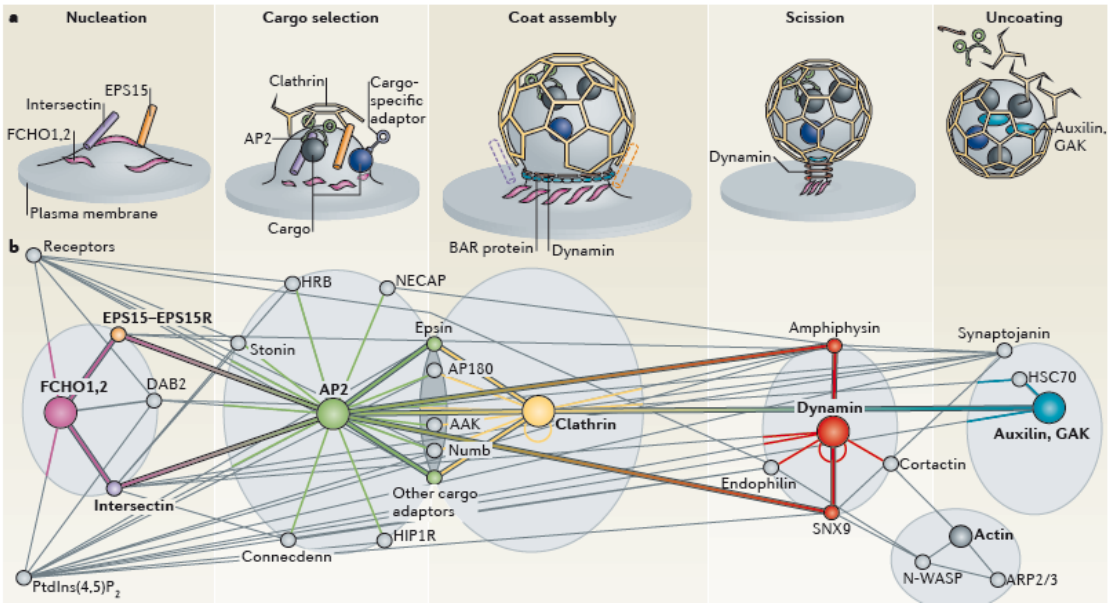

Figure 3.5 Subsequent steps of clathrin coated vesicle formation. A plethora of proteins is involved in CCP formation and maturation. After nucleation (A), cargo is selected to be incorporated into the nascent CCP (B), followed by clathrin coat assembly (C). Next, a neck is formed before scission mediated by the GTPase dynamin (D) occurs. At last the vesicle is uncoated (E) to provide the CCP components for a new cycle of clathrin-coated vesicle formation. (McMahon and Boucrot, 2011)

For efficient CME, clathrin-coated pit (CCP) formation and maturation are required, a process that can be subdivided into several steps: nucleation, cargo selection, coat assembly, scission, and uncoating (Figure 3.5).

3.3.1 Nucleation

The exact mechanism of nucleation of a nascent CCP is still debated. It was proposed to be initiated by the recruitment of Fer/Cip4 homology domain domain-only proteins (FCHo 1/2) binding to phosphatidylintositol-4,5-bisphosphate ($PI(4,5)P_2$). FCHo 1 and FCHo 2 subsequently recruit intersectins and epidermal growth factor receptor substrate 15 (Eps15) to the plasma membrane thus inducing initial membrane curvature proceeded by AP-2 binding (Ford et al., 2002; Henne et al., 2010; Pechstein et al., 2010; Saffarian et al., 2009). These findings were questioned by another model which suggests coordinated binding of a building block of two AP-2 molecules together with one clathrin triskelion to $PI(4,5)P_2$ enriched membrane followed by incorporation of a second identical building block (Cocucci et al., 2012). Undoubtedly, $PI(4,5)P_2$ is crucial for CCP initiation. Acute loss of $PI(4,5)P_2$ from the plasma membrane after 1-butanol treatment results in failure to recruit AP-2 and FCHo proteins to the plasma membrane and thus to initialize new CCP formation (Boucrot et al., 2006; Cocucci et al., 2012; Henne et al., 2010).

3.3.2 Cargo Selection

Nucleation is preceded by cargo selection. The cargo destined for CME has to be recognized by adaptors and sequestered in the growing CCP. Increased cargo concentrations significantly increase the maturation efficiency to productive CCPs. This is mediated by AP-2 as well as CLASPs (Ehrlich et al., 2004; Loerke et al., 2009).

The heterotetrameric AP-2 is the main clathrin adaptor at the plasma membrane. It recognizes cargo via binding of the µ2-subunit to the tyrosine-based YXXΦ motif (Φ is a bulky hydrophobic residue and X is any amino acid) (Collins et al., 2002; Ohno et al., 1995). Another cargo sorting signal is the acidic cluster dileucine motif [DE]XXXL[LI] which binds to a hydrophobic pocket on the AP-2 σ2-subunit (Kelly et al., 2008). Both binding sites are hidden in the inactive, closed conformation of AP-2 and become available only after induction of a conformational change induced by phosphorylation and $PI(4,5)P_2$ binding (Collins et al., 2002; Honing et al., 2005; Kelly et al., 2008).

CLASPs are cargo specific adaptors that interact with the AP-2 β-subunit, clathrin, and often $PI(4,5)P_2$. They recruit cargo to nascent CCPs which cannot bind to AP-2 itself, thereby increasing the spectrum of cargo and the possibilities of specific regulation. Some CLASPs recognize sorting signals: Eps15 and epsins interact with ubiquitinated cargo. β-arrestins are adaptors for internalization of G-protein coupled receptors. Dab2, ARH, and Numb bind to NPX[F/Y] motifs to mediate internalization of LDL receptors or integrins (Edeling et al., 2006; Traub, 2009). For other adaptors only one specific cargo is known, e.g. Stonin 2 for internalization of synaptotagmin 1 (Diril et al., 2006), AP180/CALM for synaptobrevin 2 (Koo et al., 2011), or dishevelled for Frizzled (Yu et al., 2007).

3.3.3 Coat Assembly

After cargo selection, more clathrin triskelia are recruited from the cytosol to the site of the nascent CCP by AP-2 and accessory proteins to assemble a clathrin coat eventually resembling a soccer ball. Clathrin polymerization is essential for remodeling of the plasma membrane to initialize and stabilize membrane curvature as shown by clathrin depletion which results in AP-2 positive structures lacking any curvature (Dannhauser and Ungewickell, 2012; Hinrichsen et al., 2006). Meanwhile, some early endocytic proteins such as Eps15 and epsins are displaced to the edge of the pit (Saffarian et al., 2009; Tebar et al., 1996).

3.3.4 Scission

Before scission of the CCV can occur, a neck has to be formed at the base of the clathrin cage. This is facilitated by amphiphysin and endophilin, proteins containing amphipathic α-helices that are inserted into the leaflet of the bilayer and Bin–Amphiphysin–Rvs (BAR) domains. BAR domains are banana shaped lipid binding domains which, after dimerization, recognize and bind to curved membranes by electrostatic interactions (McMahon and Gallop, 2005; Peter et al., 2004). Amphiphysin and endophilin are recruited to the CCP simultaneously where they localize to the neck and drive its constriction (Ferguson et al., 2009; Peter et al., 2004; Sundborger et al., 2011). Additionally, a requirement for the lipid $PI(3,4)P_2$, generated by PI(3) kinase C2α, has been described to enable neck formation and constriction of the CCP by recruitment of the BAR protein sorting nexin 9 (SNX9) (Posor et al., 2013). Together, the BAR proteins recruit the GTPase dynamin to the neck to facilitate further

constriction followed by scission of the CCV from the plasma membrane (Sundborger et al., 2011; Wigge et al., 1997; Wu et al., 2010). Vesicle scission requires the dynamin GTPase domain (Hinshaw and Schmid, 1995; Macia et al., 2006; Roux et al., 2006; Sweitzer and Hinshaw, 1998).

Several models for the mechanism of dynamin action have been proposed (Faelber et al., 2011). In the “constrictase model”, GTP hydrolysis drives conformational changes which lead to further constriction of the membrane followed by fission (Bashkirov et al., 2008; Hinshaw and Schmid, 1995). The “poppase model” proposed that dynamin might act as a molecular spring. In the GTP bound state dynamin rings are tightly packed together. After GTP hydrolysis, a spring like opening of the dynamin helix occurs, which increases the spacing between individual rings nearly two fold (Stowell et al., 1999). The “twistase model” describes a conformational change induced by GTP hydrolysis which results in rotation of dynamin coated membrane tubules (Roux et al., 2006). Faelber and colleagues tried to reconcile the three models and suggested a mechanism which includes all three forms of conformational changes. After a dynamin ring is closed around the neck, GTP hydrolysis is induced, resulting in bud neck constriction together with a right handed twisting of the dynamin filaments. Multiple rounds of GTP binding and hydrolysis lead to successive constriction of the dynamin helix and the bud neck. The resulting increase in membrane curvature causes further destabilization of the bud neck. Finally, GTP hydrolysis followed by dynamin dissociation will separate the dynamin filaments eventually enabling fission of the CCV (Faelber et al., 2011).

3.3.5 Uncoating

After scission, the CCV has to be uncoated to release clathrin and other coat components for a new round of CME and allow the detached vesicle to fuse with its target endosome. Vesicle uncoating is mediated by auxilin together with heat shock cognate 70 (Hsc70).

Auxilin binds with high affinity to clathrin lattices via interactions with clathrin TDs and the ankles of the triskelia (Fotin et al., 2004), with a burst of recruitment just before completion of the clathrin coat assembly (Massol et al., 2006; Taylor et al., 2011). Its binding generates a global distortion of the clathrin coat which is presumably required for further Hsc70 recruitment via its J-domain (Fotin et al., 2004; Holstein et al., 1996; Rapoport et al., 2008; Ungewickell et al., 1995). Hsc70 facilitates ATP dependent uncoating of the CCV by further destabilization of the clathrin coat resulting in release

of the clathrin triskelia from the CCV (Bocking et al., 2011; Braell et al., 1984; Schlossman et al., 1984; Xing et al., 2010). *In vitro*, maximum uncoating is obtained with one auxilin and three or fewer HSC70 molecules per triskelion (Bocking et al., 2011; Rothnie et al., 2011)

The role of the phosphatase synaptojanin in uncoating is less well defined. Possibly, it is recruited by endophilin to the bud neck, where it reduces $PI(4,5)P_2$ levels and thus mediates AP-2 release (Cremona et al., 1999; Milosevic et al., 2011; Semerdjieva et al., 2008).

After uncoating the components of the CCV are released into the cytosol and become available for a new round of CCV formation.

3.4 Clathrin-Independent Endocytosis

In addition to CME, several mechanisms of clathrin-independent endocytosis (CIE) have been described. CIE is responsible for the major fraction of membrane and fluid uptake into the cell (Howes et al., 2010). Several mechanisms of CIE have been described (Figure 3.6) (Sandvig et al., 2011). In addition to roles in uptake of specific cargo, CIE is involved in repair of defective membrane (Tam et al., 2010). Thereby, the occurence of different mechanisms of endocytosis provides larger regulatory possibilities by different regulation factors and signals (Sandvig et al., 2011). Yet, the precise function and how these pathways are interconnected still remains to be elucidated in more detail.

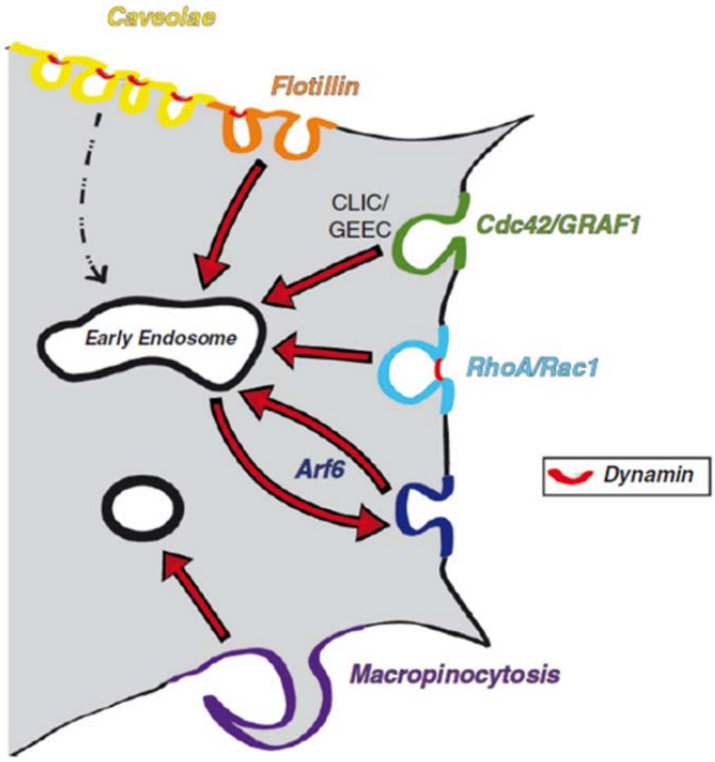

Figure 3.6 Pathways for clathrin-independent endocytosis. Several clathrin independent endocytic mechanisms have been described. Caveolae as well as endocytosis mediated by the small Rho GTPases RhoA and Rac1 is dependent on dynamin. Caveolae contain a coat of caveolin-subunits and are rather stable at the plasma membrane thus not responsible for major fractions of internalized membrane or cargo. Flotillins can internalize cargo via dynamin-dependent as well as dynamin-independent pathways. The CLIC/GEEC pathway, which depends on the small GTPase Cdc42 together with GRAF1, and Arf6 dependent endocytosis are supposedly dynamin-independent. Macropinocytosis generates large vesicles, which do not necessarily fuse with early endosomes (Sandvig et al, 2011).

3.4.1 Arf6 Dependent Endocytosis

One suggested mechanism of clathrin-independent endocytosis is ADP-ribosylation factor 6 (Arf6) dependent cargo internalization (Donaldson et al., 2009). Cargo, such as the major histocompatibility complex class I (MHCI), lacking AP-2 and clathrin targeting sequences, was described to internalize into cells in an Arf6 dependent manner. At the plasma membrane, it colocalizes with Arf6 but neither with clathrin nor cargo internalized via clathrin-mediated endocytosis (Radhakrishna and Donaldson, 1997). Overexpression of a dynamin mutant defective in GTP binding (dyn K44A) or a dominant negative C-terminal fragment of the neuronal adaptor protein AP180 (C-AP180) appear to have no effect on the internalization rates of clathrin independent

cargo while they inhibit internalization of clathrin dependent cargo such as the transferrin receptor. Simultaneously, overexpression of constitutively active Arf6 increases internalization of clathrin independent cargo only (Naslavsky et al., 2003, 2004). Meanwhile, data from other studies indicate an epsin 1 and thus clathrin dependent uptake for MHCI (Duncan et al., 2006; Goto et al., 2010), independent of Arf6 (Larsen et al., 2004).

3.4.2 Caveolae

Caveolae are flask shaped membrane invaginations at the plasma membrane proposed to contribute to internalization of glycosylphosphatidylinositol (GPI) anchored proteins, the Simian-Virus 40 (SV40), and the cholera toxin B subunit (CTxB) (Doherty and McMahon, 2009; Kumari et al., 2010; Sandvig et al., 2011). They depend on cholesterol and an intact actin cytoskeleton (Rothberg et al., 1992; Thomsen et al., 2002). However, endocytosis via caveolae remains poorly characterized. It was shown that caveolae are relatively stable structures, thus their contribution to constitutive endocytosis was suggested to be rather small (Thomsen et al., 2002). Mice with caveolin1 knockout are viable, but show defective endocytosis of the caveolar ligand fluorescein isothiocyanate-albumin (Razani et al., 2001), while internalization of SV40 (Damm et al., 2005) and CTxB (Kirkham et al., 2005) proceeds unperturbed. Thus, an alternative role for caveolae as negative regulators of entry for certain cell surface proteins has been suggested (Hernandez-Deviez et al., 2008). Additionally, recent findings hint at yet another role for caveolae as a physiological membrane reservoir to respond to sudden and acute mechanical stress (Sinha et al., 2011).

3.4.3 CLIC/GEEC Endocytosis and Flotillins

The CLIC/GEEC pathway is required for clathrin and dynamin independent endocytosis of GPI-anchored proteins. Cargo is internalized in uncoated tubovesicular clathrin independent carriers (CLICs) which subsequently fuse to GPI-anchored protein enriched early endosomal compartments (GEECs) (Sabharanjak et al., 2002). Endocytosis via the CLIC/GEEC pathway is dependent on a functional actin polymerization machinery and Cdc42 (Chadda et al., 2007; Sabharanjak et al., 2002).

Flotillins 1 and 2 are involved in dynamin dependent as well as dynamin independent endocytosis of GPI-anchored proteins, proteoglycans and CTxB (Ait-Slimane et al., 2009; Glebov et al., 2006; Payne et al., 2007). In cells, flotillins can be observed in

small membrane invaginations devoid of clathrin or caveolin1 which are dynamic and bud into the cell (Frick et al., 2007). Their relation to the GEEC/CLIC pathway is not known in detail as a role for specific RhoGTPases and cholesterol have not yet been investigated (Kumari et al., 2010).

3.5 Clathrin in Intracellular Trafficking

Clathrin's best characterized role is in CME. Yet, it can also be found on intracellular membranes of the TGN and on endosomes where it is involved in intracellular sorting of cargo (Figure 3.7).

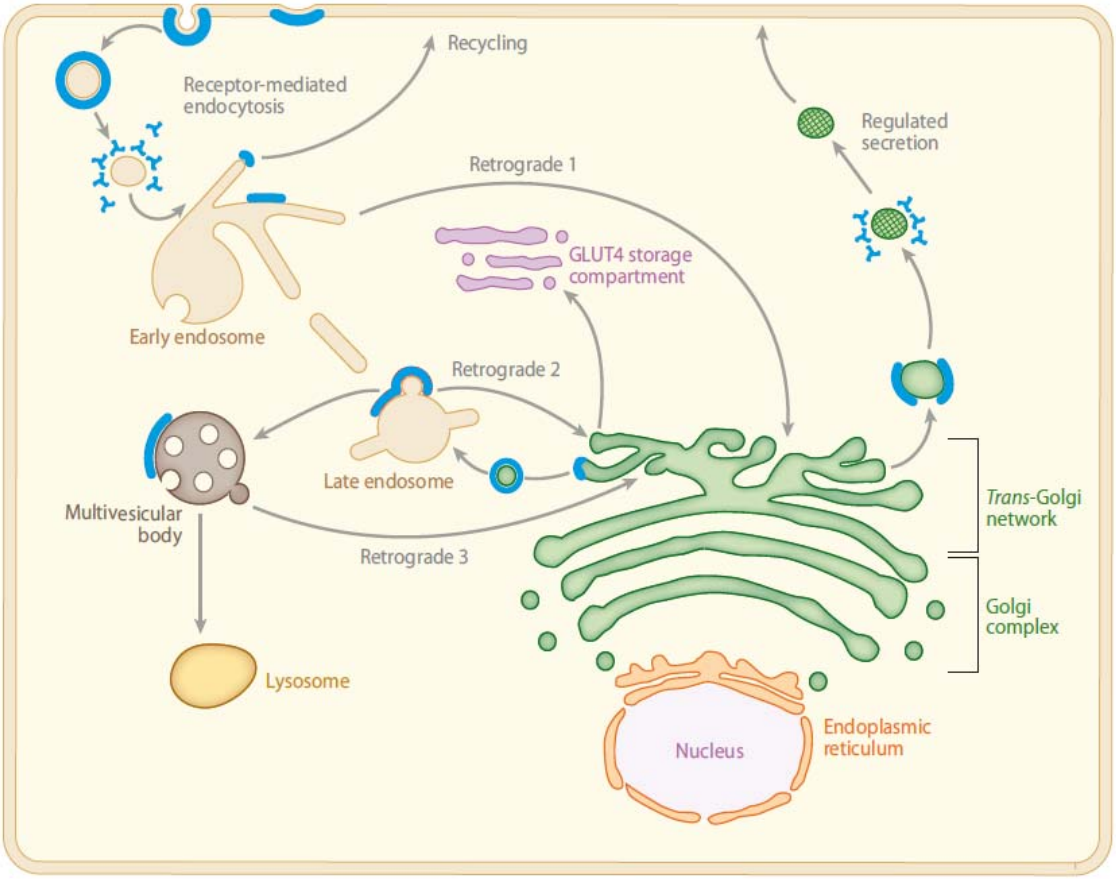

Figure 3.7 Clathrin in intracellular traffic. Clathrin (blue) is located on multiple sites in mammalian cells. In addition to plasma membrane located clathrin, it can be found on the TGN and on endosomes (modified from Brodsky 2012).

Intracellular CCP formation requires adaptor proteins such as AP-1 and GGAs, which have three mammalian isoforms, together with a variety of accessory proteins including γ-synergin (Page et al., 1999), Eps15 (Kent et al., 2002), Epsin R (Hirst et al., 2003; Mills et al., 2003; Wasiak et al., 2003; Wasiak et al., 2002), Gadkin (Maritzen et al., 2010; Schmidt et al., 2009), and amphiphysin (Huser et al., 2013), among many others (Traub, 2005).

AP-1 is a heterotetrameric adaptor homolog to AP-2 constinsting of four subunits: two large subunits γ and β1 (100 kDa, respectively) the medium μ1-subunit (47 kDa) and the small σ1-subunit (19 kDa). Like AP-2, AP-1 binds cargo via interactions with YXXΦ (Φ is a bulky residue) and [DE]XXXL[LI] motifs on the μ and β subunit (Janvier et al., 2003; Ohno et al., 1998), whereas the β-subunit is particularly important for clathrin binding (Owen et al., 2004). There are two isoforms of the AP-1 μ-subunit in mammals. While the μ1A-subunit can be found trafficking between endosomes and the TGN in all cell types, the μ1B-subunit is specifically expressed in a subset of polarized epithelial cells (Ohno et al., 1999). AP-1B with incorporated μ1B plays, together with clathrin, an important role in basolateral sorting of polarized cargo (Deborde et al., 2008; Folsch et al., 1999; Folsch et al., 2003).

The GGA family of adaptors (Golgi-localized, γ-ear-containing, ARF-binding proteins) are monomeric adaptors which are additionally to AP-1 associated with clathrin at the TGN and endosomes. GGAs are expressed in three isoforms in mammalian cells, GGA1, GGA2, and GGA3, respectively, exist. They consist of four domains: the N-terminal VHS (VPS-27, Hrs, and STAM) domain, the GAT (GGA and TOM1) domain, a hinge domain and the C-terminal GAE (γ–adaptin ear) domain which is homolog to the appendage domain of the AP-1 γ-subunit (Hirst et al., 2000; Robinson, 2004; Robinson and Bonifacino, 2001). The VHS domain recognizes cargo with acidic dileucine motifs (DXXLL), such as mannose 6-phophate receptors (MPRs). The GAT domain binds activated Arf1 and is thus required for recruitment to membranes, while the hinge domain and the GAE domain interact with clathrin and accessory proteins (Bonifacino, 2004).

Loss of either AP-1 or GGA proteins causes severe defects. Deficiency of the ubiquitously expressed AP-1 μ1A-subunit in mice is lethal during embryonic development (Meyer et al., 2000). GGA2 knockout is embryonically or neonatal lethal in mice. While deletion of GGA1 or GGA3 alone reduce birthweight of the litter, but has

no effect on lifespan and fertility, the GGA1/3 double knockout animals show increased mortality within the first three weeks after birth (Govero et al., 2012).

AP-1 and GGA recruitment to membranes depends on the lipid PI(4)P (Wang et al., 2007; Wang et al., 2003), which is enriched at the TGN and on endosomal membranes (Di Paolo and De Camilli, 2006). In contrast to AP-2, phosphoinositide binding alone is not sufficient for adaptor recruitment, but additionally requires the interaction with ADP ribosylation factor 1 (Arf1). Arf1 cycles between a cytosolic inactive form, which binds GDP, and a membrane bound active form associated with GTP (Donaldson and Jackson, 2011) that recruits AP-1 and GGAs to the TGN and endosomal membranes (Dell'Angelica et al., 2000; Ren et al., 2013; Zhu et al., 1998).

A major cellular function of AP-1- (Klumperman et al., 1998) and GGA-containing clathrin-coated carriers (Hirst et al., 2000; Puertollano et al., 2001) is the bidirectional traffic of cargo between endosomes and the TGN. For instance, AP-1 and GGAs are necessary for lysosomal delivery of MPRs from the TGN (Geuze et al., 1985; Ghosh and Kornfeld, 2003). MPRs can be found at the TGN in clathrin and AP-1 positive tubules (Geuze et al., 1985; Klumperman et al., 1998) which are highly dynamic (Waguri et al., 2003). Loss of AP-1 depletes MPRs from CCVs and results in defective MPR retrieval from endosomes to the TGN (Meyer et al., 2000; Robinson et al., 2010). Furthermore, overexpression of a dominant negative GGA1 mutant inhibits TGN exit of MPRs (Puertollano et al., 2001). It is likely that GGAs and AP-1 act together in membrane traffic. Recent studies showed that interaction with GGA proteins is required for cargo sorting into AP-1-containing clathrin-coated vesicles (Doray et al., 2002). Meanwhile, GGA2 recruitment to clathrin-coated structures on TGN / endosomal membranes is impaired in absence of AP-1 (Hirst et al., 2012), suggesting that AP-1 and GGAs are functionally linked (Daboussi et al., 2012). Yet, there are also uncoated tubules involved in constitutive secretion of vesicular stomatitis virus G protein (VSVG). These tubules deriving from the TGN seem to be distinct from the observed clathrin and AP-1 / GGA coated structures (Hirschberg et al., 1998; Polishchuk et al., 2003).

Clathrin coats have also been found on endosomal compartments. There are clathrin coated buds, located mainly on endosomal tubules (Stoorvogel et al., 1996) and flat, bilayered clathrin lattices on early endosomes which are positive for Hrs (hepatocyte growth factor-regulated tyrosine kinase substrate), a protein implicated in signaling and membrane trafficking (Raiborg et al., 2002). Yet, the precise function of clathrin at these sites is less clear. Several studies tried to shed light on these open questions. Loss-of-function of the clathrin-associated Arf6-GTPase activating protein ACAP1

(ARFGAP with coiled coil, ANK repeat, and pleckstrin homology domains) has been shown to impair recycling of several cargos including transferrin receptor (TfR), GLUT4, and integrins (Dai et al., 2004; Li et al., 2007). Furthermore, so-called gyrating clathrin (G-clathrin), characterized by localized but extremely rapid movement, has been suggested to operate in an Arf6-dependent rapid recycling route, presumably sorting cargo from along or on the ends of endosomal membrane tubules (Luo et al., 2013; Zhao and Keen, 2008). In polarized cells such as epithelia, clathrin is required to maintain basolateral polarity by sorting of cargo to the basolateral surface (Deborde et al., 2008). Clathrin was also shown to be necessary for the exit of the B-subunit of Shiga toxin from early and recycling endosomes thereby facilitating its retrograde traffic (Johannes and Popoff, 2008). In contrast, dominant interference with clathrin function by inducible overexpression of the clathrin hub domain or ligand-induced crosslinking of clathrin LCs, methods which also interfere with CME, had only minor effects on transferrin recycling (Bennett et al., 2001; Moskowitz et al., 2003). Meanwhile, it remains unclear to which degree flat clathrin coats on endosomes are necessary for Hrs-mediated degradative sorting of epidermal growth factor. They potentially retain cargo in restricted clathrin coats thereby preventing their recycling (Raiborg et al., 2006). Thus, whether and how precisely clathrin or its association with ligands are required for endosomal sorting remains to be investigated in more detail.

3.6 Clathrin in Mitosis

Independent of its well characterized role in membrane traffic, clathrin is involved in in mitotic spindle organization (reviewed in (Royle, 2012), Figure 3.8). During mitosis, endocytosis is inhibited and clathrin is redistributed to the mitotic spindle (Maro et al., 1985; Okamoto et al., 2000). Clathrin directly associates with kinetochetor fibres (k-fibers), discrete microtubule (MT) bundles of the mitotic spindle, independently from adaptor proteinss known to be involved in clathrin's function in trafficking. Chromosome congression at the metaphase plate is defective after depletion of clathrin by siRNA, caused by destabilization of the K-fibres. The consequences are delayed mitosis and multinucleated cells (Booth et al., 2011; Royle et al., 2005; Smith and Chircop, 2012).

Several studies independently identified two main interaction partners forming a complex with clathrin at the mitotic spindle (Booth et al., 2011; Fu et al., 2010; Hubner et al., 2010; Lin et al., 2010). One of them, the colonic hepatic tumor overexpressed gene (ch-TOG) is a protein essential for centrosomal MT assembly and K-fiber outgrowth (Barr and Gergely, 2008; Gergely et al., 2003). The second interaction

partner, the transforming acidic coiled-coil-containing protein 3 (TACC3), has been shown to be important for spindle MT stability and recruitment of ch-TOG to spindle MTs (Gergely et al., 2003; Kinoshita et al., 2005; Lee et al., 2001). Depletion of TACC3 phenocopies the effect of clathrin HC knockdown. However, clathrin is still recruited to the spindle in TACC3 knockdown cells while depletion of clathrin results in loss of TACC3 and ch-TOG from the mitotic spindle, indicating a role upstream of TACC3 for clathrin (Gergely et al., 2003; Lin et al., 2010; Royle et al., 2005). Recruitment of TACC3 to the mitotic spindle is regulated by clathrin and Aurora A kinase by phosphorylation of TACC3 on residue S558 (Booth et al., 2011; Kinoshita et al., 2005; LeRoy et al., 2007; Lin et al., 2010). TACC3 with mutated phosphorylation site (S558A) or inhibition of Aurora A kinase results in loss of TACC3 from spindles mimicking TACC3 or clathrin depletion (Booth et al., 2011; Cheeseman et al., 2011; Hubner et al., 2010; LeRoy et al., 2007).

The expression of spindle proteins such as TACC3 and ch-TOG is perturbed in many cancers emphasizing their important role in proliferation (Manning and Compton, 2008). Thus, determining the role of clathrin in the process of K-fibre stabilization in more detail might be a way to find new targets for anti-cancer therapeutics in the future.

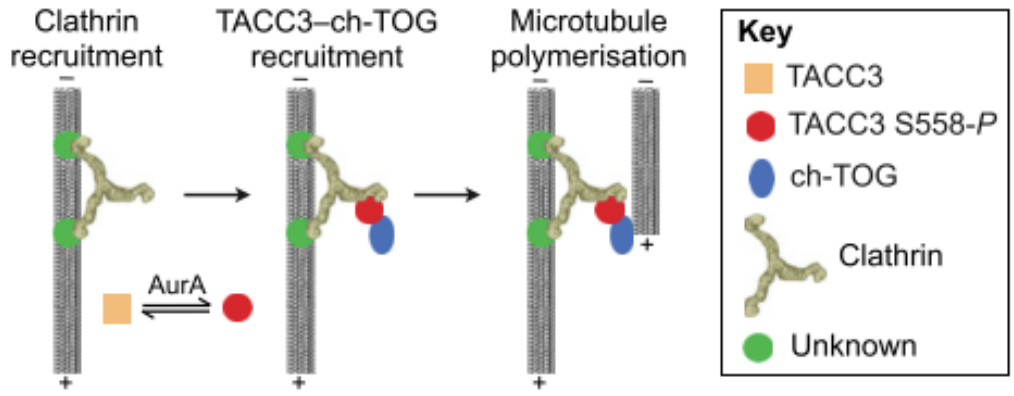

Figure 3.8 Model for clathrin function at the mitotic spindle. Clathrin is recruited to the mitotic spindle by an unknown protein, and subsequently recruits phosphorylated TACC-3 and ch-TOG (Royle, 2012).

3.7 Clathrin in Disease

Deletion of clathrin or central components of its machinery such as AP-2 and dynamin has been shown to be embryonically lethal in mice (Ferguson et al., 2009; Mitsunari et al., 2005). However, several mutations affecting the CME machinery are known to be connected to various human disorders.

There is evidence that several proteins involved in CME are perturbed in human cancer (McMahon and Boucrot, 2011). Clathrin HC fusion proteins and somatic mutations were detected in several cancers such as inflammatory myofibroblastic tumor, large B-cell lymphoma, paediatric renal carcinoma, and breast cancer (Argani et al., 2003; Bridge et al., 2001; De Paepe et al., 2003; Kan et al., 2010). Somatic mutations have been described in clathrin associated proteins and adaptors such as Eps15, HIP1, and β–arrestin (Kan et al., 2010). Other clathrin interacting proteins, such as Dab2, Numb or HIP1R, show disturbed protein levels in cancer cells (Fazili et al., 1999; Karam et al., 2007; Mok et al., 1998; Pece et al., 2004; Porpaczy et al., 2009). These changes resulting in altered CME of receptors and oncogenes and could thus influence cancer pathology. Yet, it remains to be investigated whether and how exactly these alterations are directly involved in cancerogenesis.

Epilepsy is characterized by seizures. It comprises a set of neurological disorders with multiple of them being linked to the CME machinery. Knockout studies in mice have linked the deletion of several clathrin-related proteins associated with the CME of synaptic vesicles to epileptic seizures, amongst them the neuron specific AP-3μB subunit (Nakatsu et al., 2004), endophilins (Milosevic et al., 2011), and amphiphysin (Di Paolo et al., 2002). Also perturbations in dynamin 1 function could enhance the risk for epileptic seizures as was seen in the “fitful” mutant mouse, expressing a dynamin 1 mutant which is not able to self-assemble efficiently (Boumil et al., 2010).

Furthermore, recent evidence indicates an involvement of a dysfunctional CME machinery in psychotic disorders (Schubert et al., 2012). On the one hand, several proteomic studies suggest alterations of clathrin- and AP-2-interacting proteins, such as dynamin I, HSC 70, amphiphysin, and Stonin 2, in patients with psychotic diseases (English et al., 2009; Focking et al., 2011; Luan et al., 2011). CME is required to regulate protein levels of receptors involved in psychotic disorders at synaptic membranes, amongst them receptors such as dopamine, NMDA, AMPA, and GABA(A) receptors (Harel et al., 2011; Kim et al., 2004; Kittler et al., 2000; Lau and Zukin, 2007; Paspalas et al., 2006; Schubert et al., 2012; Thompson and Whistler, 2011). On the other hand, many antipsychotic drugs directly interact with clathrin interacting proteins.

Phenothiazines, such as chlorpromazine and trifluoreperazine, inhibit CME by preventing AP-2 binding to the plasma membrane (Wang et al., 1993). First and second generation antipsychotics and the mood stabilizer lithium interfere with recruitment of the endocytic adaptor β-arrestin to dopamine receptors after stimulation with dopamine or quinpirole (Beaulieu et al., 2008; Masri et al., 2008). Thus perturbations of the clathrin interactome may contribute to an increased risk for psychotic diseases, even though a direct link between the gene perturbations and the disease onset still has to be established.

Many pathogens hijack the CME machinery to gain entry into cells. After binding to specific cell surface receptors, the pathogens are internalized. Thereby, they take advantage of endocytosis as their internalization leaves no traces at the cell surface, and thus conceals the pathogen from the immune system. Subsequently, they are transported to early and late endosomes where they exploit the increasingly acidic milieu to achieve fusion and release into the cytoplasm (Mercer et al., 2010). Several viruses have been reported to infect cells via CME, amongst them for example the, dengue virus (van der Schaar et al., 2008), ebola virus (Bhattacharyya et al., 2010), or hepatitis C virus (Blanchard et al., 2006; Helle and Dubuisson, 2008; Meertens et al., 2006). The human immunodeficiency virus (HIV) has long been believed to infect cells by direct fusion with the plasma membrane. However, recent studies suggest clathrin-dependent internalization followed by viral fusion in endosomes (Daecke et al., 2005; Miyauchi et al., 2009). Others, such as the Influenza virus, can infect cells using clathrin-dependent and -independent routes (Sun and Whittaker, 2013). However, the clathrin machinery is not only hijacked by viruses but also by bacteria. So-called “zippering” bacteria such as *Listeria monocytogenes* enter cells in a clathrin dependent manner (Veiga et al., 2007), while Shigella flexneri hijacks the clathrin machinery to facilitate its spreading between cells (Fukumatsu et al., 2012).

Together this shows that components of the CME machinery are implicated in a number of human disorders. Direct targeting of clathrin might help to understand the underlying mechanisms of the diseases and provide insights for the development of new drugs.

3.8 Interference with Clathrin Dependent Processes

3.8.1 Depletion Using Small Interfering RNA

A method routinely used for to interefere with clathrin function is small interfering RNA (siRNA) mediated depletion of a protein of interest. The effects of clathrin HC depletion on cells were first shown in 2003 by two different groups (Hinrichsen et al., 2003; Motley et al., 2003). In both studies, the clathrin dependency of transferrin (tf) internalization could be confirmed while adaptor distribution was unaffected. Contradictory results with regards to EGF uptake were probably due to different transfection protocols used in the studies resulting in incomplete clathrin knockdown and thus no inhibition of EGF internalization (Hinrichsen et al., 2003; Motley et al., 2003). Reduced growth rates indicated a block in mitosis or cytokinesis (Motley et al., 2003). Since then siRNA mediated clathrin depletion was used in numerous studies to investigate clathrin dependent processes. However, siRNA knockdown of clathrin has its limitations. To obtain a maximum of clathrin depletion, double transfection and long incubation periods of 72-96 hours are required. Therefore, compensatory effects cannot be excluded.

3.8.2 Overexpression of Dominant Negative Mutants

Transfection of cells with dominant negative mutants is commonly used to investigate clathrin mediated endocytosis. The GTPase defective dynamin mutant (dynK44A) inhibits the scission of vesicles with and without clathrin coat. The vesicles have elongated necks with associated dynK44A. The lack of scission results in efficient inhibition of dynamin dependent endocytosis (Damke et al., 1994). However, dynK44A expression does not allow to distiniguish between clathrin-dependent and clathrin-independent mechanisms of endocytosis and is therefore a rather unspecific method. Overexpression of the C-terminus of AP180 or of Eps15 lacking the EH domain sequester clathrin and thus prevents coat formation resulting in inhibited CME, as shown for transferrin or EGF receptor (Benmerah et al., 1999; Ford et al., 2001; Zhao et al., 2001). However, this approach, like siRNA knockdown, requires transfection and thus long expression times (at least 16 h) resulting in possible compensatory effects which might be indistinguishable from direct effects.

3.8.3 Chemical Interference

Additionally, chemical interference obtained by altering the composition of the cell medium can be used to acutely interfere with CME. Potassium depletion to less than 40 % of cellular levels reversibly disrupts CCPs and thus decreases CME by 70-95% (Larkin et al., 1983). However, potassium depletion also alters cell morphology and disrupts focal adhesion formation suggesting that other important cellular functions may be affected (Altankov and Grinnell, 1993). Additionally, it might affect internalization of clathrin-independent cargo such as cholera toxin and horseradish peroxidase (Carpentier et al., 1989). Furthermore, CME of EGF and transferrin are reversibly inhibited by cytosolic acidification to a pH below 6.5 or treatment with high sucrose (Cosson et al., 1989; Daukas and Zigmond, 1985; Sandvig et al., 1987). In both cases, inhibition of CME is due to an altered structure of the clathrin lattices which round up but fail to pinch off and build unusually small microcages devoid of membrane. While transferrin receptor still accumulates normally in CCPs under low pH, LDL receptor fails to be incorporated (Heuser, 1989; Heuser and Anderson, 1989). Possible side effects of acidification or hypertonic sucrose have not been investigated but are expected to influence cell physiology.

3.8.4 Acute Perturbation by Dimerization

As a method to acutely perturbe protein function, Spencer and colleagues developed a technique based on the highly specific interaction of the immunosuppressant FK506 and its target, FK506-binding protein 12 (FKBP). Cell permeable synthetic dimers of FK506 (FK1012 molecules) bind two separate FKBP molecules. Proteins fused to FKBP dimerize within minutes upon addition of the dimerizer (Spencer et al., 1993). Overexpression of FKBP fused to clathrin light chain together with a GFP-tag (EGFP-FKBP-CLC) followed by incubation with the crosslinker FK1012-A resulted in EGFP-FKBP-CLC dimer formation in cells. Even though clathrin triskelia are still observed on membranes, the lattice formation is disrupted resulting in inefficient triskelia exchange and decreased transferrin and LDL internalization (Moskowitz et al., 2003).

Using the same technique it was confirmed that clathrin is required for polarity of basolateral plasma membrane proteins in epithelial cells, such as tf receptor, VSVG, and E-cadherin (Deborde et al., 2008). As FKBP-CLC dimerization results in accumulation of clathrin triskelia on membranes (Spencer et al., 1993), it cannot be excluded that clathrin still fulfills functions in protein recruitment to membranes. This can be circumvented by using a “knocksideways” system where proteins of interest are

re-routed to a compartment of choice by rapamycin induced heterodimerization. Rapamycin binds to FKBP and the rapamycin binding (FRB) domain from mTOR. Proteins which are fused to FKBP and the FRB domain will dimerize in presence of rapamycin (Robinson et al., 2010). In a recent study, the AP-1 γ-subunit was fused to FKBP which dimerizes with FRB-YFP-Mito on mitochondria in presence of rapamycin (Figure 3.9). Acute re-routing of AP-1 to mitochondria depletes CI-MPR from CCVs and leads to its accumulation in peripheral rather than perinuclear compartments thereby confirming a requirement for AP-1 in intracellular transport CI-MPR (Robinson et al., 2010).

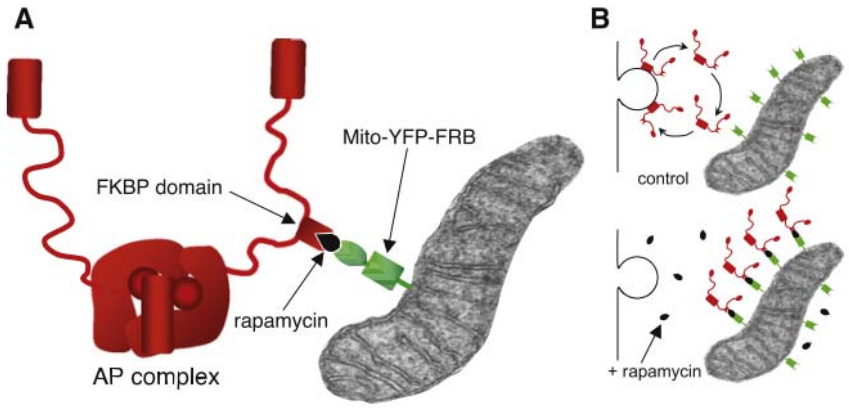

Figure 3.9 Schematic diagram of the knocksideways strategy. (A) FKBP is fused to a subunit of an adaptor complex such as AP-1, while FRB is fused to a mitochondrial targeting signal. Both of them bind rapamycin. (B) In presence of rapamicin they dimerize within minutes resulting in loss of AP-1 from its original membranes and re-routing to mitochondria (Robinson et al., 2010).

3.8.5 Small Molecule Inhibitors of CME and Intracellular Trafficking

Different small molecule inhibitors have been used to interfere with clathrin mediated endocytosis (Figure 3.10, (von Kleist and Haucke, 2012)). The dynamin inhibitors Dynasore (Macia et al., 2006), Dyngo-4a (Harper et al., 2011; McCluskey et al., 2013), or Arbidol (Blaising et al., 2013) can be used to prevent fission of clathrin coated pits. However, they lack specificity due to their involvement in clathrin independent membrane fission (Cao et al., 2007; Henley et al., 1998; Pelkmans et al., 2002). Moreover, it was recently shown that Dynasore and Dyngo-4a have unspecific effects on fluid phase endocytosis and peripheral membrane ruffling in dynamin triple

knockdown cells which lack all three mammalian dynamin isoforms (Park et al., 2013). Cationic amphiphilic drugs, such as chlorpromazine, are antipsychotic drugs which efficiently inhibit CME (see also 3.7). Chlorpromazine induces clathrin disassembly and relocation of AP-2 onto intracellular membranes (Wang et al., 1993). Yet, its specificity is still debated, as it might also affect other pathways and influence membrane fluidity (Elferink, 1979; Ogiso et al., 1981). Bolinaquinone is a small molecule which directly binds clathrin and reduces uptake of 488-BSA into cells. Compared to other endocytosis inhibitors, bolinaquinone effects appear rather weak with incomplete inhibition of endocytosis in the micromolar range and have not been investigated in much detail (Margarucci et al., 2011).

There are also examples for small molecules targeting intracellular traffic (Figure 3.10). The fungal metabolite brefeldin A (BFA) causes dramatic changes in Golgi morphology by inhibition of the small GTPase Arf1. The Golgi disassembles and its components redistribute into the ER, thus inhibiting secretion. Furthermore, BFA causes massive tubulation of endosomes, lysosomes and the TGN (Chardin and McCormick, 1999; Klausner et al., 1992; Lippincott-Schwartz et al., 1989). Exo1 and Exo2 are inhibitors that interfere with ER to Golgi transport by causing a collapse of the Golgi into the ER-Golgi intermediate compartment (ERGIC). Yet, their precise mechanism of action and their molecular target remains unknown (Feng et al., 2004; Feng et al., 2003). Secramine results in disrupted protein export from the Golgi by inhibition of activation of the Rho-familiy GTPase Cdc42. However, secramine also reduces polarization during cell migration and alters actin organization regulated by Cdc42 (Pelish et al., 2006). The small molecule Dispergo reversibly inhibits VSVG-GFP export from the ER to the Golgi. Using a mechanism which is still unclear, it induces extensive ER tubulation and loss of ER cisternae while cargo is retained at ER exit sites. Long incubation times result in loss of the Golgi apparatus, a secondary effect due to cargo and membrane retention in the ER (Lu et al., 2013).

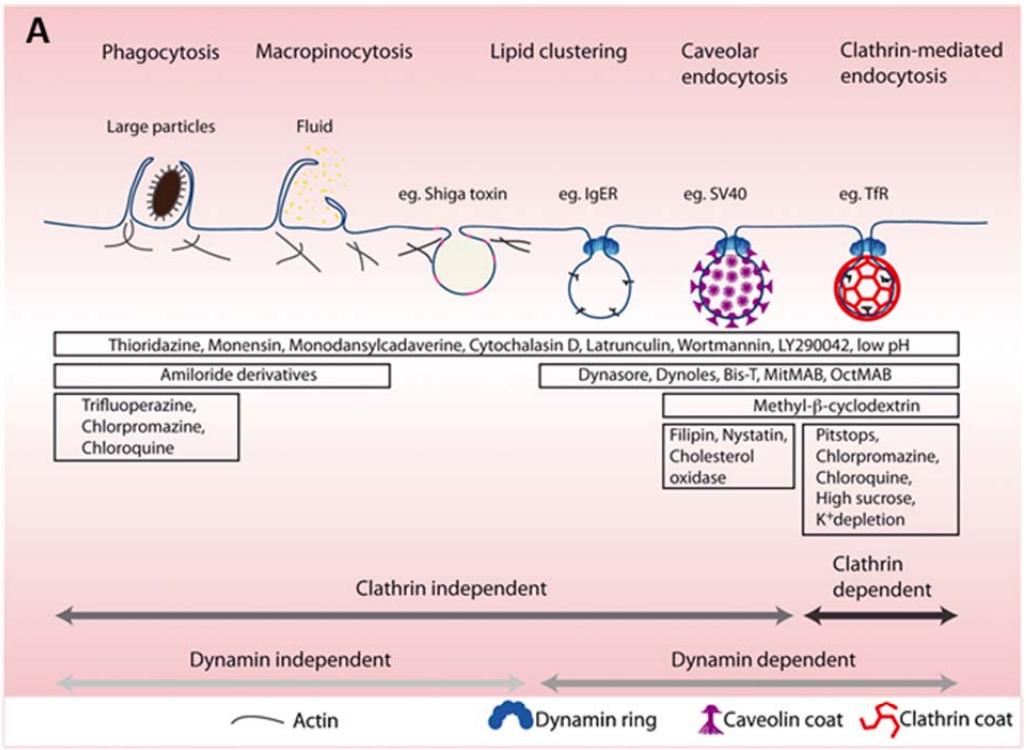

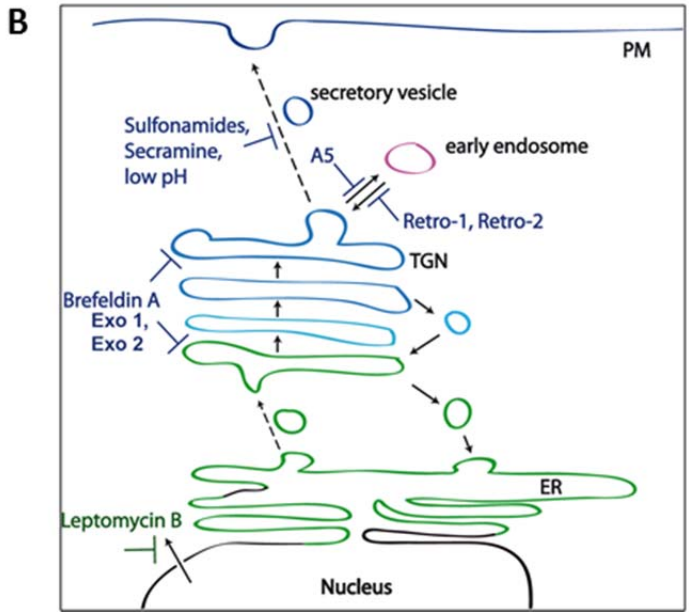

Figure 3.10 Small molecule mediated inhibition of membrane trafficking. (A) Scheme of entry routes into eukaryotic cells and exemplary cargo listed together with compounds known to perturb internalization into cells. The pathways can be distinguished based on their dependence on clathrin or the GTPase dynamin and the size of the internalized cargo. (B) Scheme of small molecules known to interfere with secretion and intracellular sorting (von Kleist and Haucke, 2012).

3.9 Pitstops as Inhibitors of Clathrin Function

So far inhibition of endocytosis or intracellular traffic did not specifically and effectively target clathrin itself. Recently we described the first specific inhibitors of clathrin function termed Pitstops (von Kleist et al., 2011). Pitstop®-1 and Pitstop®-2 efficiently inhibit *in vitro* binding of proteins containing clathrin box motifs with an IC_{50} in the low micromolar range. X-ray crystallography showed that the small molecule inhibitors directly bind the clathrin terminal domain at the interface between blade one and two, thus competing out the clathrin box and interfering with clathrin TD interactions with endogenous clathrin box containing ligands (Figure 3.11). In contrast to Pitstop®-1, Pitstop®-2 is cell permeable and can thus be used to study clathrin function by acute inhibition *in vivo*. Pitstop®-2 inhibits CME of transferrin and EGF as well as the internalization of HIV into cells (von Kleist et al., 2011).

Pitstops provide tools to address clathrin function in cell physiology. Since its discovery, Pitstop®-2 has been successfully used in several studies. As described previously (see also 3.6), clathrin plays a role in mitotic spindle organization and stabilization during mitosis. In a recent study Pitstop®-2 was used to confirm clathrin function at the mitotic spindle and to investigate potential anti-cancer properties of the compound (Smith et al., 2013). Even though clathrin lacking the terminal domain cannot bind to the mitotic spindle, clathrin TD/ ligand interactions via the clathrin box are not required for clathrin recruitment in HeLa cells. In presence of Pitstop®-2, clathrin was still recruited to K-fibers, yet a loss of mitotic spindle integrity was observed phenocopying clathrin HC depletion or treatment with an Aurora A kinase inhibitor. Together, the data confirm the role of clathrin TD-ligand interactions in mitosis (Smith et al., 2013).

In another study, the interplay between vascular endothelial growth factor receptor 2 (VEGFR2) endocytosis and downstream signaling was investigated. After vascular endothelial growth factor (VEGF) binding, VEGFR2 undergoes CME and eventually activates extracellular related kinases 1/2 (ERK1/2) which results in induction of angiogenesis. VEGF is expressed in most solid cancers and thus an interesting therapeutical target (Koch and Claesson-Welsh, 2012; Lampugnani et al., 2006). Gourlaouen and colleagues stimulated Pitstop®-2- or dynasore-treated cells with VEGF. They demonstrated that VEGFR2 was not internalized into the cells, but still activated in presence of inhibitor. However, activation of the downstream targets ERK1/2 was abrogated, revealing that VEGFR2 endocytosis is necessary for activation of more distal kinases in the signaling cascade (Gourlaouen et al., 2013).

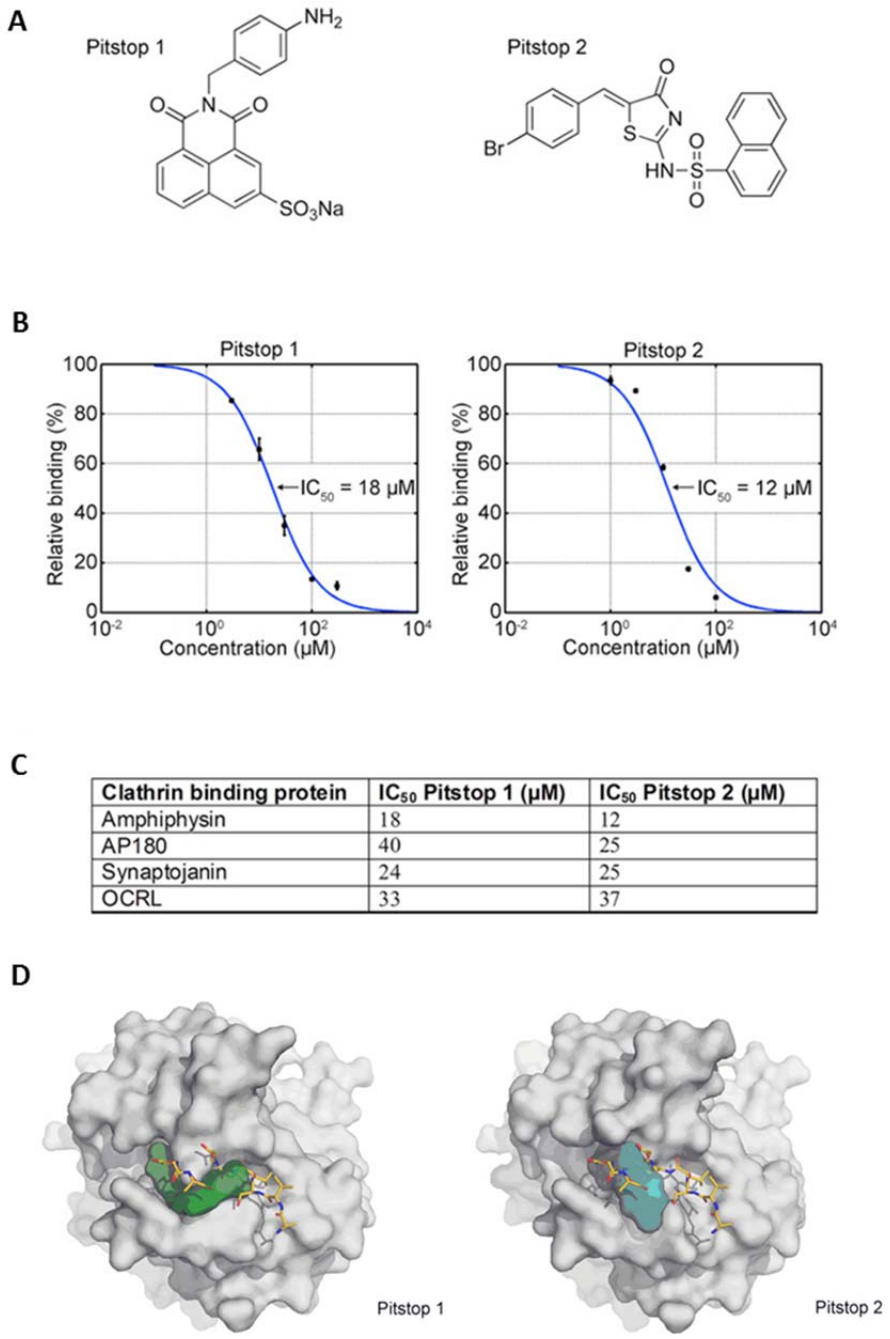

Clathrin binding protein	IC_{50} Pitstop 1 (µM)	IC_{50} Pitstop 2 (µM)
Amphiphysin	18	12
AP180	40	25
Synaptojanin	24	25
OCRL	33	37

Figure 3.11 Pitstops selectively inhibit ligand association with the clathrin terminal domain. (A) Shown are the chemical structures of Pitstop®-1 and Pitstop®-2. (B) Pitstops interfere with clathrin TD-amphiphysin complex formation in a dose dependent manner determined by ELISA. (C) IC_{50} values of Pitstop-mediated interference with clathrin TD and clathrin box containing ligands determined by ELISA. (D) View on the binding sites for Pitstop®-1 and Pitstop®-2. For comparison the clathrin box containing AP-3 β3 hinge region is depicted with yellow sticks demonstrating that Pitstops bind the same site on the terminal domain (modified from von Kleist et al., 2011).

Furthermore, Pitstop®-2 was used to investigate internalization of Crimean-Congo hemorrhagic fever virus (CCHFV) which has been reported to enter cells via CME. Garrison and colleagues confirmed clathrin-dependent internalization of the virus using Pitstop®-2 and siRNA mediated knockdown of AP-2 and clathrin (Garrison et al., 2013).

Recently, the specificity of Pitstop®-2 was questioned by findings that the internalization of clathrin independent cargo, such as MHCI (major histocompatibility complex class I) and CD98, is inhibited in the presence of Pitstop®-2 (Dutta et al., 2012). However, other studies suggest Epsin 1 and, thus, clathrin / AP-2-dependent internalization for MHCI (Duncan et al., 2006; Goto et al., 2010; Larsen et al., 2004).

In summary this shows that Pitstop®-2 is a valuable tool which has already been used in several studies. However, many questions about the effects of acute perturbation of endocytosis and intracellular traffic remain to be answered.

4 Aims of the study

The work described in this thesis is based on the development of Pitstops, the first known small molecule inhibitors of clathrin functionThe cell permeable small molecule Pitstop®-2 interferes with clathrin terminal domain-ligand interactions within minutes after addition and is, thus, a valuable tool to investigate clathrin function by acute perturbation. In this study, Pitstop®-2 was used to investigate the role of the clathrin terminal domain in CME and in the regulation of CCP dynamics. Additionally, the role of clathrin TD-ligand interactions in intracellular traffic were elucidated.

5 Materials and Methods

5.1 Materials

5.1.1 Chemicals and Consumables

Chemicals and consumables were purchased from GE Healthcare (Freiburg), Gibco (Eggenstein), Greiner (Solingen), Life Technologies (Gaithersburg, USA), Merck (Darmstadt), Roth (Karlsruhe), Serva (Heidelberg), Sarstedt (Nümbrecht), Schott (Mainz), Sigma-Aldrich (St. Louis, USA), and Thermo Scientific (Schwerte).

5.1.2 Markers and Loading Dyes

DNA markers were purchased from Fermentas (GeneRuler 1 kb DNA ladder), protein markers from NEB (broad range protein marker, pre-stained broad range protein marker) or Fermentas (page ruler prestained protein ladder). 6x DNA loading dye solution contained 0.05 % bromphenol blue, 0.05 % xylene cyanol, 30 % glycerol in ddH_2O. 6x sample buffer for SDS-PAGE was prepared in a total volume of 50 ml containing 375 mM Tris, 60 % (v/v) glycerin, 30 % (v/v) β-mercaptoethanol, 18 % (w/v) SDS and a “tip of a spatula” bromphenol blue.

5.1.3 Enzymes and Reaction Kits

Phusion polymerase and restriction enzymes were purchased from New England Biolabs (NEB, Schwalbach). Taq polymerase was from Genaxxon (Ulm). Calf intestinal phosphatase (CIP) and T4 DNA ligase were obtained from Fermentas (St. Leon-Rot). The NucleoSpin Extract II kit was used for DNA extraction from agarose gels, the NucleoSpin Plasmid kit for small scale plasmid purification from *Escherichia coli* (E.coli), both from Macherey-Nagel (Düren), for large scale plasmid purification the plasmid midi prep kit from Qiagen (Hilden).

5.1.4 Bacterial Strains

The following bacterial strains were used:

Strain	Application	Source
E. coli TOP10	Plasmid amplification	Invitrogen
E. coli BL21	High level expression of heterologous proteins	Invitrogen
E. coli ER2566	High level expression of heterologous proteins	Stratagene

5.1.5 Vectors

The following vectors were used for mammalian and bacterial expression:

Plasmid	Description	Tag	Resistance	Source
pEGFP-C1	mammalian expression vector	EGFP	Kanamycin	Clontech
pEGFP-C2	mammalian expression vector	EGFP	Kanamycin	Clontech
pEGFP-C3	mammalian expression vector	EGFP	Kanamycin	Clontech
pcDNA3	mammalian expression vector	None	Ampicillin	Invitrogen
pKaede-MN1	mammalian expression vector	pKaede	Kanamycin	MBL
pCDM8.1	mammalian expression vector	None	Ampicillin	Invitrogen
pGEX-4T1	bacterial expression vector	GST	Ampicillin	GE Healthcare
pET28a(+)	bacterial expression vector	HIS_6	Kanamycin	Novagen

5.1.6 Constructs

Construct	Amino acids	Mutations	Vector	origin
CLC	Full length		pKaede-MN1	
CHC TD	1-364		pGEX-4T1	Lisa von Kleist
Amphiphysin1 B/C	250-578		pET-28a(+)	Lisa von Kleist
CHC WT	Full length		pcDNA3	Lisa von Kleist
CHC 3x mut	Full length	R64A, Q89M, F91A	pcDNA3	Lisa von Kleist
CHC ΔTD	365-1675		pcDNA3	Lisa von Kleist
GGA1	Full length		pEGFP-C1	Julia Mössinger
GGA2	Full length		pEGFP-C2	Julia Mössinger

Construct	Amino acids	Mutations	Vector	origin
GGA3	Full length		pEGFP-C2	Julia Mössinger
εCOP	Full length		pEGFP-C3	gift from J. Lippincott-Schwartz (NIH, USA) (Ward et al., 2001)
VSVG	Full length	F204S	pCDM8.1	gift from J. Lippincott-Schwartz (NIH, USA) (Presley et al., 1997)
GFP-GPI	Full length		pcDNA3	gift from J. Lippincott-Schwartz (NIH, USA) (Nichols et al., 2001)

5.1.7 Oligonucleotides

Oligonucleotides were purchased from MWG (Martinsried):

Primer	Sequence	Restriction site
CLC-Kaede fw	atat CTGCAG caatggctgagttggatcc	PstI
CLC-Kaede rev	atat GCGGCCGC atgcaccaggggc	NotI

5.1.8 siRNA

For depletion of proteins the following siRNAs were purchased from MWG Biotech (Martinsried).

Target	Sequence
clathrin heavy chain	AUCCAAUUCGAAGACCAAU
clathrin heavy chain	AAGCAAUGAGCUGUUUGAAGA
AP-2(μ2)	GUGGAUGCCUUUCGGGUCATT

5.1.9 Mammalian Cell Lines

The following cell lines were used in experiments

Cell line	Origin	Morphology
HeLa	Human cervix carcinoma cells	Epithelial cells
COS-7	African green monkey kidney cells	Fibroblasts
BSC-1	African green monkey kidney cells	Epithelial cells
NIH/3T3	Mouse embryonic fibroblasts	Fibroblasts

Stable cell lines	Description	Origin
HeLa GFP-CI-MPR	HeLa cells stably expressing the CI-MPR cytosolic tail fused to GFP	From B. Hoflack (Waguri et al., 2003)
COS-7 CLC-EGFP	COS-7 cells stably expressing clathrin light chain fused to EGFP	Made by Kira Gromova
BSC-1 EGFP-σ1	BSC-1 cells stably expressing the AP-1 σ1 subunit fused to EGFP	From T. Kirchhausen (Anitei et al., 2010)
3T3 EGFP-σ2	3T3 cells stably expressing the AP-2 σ2 subunit fused to EGFP	Made by Kira Gromova

5.1.10 Antibodies and Fluorescent Ligands

The antibodies and fluorescent ligands used are listed below.

Primary antibodies

antibody	Clone	species	source	Method (dilution)
AP-1 γ-adaptin	100/3	Mouse	Sigma (A4200)	IF (1:200)
AP-1 γ-adaptin	88/ Adaptin γ	Mouse	BD transduction (610386)	WB (1:2000)
AP-2 α-adaptin	AP-6	Mouse	Abcam (Ab2730)	IF (1:100)
AP-2 α-adaptin	AC1M11	Mouse	Dianova (MA3-061)	WB (1:2000)
AP-3 μ-adaptin	p47	Mouse	BD transduction (610901)	WB (1:250)
β-actin	AC-15	Mouse	Sigma (A-5441)	WB (1:5000)

antibody	Clone	species	source	Method (dilution)
CD63	RFAC4	Mouse	Millipore (CBL553)	IF (1:100)
Clathrin heavy chain	X22	Mouse	Affinity Bioreagents (MA1065)	IF (1:100)
Clathrin heavy chain		Rabbit	Abcam (ab21679)	IF (1:200)
Clathrin heavy chain	TD1	Mouse	homebrew	WB (1:500)
Dynamin 1/2/3	Hudy-1	Mouse	Upstate (05-319)	IF (1:100)
EEA1	14/EEA1	Mouse	BD transduction (610456)	IF (1:100)
EGF receptor	D38B1	Rabbit	Cell signaling (4267S)	WB (1:1000)
FCHo1/2	Ra103	Rabbit	H. McMahon	IF (1:300)
Gadkin		Rabbit	homebrew (Schmidt et al., 2009)	IF (1:100)
Intersectin	S750	Rabbit	T. Südhof	IF (1:200)
LC3	4E12	Mouse	MBL (M152-3)	IF (1:100)
MHC class I	w6/32	Mouse	eBiosciences (14-9983-82)	Internalization (1:200)
CI-M6PR	2G11	Mouse	Affinity bioreagents (MA1-066)	IF (1:100)
P62 LCK ligand	3	Mouse	BD transduction (610832)	IF (1:400)
Sorting nexin 9		Rabbit	S. Carlsson	IF (1:200)
TGN46		Sheep	Serotec (AHP500G)	IF (1:200)
Transferrin receptor	H68.4	Mouse	Zymed (13-6800)	IF (1:400)

Secondary antibodies

antibody	conjugate	source	Method (dilution)
GαM^{488}	Alexa Fluor^{TM} 488 goat anti-mouse IgG	Life technologies	IF (1:200)
GαM^{568}	Alexa Fluor^{TM} 568 goat anti-mouse IgG	Life technologies	IF (1:200)
GαM^{647}	Alexa Fluor^{TM} 647 goat anti-mouse IgG	Life technologies	IF (1:200)
GαR^{488}	Alexa Fluor^{TM} 488 goat anti-rabbit IgG	Life technologies	IF (1:200)
GαR^{568}	Alexa Fluor^{TM} 568 goat anti-rabbit IgG	Life technologies	IF (1:200)
GαR^{647}	Alexa Fluor^{TM} 647 goat anti-rabbit IgG	Life technologies	IF (1:200)
DαS^{647}	Alexa Fluor^{TM} 647 donkey anti-sheep IgG	Life technologies	IF (1:200)

antibody	conjugate	source	Method (dilution)
$G\alpha M^{unlabelled}$	Goat Anti-Mouse IgG, no conjugate	Jackson	IF (1:10)
$G\alpha M^{HRP}$	HRP-conjugated goat anti-mouse IgG	Jackson	WB (1:5000)
$G\alpha R^{HRP}$	HRP-conjugated goat anti-rabbit IgG	Jackson	WB (1:5000)
$R\alpha GST^{HRP}$	HRP-conjugated rabbit anti-Gluthathione-S-Transferase	Sigma	Elisa (1:5000)

Fluorescent ligands

Fluorescent ligand	source
Alexa Fluor™488 conjugated Transferrin	Life technologies
Alexa Fluor™568 conjugated Transferrin	Life technologies
Alexa Fluor™488 conjugated EGF	Life technologies

5.1.11 Buffers, Media and Solutions

Molecular biology	
LB medium:	0.5 % (w/v) yeast extract 1 % (w/v) trypton 0.5 % (w/v) NaCl pH 7.2
2x YT medium:	1 % (w/v) yeast extract 1.6 % (w/v) trypton 0.5 % (w/v) NaCl pH 7.2
Ampicillin stock (500x):	50 mg / ml in ddH_2O Sterile filtered
Kanamycin stock (200x):	10 mg / ml in ddH_2O Sterile filtered
10x TBE (1L):	108 g Tris base 55 g boric acid 7.4 g EDTA
Ethidium bromide stock solution:	10 mg / ml in ddH2O

Molecular biology	
6x loading dye for DNA:	0.25 % (w/v) bromophenol blue 0.25 % (w/v) xylene cyanol 30 % (v/v) glycerol
TE-buffer:	10 mM Tris-HCl pH 7.5 1 mM EDTA

Biochemistry	
PMSF stock solution:	100 mM in DMSO
Cell lysis buffer with detergent:	20 mM HEPES pH 7.4 100 mM KCl 2 mM $MgCl_2$ 1 % (v/v) Triton X-100 1 mM PMSF 0.3 % (v/v) protease inhibitor cocktail (Sigma)
Cell lysis buffer without detergent:	20 mM HEPES pH 7.4 100 mM KCl 2 mM MgCl2 1 mM PMSF 0.3 % protease inhibitor cocktail (Sigma)
ELISA assay buffer:	20 mM HEPES pH 7.4 50 mM NaCl 10 mM DTT 1 mM PMSF
ELISA blocking buffer:	20 mM HEPES pH 7.4 50 mM NaCl 1 mM DTT 2 % (w/v) BSA 2.5 % (w/v) non-fat dry milk
ELISA wash buffer:	20 mM HEPES pH 7.4 50 mM NaCl 0.05 % (v/v) Tween 20
2x Bradford Reagent (500 ml):	70 mg (w/v) Coomassie G250 100 ml 85 % H_3PO_4 50 ml ethanol In ddH_2O, filtered

Biochemistry	
6x SDS-PAGE sample buffer:	375 mM Tris pH 6.8 60 % (v/v) glycerol 30 % (v/v) 2-mercaptoethanol 18 % (w/v) SDS added bromophenol blue
4x SDS-PAGE separating gel buffer:	1.5 M Tris pH 8.8 0.4 % (w/v) SDS
4x SDS-PAGE stacking gel buffer:	0.5 M Tris pH 6.8 0.4 % (w/v) SDS
10x SDS-PAGE running buffer:	246 mM Tris pH 8.8 1.92 M glycine 1 % (w/v) SDS
1x blotting buffer:	90 % SDS-PAGE running buffer 10 % methanol
Ponceau staining solution:	0.2 % (w/v) Ponceau S 1 % (v/v) acetic acid
Ponceau de-staining solution:	1 % (v/v) acetic acid
10x TBS:	200 mM Tris 1.4 M NaCl pH 7.6
Blocking solution:	4 % (w/v) non-fat dry milk in TBS
IB antibody solution:	2 % (w/v) BSA 0.01 % (w/v) azide in TBS

Cell Biology	
Cell culture medium:	DMEM (Dulbecco's modified Eagle's medium) 4.5 g / l glucose from Gibco 10 % (v/v) heat inactivated fetal calf serum (FCS) Antibiotics (50 units / ml Penicillin, 50 µg / ml Streptomycin)
Optimem:	from Gibco
Imaging medium:	Hank's balanced salt solution with Ca^{2+} and Mg^{2+} (HBSS) from Gibco 0.1 % (v/v) heat inactivated fetal calf serum (FCS) 10 mM HEPES pH 7.4

Cell Biology	
10x PBS:	1.37 M NaCl 27 mM KCl 43 mM Na_2HPO_4 14 mM NaH_2PO_4 pH 7.4
Fixative:	4 % (w/v) paraformaldehyde 4 % (w/v) sucrose in PBS
1 M sodium phosphate buffer (100 ml):	77.4 ml 1 M Na_2HPO_4 22.6 ml 1 M NaH_2PO_4 pH 7.4
Goat serum dilution buffer (GSDB):	10 % (v/v) goat serum 20 mM sodium phosphate buffer pH 7.4 100 mM NaCl 0.3 % (v/v) Triton-X-100
Acid wash buffer:	0.1 M Sodium-Acetat pH 5.3 0.2 M NaCl

5.2 Devices and Equipment

Device	**Company**
Autoclave Systec model V-65	Systec (Wettenberg)
Centrifuge Eppendorf 5417-R	Eppendorf (Hamburg)
Centrifuge Beckman J2-21 Rotors: JA-10, JA-17	Beckman Coulter (Krefeld)
Centrifuge Beckman Avanti J-26XP Rotors: JS-5.3, JA-25.50	Beckman Coulter (Krefeld)
Ultracentrifuge Optima TLX Rotors: TLA 100-10	Beckman Coulter (Krefeld)
Incubator for microbiological organisms	Memmert (Schwabach)

Device	Company
Incubator Heraeus for tissue culture	ThermoElectron (Langenselbold)
Microscope Axiovert 200M	Carl Zeiss (Jena)
TIRF System	Visitron Systems GmbH (Puchheim)
Spinning Disc Confocal microscope	Perkin Elmer (Rodgau)
Nikon Ti Eclipse - epifluorescence microscope	Nikon (Düsseldorf)
Olympus CKX31	Olympus (Hamburg)
Magnetic stirrer RCT basic	IKA-Werke (Staufen)
pH meter SevenEasy electrode (InLab410)	Mettler-Toledo (Gießen)
Plate reader GeniosPro	Tecan AG (Männedorf)
Power Supply Standard Power Pack P25	Whatman Biometra (Göttingen)
Semi-dry Blotter Fastblot B44	Whatman Biometra (Göttingen)
Sonicator Microtip System Sonopuls	Bandelin (Berlin)
Spectrophotometer Eppendorf Bio Photometer	Eppendorf (Hamburg)
Thermocycler T3	Thermocycler Biometra (Göttingen)
UV table UVT-28 ME	Herolab (Wiesloch)
Water purification Milli-Q Ultrapure Water Purification System	Millipore (Schwalbach)

5.3 Software and Internet Sources

Software	Application	Source
Adobe Acrobat	PDF	Adobe Systems (San José, USA)
Adobe Illustrator	Graphics	Adobe Systems (San José, USA)
Adobe Photoshop	Image, figure assembly	Adobe Systems (San José, USA)
ApE free software	DNA sequence analysis, primer design	Programmed by M.Wayne Davis http://biologylabs.utah.edu/jorgensen/wayned/ape/
Chem3D Ultra	Chemical structures	Cambridge Soft (Cambridge, USA)
EasyWin32	UV visualization	
ExPASy	DNA-protein translation	www.expasy.org
GraphPad Prism 5	Tables and graphs	GraphPad Software (La Jolla, USA)
GraphPad QuickCalcs t test calculator	Data statistics	http://www.graphpad.com/quickcalcs/ttest1.cfm

Software	Application	Source
ImageJ / Fiji	Microscopy image analysis	Wayne Rasband (NIH, USA) http://rsb.info.nih.gov/ij/
Micromanager	Microscopy image acquisition	Wayne Rasband (NIH, USA) http://rsb.info.nih.gov/ij/
Microsoft Office	Text processing, tables, graphs	Microsoft (Redmond, USA)
NCBI	Literature search (PubMed)	www.ncbi.nlm.nih.gov
NCBI Blast	DNA and protein sequence handling	www.ncbi.nlm.nih.gov/BLAST/
Slide Book 5	Microscopy image acquisition and analysis	Intelligent Imaging Innovations (Göttingen)
Volocity	Microscopy image acquisition and analysis	Perkin Elmer (Rodgau)

5.4 Molecular Biology

5.4.1 Polymerase Chain Reaction

Polymerase chain reaction (PCR) was performed to amplify DNA fragments from cDNA or plasmids for further cloning or to screen for *E.coli* colonies positive for the transformed plasmid. For cloning Phusion polymerase was used in the following PCR mix:

5x Phusion buffer HP	10	µl
10 mM dNTPs (200 µM each)	1	µl
0.5 µM forward primer	2.5	µl
0.5 µM reverse primer	2.5	µl
Template DNA (1-10 pg plasmid, 50-500 ng genomic DNA)	1	µl
Phusion polymerase	0.5	µl
H_2O	32.5	µl
	50	µl

The PCR-Mix was incubated in the thermocycler using the following standard programme:

Cycle step	*temperature*	*time*	*Cycle number*
Initial denaturation	98°C	30 sec	1
Denaturation	98°C	10 sec	
Annealing	TM + 3°C	30 sec	25-35
Extension	72°C	15-30 sec / kb	
Final extension	72°C	10 min	1
	4°	∞	

TM: melting temperature of the primer.

To analyze the efficiency of *E.coli* transformation a colony PCR was performed. The PCR-mix contained Taq polymerase and was composed as follows:

10x Genaxxon buffer	1	µl
5 mM dNTPs	0.32	µl
0.4 µM forward primer	0.375	µl
0.4 µM reverse primer	0.375	µl
H_2O	6.87	µl
Taq polymerase	0.06	µl
Bacteria suspension	1	µl
	10	µl

The mix was incubated in a thermocycler using the following programme:

Cycle step	**temperature**	**time**	**Cycle number**
Initial denaturation	95°C	6 min	1
Denaturation	95°C	30 sec	
Annealing	TM – 2°C	90 sec	30
Extension	72°C	1 min / kb	
Final extension	72°C	10 min	1
	4°C	∞	

5.4.2 DNA Restriction Digest

DNA fragments obtained by PCR and plasmids were digested using restriction enzymes (NEB) together with the according buffers. The DNA from one PCR reaction or 1 µg of plasmid DNA was digested in a mix containing 10x NEbuffer and 10 units per 1 µg of DNA restriction enzymes in a final volume of 30 µl. After 3 h incubation at 37°C for a preparative digest or 1 h at 37°C for a fast, analytic digest, the DNA fragments were loaded in an agarose gel for analysis.

5.4.3 Agarose Gel Electrophoresis and Gel Extraction

Agarose gel electrophoresis was used after PCR or restriction digest in order to purify DNA fragments and separate them by size.

To prepare the gel 1 % (w/v) agarose was dissolved in 1x TBE by heating the mixture. After polymerization at room temperature the DNA mixed with 6x sample buffer was loaded into the gel pockets and separated at 90 V. Afterwards, the gel was incubated 10 min in a water bath supplemented with ethidium bromide. The DNA bands were visualized under UV light. Bands running at the correct size were excised and extracted using the NucleoSpin Extract II kit from Macherey-Nagel according to manufacturer's instructions.

5.4.4 Ligation of DNA Inserts Into Linearized Vectors

Ligation was done using T4-Ligase (Fermentas) in 10 µl final volume. 50 ng of digested plasmid and insert were combined in a 1:3 molar ratio in a ligation mix together with 1 unit of T4-Ligase and 1 µl of 10x ligase buffer. Samples were incubated for 1 h at room temperature or overnight at 12°C before transformation into chemically competent *E.coli*.

5.4.5 Preparation of Chemically Competent *E.coli* Cells

To prepare chemically competent *E.coli*, a fresh colony was picked from an agar plate and inoculated in 5ml LB medium. It was grown overnight at 37°C then re-inoculated into 50 ml LB medium and further grown until the bacterial suspension reached an OD_{600} of 0.4. The cells were harvested by centrifugation at 4°C for 10 min at 2500x g in a sterile centrifuge tube. The bacterial pellet was resuspended in 10 ml cold 0.1 M calcium chloride and incubated on ice for 10 min to 3 h. Subsequently cells were

harvested like before, resuspended in 2 ml 0.1 M calcium chloride. 50 µl aliquots were prepared after addition of glycerol to a final concentration of 10 % (v/v). Cells were frozen in liquid nitrogen and stored at -80°C.

5.4.6 Transformation of Chemically Competent *E. coli* Cells

For heat shock transformation aliquots of chemically competent *E.coli* were thawed on ice. One ligation sample or 10 ng of plasmid DNA were added to the cells and incubated on ice for 20 min. For the heat shock, cells were incubated at 42°C for 1 min and immediately afterwards on ice for additional 5 min. Subsequently 250 µl of LB medium was added to the cells and they were shaken for 60 min at 37°C to induce antibiotic resistance. Afterwards, cells were pelleted (1 min, 3000x g) and plated on LB-agar plates supplemented with the corresponding antibiotic. The plates were incubated overnight at 37°C. The next day, colonies were picked and inoculated into LB medium for further proceedings.

5.4.7 Plasmid DNA Preparation

For small scale purification of plasmid DNA, *E.coli* cells were grown overnight in 3 ml LB medium at 37°C and purified using the NucleoSpin Plasmid kit (Macherey-Nagel) following the manufacturer's instructions. For mammalian cell line transfection high purity DNA was isolated from 100 ml overnight cultures using the plasmid midi prep kit from Qiagen according to manufacturer's instructions.

5.4.8 DNA Sequencing

To verify the constructs 1.5 µg of purified plasmid DNA were sequenced by MWG. The obtained sequences were aligned using the programme ApE (A Plasmid Editor).

5.4.9 Glycerol Stocks

E.coli clones hosting plasmid DNA were frozen in 1 ml LB medium supplemented with 20 % (v/v) sterile glycerol at -80°C for long term storage.

5.5 Biochemistry

5.5.1 Overexpression of Recombinant Proteins in *E. coli*

For the overexpression of recombinant protein, *E.coli* bacteria hosting the required plasmid were inoculated from glycerol stocks into 100 ml LB medium and grown overnight at 37°C. The next day, the bacteria were diluted 1:20 in 2xYT medium. Overexpression was induced at an OD_{600} value of 0.8 by addition Isopropyl-β-D-thioglactopyranoside (IPTG) to a final concentration of 0.5 mM. After 4 h incubation at 25°C the cells were harvested by 15 min centrifugation at 4000x g, 4°C and the cell pellets either frozen or used immediately for protein purification.

5.5.2 Affinity-Purification of Recombinant GST- and HIS_6-Fusion Proteins

Cell pellets from 500 ml cultures were resuspended in 35 ml ice-cold PBS for GST-fusion proteins or in 20 mM Tris-HCl (pH 7.4), 500 mM NaCl for HIS_6-tagged proteins and supplemented with 1 mM Dithiothreitol (DTT), 1 mM phenylmethylsulfonylfluoride (PMSF), 100 units of benzonase endonuclease (Sigma) and a “tip of a spatula” of lysozyme (Roth). After 10 min incubation on ice 1 % Triton-X-100 (GST-fusion proteins) or 2 % Chaps (HIS_6-tagged proteins) was added. The samples were sonicated twice for 1 min on ice using 70 % power and 50 % duty cycle to break the cells and kept on ice for additional 10 min. Next, the cells were centrifuged at 17000x rpm at 4°C for 15 min before the supernatant containing the GST-tagged proteins were loaded on 0.5 ml pre-washed GST-binding resin (Novagen). The supernatant of HIS_6-tagged proteins was supplemented with 10 mM imidazole before addition to 0.5 ml pre-washed Ni-NTA agarose (Qiagen). The suspension was incubated for 2 h at 4°C on a rotating wheel to allow binding to the resin. The beads were centrifuged at 4°C for 3 min, 2000x g and supernatant discarded, then washed three times with PBS (GST-fusion proteins) or 20 mM Tris buffer pH 7.4, 500 mM Nacl, 10 mM imidazole (HIS_6-tagged proteins). After washing, GST-fusion proteins were eluted in 0.5 ml PBS containing 20 mM reduced glutathione, HIS_6-tagged proteins in 0.5 ml 20 mM Tris-HCl pH 7.4, 500 mM NaCl, 300 mM imidazole for 1 h at 4°C on a rotation wheel. Proteins were dialyzed in 2 L ELISA buffer at 4°C for 2 h and overnight. The following day, the proteins were ultracentrifuged for 30 min at 50000x g, 4°C to remove aggregates. After addition of 10 % (v/v) glycerol and 1 mM DTT, protein concentration was determined by Bradford assay, the proteins were aliquoted, frozen in liquid nitrogen and stored at -80°C for later use.

5.5.3 ELISA-Based Binding Assays

An ELISA-based binding assay was performed to measure inhibition of protein-protein interactions in presence of small molecule inhibitors.

First, 384-well plates (highbinding PS Microplate, Greiner Bio-One) were coated with 80 ng HIS_6-amphiphysin B/C diluted to a total volume of 50 µl in ELISA buffer (10 mM HEPES pH 7.4, 50 mM NaCl, 1mM DTT, 1 mM PMSF). BSA diluted in ELISA buffer served as negative control. After 1 h incubation at room temperature, 50 µl of ELISA blocking buffer (10 mM HEPES pH 7.4, 50 mM NaCl, 1 mM DTT, 1 mM PMSF, 2 % BSA, 2.5 % Milk) was added to block unspecific protein binding. The plate was sealed with aluminium foil and incubated over night at 4°C. The next day, plates were washed thoroughly 5x with ELISA wash buffer (10 mM HEPES pH7.4, 50 mM NaCl, 1 mM DTT, 0.05 % Tween). Subsequently, chemical compounds diluted in DMSO were added together with 600 ng of GST-clathrin TD in ELISA buffer and incubated for 1 h at room temperature. The plates were washed 5x before 50 µl anti-GST-HRP antibody (dilution 1:5000) was added and incubated for 15 min at room temperature. The antibody was removed and the wells were washed 5x in ELISA wash buffer. To detect the bound antibody, 50 µl Tetramethylbenzidine (TMB) substrate (Pierce Biotechnology) was added and the plate was incubated for 15 min at room temperature. HRP reacted with TMB yielding in a soluble blue reaction product. Addition of 50 µl 2N H_2SO_4 terminated the reaction leading to a yellow reaction product which could be detected by measuring the absorbance at 450 nm in a plate reader (Tecan). Relative binding was calculated as relative amount of DMSO control after background subtraction.

5.5.4 Preparation of Cell Lysates

To analyze knockdown efficiency or protein degradation, whole cell lysates were prepared from HeLa cells grown in a 6 well plate. The cells were transferred to ice, washed 3x with cold PBS supplemented with 10 mM $MgCl_2$, and scraped in 500 µl PBS. After centrifugation for 3 min at 4°C, 1000x g, the PBS was replaced by 50 µl cell lysis buffer (20 mM HEPES pH 7.4, 100 mM KCl, 2 mM $MgCl_2$, 1% Triton X-100, 1 mM PMSF, and 0.3% (v/v) protease inhibitor cocktail). The lysates were incubated for 30 min on ice and then centrifuged for 10 min at 17000x g, 4°C to remove cell debris. Protein concentrations were determined by Bradford assay, sample buffer (62.5 mM Tris pH 6.8, 10 % glycerol, 5 % 2-mercaptoethanol, 3 % SDS, and 0.05 % bromphenol blue; final concentration) was added and the lysates were boiled for 5 min.

5.5.5 EGFR Degradation Assay

HeLa cells were grown in 6 well plates, starved for 2 hours in DMEM supplemented with 0.1 % FCS and 10 mM HEPES and then stimulated with 500 ng / ml of unlabeled EGF in presence of 10 µg / ml cycloheximid. Immediately after stimulation the cells were transferred to ice, washed twice in cold PBS + 10 mM $MgCl_2$. Whole cell lysates were prepared like described before to define the initial amount of EGF receptor. The remaining cells were treated with 30 µM Pitstop®-2, 30 µM Pitnot-2 or 0.1 % DMSO in DMEM + 10 mM HEPES, 0.1 % FCS 30 min after stimulation to follow further EGF degradation in presence of Pitstop2. Cell lysates were prepared 30 min, 60 min, 120 min, and 180 min after stimulation, equivalent to 0 min, 30 min, 90 min, and 150 min after Pitstop®-2 addition.

5.5.6 Cytosol / Membrane Fractionation

For a cytosol / membrane fractionation, mock HeLa cells and cells depleted of endogenous clathrin heavy chain were splitted onto 6 cm dishes and incubated with 30 µM Pitstop®-2 or 0.1 % DMSO in DMEM supplemented with 0.1 % FCS and 10 mM Hepes (pH 7.4) for 20 min at 37°C. Next, cells were washed twice on ice with cold PBS + 10 mM $MgCl_2$. After complete removal of the washing buffer, cells were harvested in 100 µl of lysis buffer without detergent (20 mM HEPES pH 7.4, 100 mM KCl, 2 mM $MgCl_2$, 0.3 % protease inhibitor cocktail (Sigma), and 1 mM PMSF) using a cell scraper. Afterwards, the cells were lysed by freezing them three times in liquid nitrogen and immediately thawing them in a water bath at room temperature. Next, the lysates were pushed 20 times through a 27g needle to homogenize them. Subsequent centrifugation for 3 min at 4°C, 1000x g was performed to remove nuclei and large debris. The supernatant was collected, 20 µl were saved for analysis as total cell lysates in western blot, while the rest was transferred to TLA tubes and spun at 4°C with 180000x g. The supernatant, defined as the cytosolic fraction, was collected, protein concentration was determined and 6x sample buffer was added. The membrane pellet was resuspended in a volume of 1x sample buffer that equals the volume of the cytosolic fraction. Samples from three independent experiments were used in SDS-PAGE and western blot to compare the degree of membrane binding of different proteins.

5.5.7 Protein Concentration Determination by Bradford Assay

To determine the protein concentration of cell lysates or purified protein a Bradford assay was performed. 500 µl of 2x Bradford solution was added to 1 - 5 µl of protein solution in 500 µl water. After 5 min incubation at room temperature the absorption at 595 nm was measured. 1x Bradford solution served as a blank. The protein concentration from samples measured in duplicates or triplicates was calculated from a reference curve generated using BSA as standard.

5.5.8 SDS Polyacrylamide Gel Electrophoresis (SDS-PAGE)

SDS-PAGE was performed to separate proteins according to their size. Equal amounts of protein mixed with sample buffer and denatured for 5 min at 95°C were loaded on SDS gels with the following composition:

	Separating gel (15ml)		**Stacking gel (5 ml)**
	8 %	10 %	3.8 %
ddH_2O	7 ml	6 ml	3.25 ml
4 x separating gel buffer	3.75 ml	3.75 ml	-
4 x stacking gel buffer	-	-	1.25 ml
30 % acrylamide / 0.8 % bis-acrylamide	4 ml	5 ml	0.625 ml
10 % ammonium persulfate (APS)	75 µl	75 µl	75 µl
TEMED	7.5 µl	7.5 µl	7.5 µl

Separation of the proteins was performed after complete polymerization of the gel in 1x SDS-PAGE running buffer at 15 mA per gel until the bromphenol band of the marker reached the end of the gel.

5.5.9 Immunoblotting

The proteins separated with SDS-PAGE were transferred from the polyacrylamid gel to a nitrocellulose membrane (Whatman Biometra) using a semi dry blotting system (FastBlot B44, Biometra). Three layers of whatman paper, the nitrocellulose membrane, the polyacrylamide gel and three more layers of whatman paper (bottom to top) were assembled in the semi-dry blotter after soaking them in blotting buffer. The

electrotransfer was performed for 180 min at 45 mA per membrane. To determine efficiency of the transfer, the nitrocellulose membrane was stained with Ponceau S and briefly destained with 1 % acetic acid before scanning for documentation. The blot was washed in TBS and then incubated in blocking buffer for 1 h at room temperature. After washing the membrane three times for 10 min in 1x TBS, it was incubated with the primary antibody in IB antibody solution (TBS supplemented with 2 % BSA and 0.01 % azide) over night at 4°C. The next day the nitrocellulose membrane was washed three times in 1x TBS before incubation with secondary antibody conjugated to horseradish peroxidase (HRP; 1:5000) in blocking buffer for 1 h at room temperature. After three washes with 1x TBS, the antibodies were detected using enhanced chemoluminescence (ECL) Western Blotting Detection Reagents (GE Heathcare). ECL together with HRP leads to a luminescent signal which was detected by exposing a light sensitive film (Hyperfilm ECL, Amersham Biosciences) on the membrane. If required, quantification of the signal was done using the ImageJ gel analysis plugin.

5.6 Cell biology

5.6.1 Mammalian Cell Culture

Mammalian cell lines (HeLa, HeLa GFP-CI-MPR, COS-7, COS-7 CLC-EGFP, BSC-1 EGFP-σ1, and 3T3 EGFP σ2) were incubated in humidified incubators (Thermo Electron) with 5 % CO_2 at 37°C. They were grown in Dulbecco's modified Eagle's medium (DMEM, Gibco) containing 4.5 g / l glucose supplemented with 10 % (v/v) heat inactivated (30 min, 56°C) fetal calf serum (FCS) and 1 % (v/v) antibiotics (50 units / ml penicillin, 50 µg / ml streptomycin). Medium for stable cell lines was supplemented with additional antibiotics: 0.4 µl / ml puromycin for COS-7 CLC-EGFP, 0.3 µl / ml for 3T3 EGFP-σ2, and 20 µl / ml geneticin for BSC-1 EGFP-σ1 and HeLa GFP-CI-MPR. Cells were passaged every two to four days after 5 min trypsinization with trypsin / EDTA solution (Gibco) and plated in 1:2 – 1:20 dilutions in a new cell culture dish.

5.6.2 Transfection of Mammalian Cells with Plasmid DNA

Transient overexpression of fluorescently tagged proteins was done with Lipofectamine 2000 (Life Technologies) according to the manufacturer's instructions. First, the plasmid DNA and the Lipofectamine 2000 were diluted separately in Optimem (Gibco) in a poly-styrol reaction tube. After 5 min at room temperature the samples were mixed

and incubated for additional 20 min at room temperature. Next the transfection mix was added dropwise to cells with a confluency of approximately 80 % in antibiotic free DMEM. The transfection medium was changed after 4 h incubation at 37°C. 6-8 h post transfection cells were splitted on Matrigel coated coverslips for use one day after transfection.

Plate	**DNA mix**		**Lipofectamine mix**		**Antibiotic free DMEM**
	DNA	Optimem	Lipofectamine	Optimem	
12-well	1 µg	100 µl	2 µl	100 µl	800 µl
6-well	2 µg	200 µl	4 µl	200 µl	1600 µl
6 cm	4 µg	400 µl	8 µl	400 µl	3200 µl
10 cm	10 µg	1000 µl	20 µl	1000 µl	8000 µl

5.6.3 siRNA Knockdown of Proteins

For depletion of endogenous protein, two rounds of siRNA knockdown were performed in 6-well plates using Oligofectamine (Life Technologies) as transfection reagent according to the manufacturer's manual. First 2 µl of siRNA were diluted in 175 µl Optimem while 2 µl Oligofectamine were diluted in 25 µl Optimem in poly-styrol reaction tubes. After 5 min at room temperature, the two samples were combined and incubated for additional 20 min at room temperature. The medium of cells in a 6 well plate with a confluency of approximately 50 – 60 % was exchanged with 800 µl of Optimem, before the transfection mix was added dropwise. After 4 h incubation at 37°C, 1 ml of rescue medium (DMEM supplemented with 20 % (v/v) FCS and 2 % (v/v) antibiotics) was added to the cells. After 24 h, cells were passaged to reach a confluency of 50 – 60 % the next day for a second round of transfection following the same protocol. The day after the second siRNA transfection, cells were splitted on Matrigel coated coverslips or into 6 well plates for lysate preparation, and used in experiments the following day.

5.6.4 Transferrin Uptake

Transferrin uptake experiments were performed in HeLa cells to quantitatively analyze clathrin-mediated endocytosis. After 1 h starvation at 37°C in serum free DMEM, HeLa cells were preincubated with compound or according amounts of DMSO as negative control for 15 min at 37°C in DMEM supplemented with 10 mM HEPES pH 7.4 and 0.1

% FCS. For the uptake 20 µg / ml Alexa-488/568 coupled transferrin ($tf^{488/568}$, life technologies) was diluted in the medium containing the inhibitor and added to the cells for 15 min at 37°C. After washing three times in ice cold PBS + 10 mM $MgCl_2$, the cells were fixed in fixation solution (4 % PFA, 4 % sucrose in PBS pH 7.4) for 15 min at room temperature. The samples were mounted onto glass slides in Immomount supplemented with 0.5 µg / ml 4',6-Diamidino-2-phenylindole (DAPI) and imaged with an inverted epifluorescence microscope (Axiovert 200M, Zeiss) controlled by Slidebook 5 software (Intelligent Imaging Innovations). For quantification of the experiments, the sum intensities in a region of interest (ROI) including the cells to be analyzed were defined. After background subtraction, the obtained intensity values were divided by the cell number to get the average sum intensity per cell. Data was normalized to controls.

5.6.5 Transferrin Recycling

HeLa cells were splitted on coverslips in 12 well plates. The next day, 70 % confluent cells were starved for 1h in serum free DMEM. Subsequently a transferrin uptake was performed using 20 µg / ml tf^{488} (Life Technologies) for 30 min at 37°C. After washing the cells twice in PBS + 10 mM $MgCl_2$ on ice, an acidic wash was done on ice in 0.1 M sodium-acetate (pH 5.3) + 0.2 M NaCl for 3 min. Afterwards cells were rinsed twice in PBS + 10 mM $MgCl_2$. The 0 min timepoint was fixed for 15 min in fixation solution (4 % PFA, 4 % sucrose in PBS pH 7.4). To the remaining cells pre-warmed DMEM containing 1 mg / ml unlabelled transferrin and 30 µM Pitstop®-2, 30 µM control compound 1 or corresponding amounts of DMSO, respectively, were added, immediately before shifting them to 37°C. After 7.5 min or 15 min cells were transferred to ice, washed twice with PBS + $MgCl_2$, fixed and processed for microscopy. Microscopy and image analysis was performed like described above (5.6.4).

5.6.6 Degradation of Fluorescently Labelled EGF

HeLa cells were split on coverslips in 12 well plates. The next day, cells were starved for 1h in serum-free DMEM. Then an EGF uptake was performed using 100 ng / ml $EGF^{Alexa647}$ (Invitrogen) for 20 min at 37°C. After washing the cells twice in PBS + 10 mM $MgCl_2$ on ice, the 0 min time point was fixed for 15 min in 4 % PFA. To the remaining cells pre-warmed DMEM containing 500 ng / ml unlabeled EGF and 30 µM Pitstop-2, 30 µM control Pitnot-2 or corresponding amounts of DMSO, respectively,

were added and they were shifted to 37°C immediately. After 30 min, 60 min, 90 min, or 120 min the cells were transferred on ice, washed with PBS + $MgCl_2$, subsequently fixed and prepared for microscopy.

5.6.7 Cargo Accumulation in Clathrin Coated Pits

To allow cargo accumulation at the plasma membrane, COS-7 cells were seeded on matrigel coated coverslips. After 24 h, they were starved for 2 h in serum free DMEM. Cells were then incubated in DMEM supplemented with 0.1 % FCS and 10 mM HEPES (pH 7.4) containing 100 ng / ml Alexa-488 coupled EGF (EGF^{488}) in presence of 30 µM Pitstop®-2 or 0.1 % DMSO for 30 minutes at 8°C. After quick washing in PBS + 10 mM $MgCl_2$, cells were fixed in fixation solution (4 % PFA, 4% sucrose in PBS pH 7.4) for 15 minutes at room temperature and stained for endogenous AP-2 as a clathrin coated pit marker. Cells were imaged using a total internal reflection (TIRF) microscopy system (Visitron). Acquisition and analysis of the data was done with Slidebook 5 software (Intelligent Imaging Innovations). Colocalization was analyzed by determining the Pearson's correlation coefficient between EGF and AP-2 using Slidebook 5 software.

5.6.8 MHCI Internalization

For MHC class I internalization experiments, HeLa cells were seeded on matrigel coated glass coverslips. 24 hours after seeding the cells were incubated with antibody against MHC class I (clone w6/32, eBiosciences) in DMEM supplemented with 10mM HEPES pH 7.4 and 0.1 % FCS for 15 min on ice. After brief washing in PBS + 10mM $MgCl_2$, cells were allowed to internalize the surface bound antibody in the presence of 30 µM compound (Pitstop®-2, Pitstop2-100, control compound 1, control compound 2), or 0.1 % DMSO in HBSS supplemented with 0.1 % FCS and 10mM HEPES pH 7.4 for 30 min at 37°C. After washing three times in ice-cold PBS + 10 mM $MgCl_2$, the cells were fixed in fixation solution (4 % PFA, 4% sucrose in PBS pH 7.4) for 15 minutes at room temperature. To bind surface epitopes of non-internalized MHC class I, cells were incubated overnight at 4°C with an unlabeled goat anti mouse antibody (1:10) in goat serum dilution buffer (10 % goat serum, 15 mM sodium phosphate buffer pH 7.4, 100 mM NaCl) without detergent. The next day, the cells were permeabilized with goat serum dilution buffer supplemented with 1 mg / ml Saponin for 20 min at room temperature before staining of internalized MHC class I antibody with an Alexa488 labelled fluorescent goat anti mouse secondary antibody. The samples were imaged using a spinning disc confocal microscope (Perkin Elmer) with Volocity Software

(Improvision). Quantification of internalized antibody was performed like described above (5.6.4).

5.6.9 *De novo* Formation of Clathrin Coated Pits

To analyze the effect of Pitstop®-2 on de novo formation of clathrin coated pits, COS-7 cells stably expressing EGFP-clathrin light chain were seeded on matrigel coated coverslips to reach a density of approximately 70%. The next day, living cells were imaged in imaging buffer (HBSS supplemented with 0.1 % FCS and 10 mM HEPES pH 7.4) at 37°C using TIRF microscopy (Visitron) together with Slidebook 5 software (Intelligent Imaging Innovations). Images of untreated cells in HBSS were acquired first, then 2 % 1-butanol in HBSS was added together with 0.1 % DMSO or 30 µM Pitstop®-2 to deplete clathrin coated pits. After 5 minutes, the 1-butanol was washed out by exchanging the old medium with HBSS containing 0.1 % DMSO or 30 µM Pitstop®-2. This allows de novo clathrin coated pit formation at the plasma membrane. Images of the same cell were acquired before treatment, in the presence of 1-butanol, and 3 minutes after washout.

5.6.10 VSVG-GFP Secretion Assay

HeLa cells were splitted on coverslips in 12 well plates. The next day, the 80-90 % confluent cells were transfected with VSVG-SP-GFP using Lipofectamine 2000 (Invitrogen). After 4 h incubation at 37°, the medium was replaced and cells were shifted to 39°C for additional 6 hours, to trap VSVG-SP-GFP in the ER during expression. After 10 h total expression time, the cells were incubated with 10 µg / ml cycloheximid and shifted to 19°C to allow VSVG-SP-GFP trafficking to the TGN. One hour later, 30 µM Pitstop®-2, 30 µM control compound 1 or the according amount of DMSO (0.1 %) in DMEM containing 0.1 % FCS and 10 mM HEPES (pH 7.4) were added to the cells and preincubated for additional 10 min at 19°C. Then the timepoint “0 min chase” was washed with PBS + 10 mM $MgCl_2$ on ice and fixed for 15 min in fixation solution (4 % PFA, 4 % sucrose in PBS pH 7.4). The remaining cells were transferred to 32°C, chased for 60 min, washed and fixed as described above. The fixed samples were processed for micrsocopy and imaged with an inverted epifluorescence microscope (Axiovert 200M, Zeiss) controlled by Slidebook 5 software (Intelligent Imaging Innovations). VSVG-SP-GFP distribution in the cell was analyzed using ImageJ.

5.6.11 Immunofluorescence Staining

HeLa cells were seeded on matrigel coated glass coverslips 24 h before the experiment. Prior to the staining, cells were fixed in fixation solution (4 % PFA, 4 % sucrose in PBS, pH 7.4) for 15 min at room temperature, or in Methanol for 7 min at -20°C. After permeabilization with goat serum dilution buffer (10 % goat serum, 15 mM sodium phosphate buffer pH 7.4, 100 mM NaCl) supplemented with 0.3 % Triton-X-100 or 1 mg / ml saponin as detergent, antibody stainings were performed. Coverslips were incubated upside down in 30 µl primary antibody solution for 1 h at room temperature, and then washed 3 times. Subsequently they were stained with 30 µl of the corresponding secondary antibody in a 1:200 dilution for 1 h at room temperature. After mounting in Immomount supplemented with 0.5 µg / ml 4',6-Diamidino-2-phenylindole (DAPI), the samples were imaged using an inverted epifluorescence microscope (Axiovert 200M, Zeiss), a spinning disc confocal microscope (Perkin Elmer), or a total internal reflection (TIRF) microscopy system (Visitron).

5.7 Microscopy

5.7.1 Epifluorescence Microscopy

VSVG-secretion, transferrin uptake, transferrin recycling and EGF degradation assays were imaged using an inverted epifluorescence microscope (Zeiss Axiovert 200M) controlled by Slidebook 5 software (Intelligent Imaging Innovations). Images were analyzed using Slidebook 5 Software or ImageJ.

5.7.2 Confocal Microscopy

Confocal microscopy has an improved resolution compared to epifluorescence microscopy due to better resolution in the z-axis and thus reduction of out of focus fluorescence. MHCI internalization assays, stainings of intracellular markers, live cell imaging of intracellular proteins, and FRAP experiments were performed using a spinning disc confocal microscope (Perkin Elmer) with Volocity software (Improvision).

5.7.3 Live Cell Imaging

For live cell microscopy of adaptor protein dynamics, cells were splitted on matrigel coated coverslips. The next day, time series of 2 min with 0.5 frames per second were acquired at 37°C 5-30 min after the addition of 0.1 % DMSO, or 30 µM compound (Pitstop®-2, Pitstop2-100, Pitnot-2, or Pitnot-2-100) in imaging buffer (HBSS supplemented with 10 mM Hepes pH 7.4 and 0.1 % FCS). Analysis of time lapse series and generation of kymographs was acquired with Volocity software (Perkin Elmer). Lifetimes and movement were analyzed by manual tracking.

Images of GFP-CI-MPR were acquired at 37°C 5-30 min or 60-90 min in imaging buffer with 30 µM Pitstop®-2 or DMSO (0.1 %). Analysis of the number and size of GFP-CI-MPR positive puncta was performed using Volocity Software (Improvision).

5.7.4 Fluorescence Recovery after Photobleaching (FRAP)

Fluorescence recovery after photobleaching (FRAP) experiments were performed using a spinning disc confocal microscope (Perkin Elmer) together with Volocity software (Improvision). After one wash in PBS the cells were incubated in imaging buffer supplemented with 30 µM Pitstop®-2, 30 µM Pitstop2-100, 30 µM Pitnot-2, 30 µM Pitnot-2-100, or 0.1 % DMSO. After 5 min compound incubation, FRAP experiments were performed at 37°C. To analyze the recovery of clathrin in clathrin coated pits, COS-7 cells stably expressing CLC-EGFP were imaged for 12 s, then bleached in a region of 15x15 μm^2, and directly afterwards imaged for additional 120 s, acquiring 0.5 frames per second. Cells transiently expressing GPI-GFP were used to investigate membrane mobility. Cells were imaged for five seconds at a framerate of 1 frame per second, and afterwards bleached in a round area with a diameter of 125 μm^2. Immediately after bleaching the cells were imaged for another 60 seconds at a framerate of 2.5 images per second. Fluorescence recovery was analyzed by comparing fluorescence intensities in the bleached area before and after bleaching. To correct for photobleaching the values were related to a control area, which was not actively bleached.

5.7.5 Photoconversion of CLC-Kaede

CLC-Kaede photoconversion experiments were performed using a spinning disc confocal microscope (Perkin Elmer). Cells transiently overexpressing CLC-Kaede were imaged 5-30 min after addition of 30 µM Pitstop®-2, 30 µM Pitnot-2, or DMSO (0.1 %)

in imaging buffer. After 10 s of imaging, the TGN region of a cell was photoconverted from Kaede488 to Kaede568 using the 405 nm laser line. Immediately afterwards, a time lapse series was acquired for additional 2 min with a framerate of 2 s per frame. Quantifications of fluorescence intensities and Pearson's Correlations were obtained using Volocity software (Improvision).

5.7.6 TIRF microscopy: Live and Fixed

TIRF microscopy can be used to monitor processes at the surface of cells. Illumination of the fluorescent sample with an angle of approximately 60° leads to excitation of fluorophores in an evanescent field of only 100 nm thickness. Intracellular fluorophores are not excited. EGF accumulation in clathrin coated pits (5.6.6) and de novo formation of clathrin coated pits (5.6.9) were described before. For live cell TIRF microscopy COS-7 cells stably expressing EGFP-clathrin light chain, or 3T3 cells stably expressing sigma2-EGFP were used. Imaging was performed and analyzed like described before (5.7.3). Dynamics were analyzed by manual tracking.

5.8 Statistics

Statistical analyses were performed using the Excel microsoft software and the unpaired Student's t test (GraphPad Software). The data are presented as mean with standard error of the mean (SEM), n indicates the number of samples examined. Asterisks were used to indicate significance ($p > 0.05$ not significant (ns); * $p < 0.05$; ** $p < 0.001$; *** $p < 0.0001$).

6 Results

Recently two small molecule inhibitors of clathrin terminal domain (TD)-ligand interactions termed Pitstop®-1 and Pitstop®-2 were identified using an ELISA-based screen followed by medicinal chemistry approaches. X-ray crystallography confirmed that Pitstops directly bind to the clathrin terminal domain (TD). In contrast to Pitstop®-1, Pitstop®-2 is cell permeable and can thus be used to investigate the effects of acute clathrin inhibition *in vivo* (von Kleist et al., 2011).

6.1 The Pitstop Family of Small Molecule Inhibitors

In this study, Pitstop2 (Figure 6.1A) was used to characterize the effects of acute clathrin inhibition on cellular processes. Focused library synthesis resulted in more structurally related compounds (Adam McCluskey, Newcastle). In order to ensure specificity, we included three structurally similar compounds from this focused library in some of the experiments, an active compound Pitstop2-100, and two inactive control compounds (Pitnot-2 and Pitnot-2-100) (Figure 6.1A). Using an ELISA based binding assay we were able to show that Pitstop®-2 and Pitstop2-100 inhibit the interaction between clathrin terminal domain and amphiphysin to the same degree (Figure 6.1B), while both control compounds do not have an effect on the interaction (Lisa von Kleist, not shown).

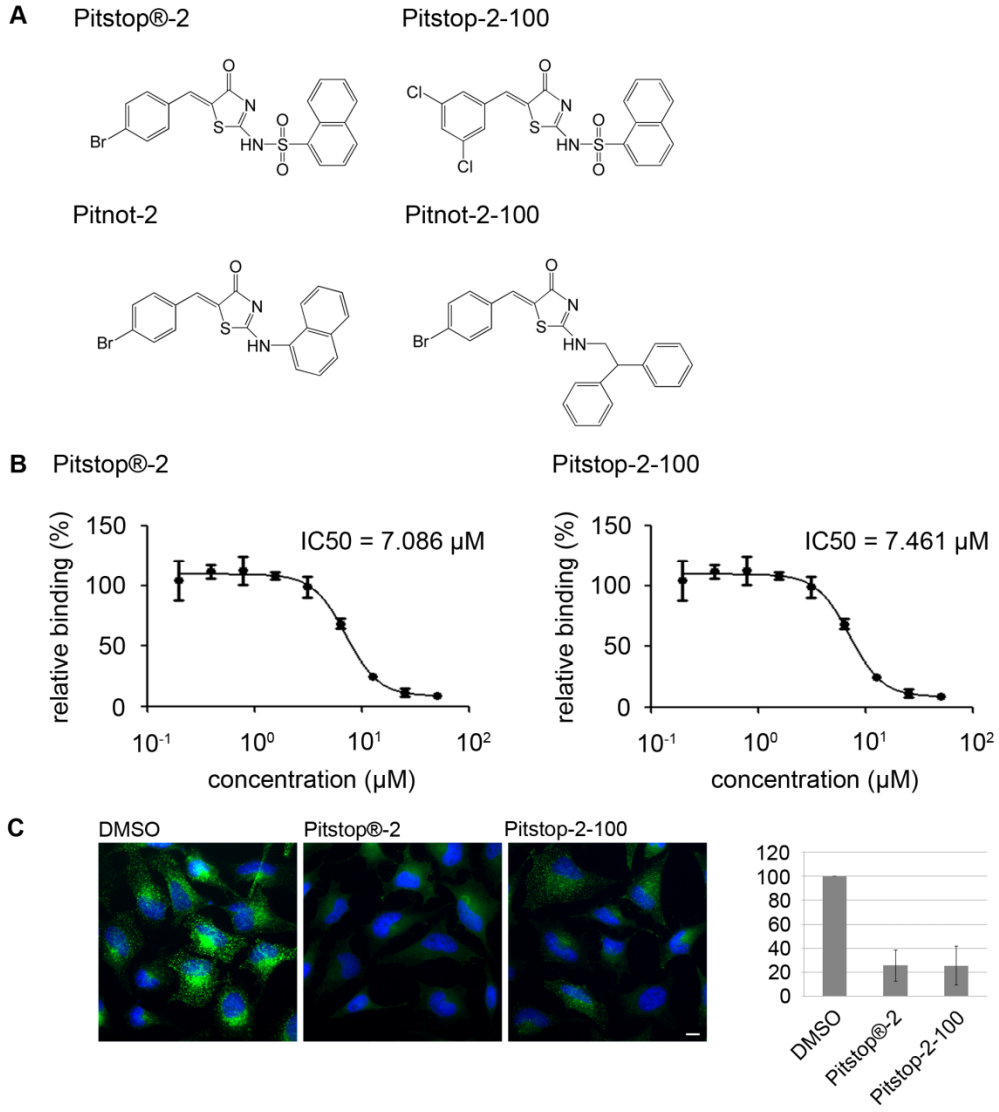

Figure 6.1 The Pitstop family of small molecule inhibitors. (A) The chemical structures of Pitstop®-2, Pitstop2-100, and two inactive control compounds (Pitnot-2 and Pitnot-2-100) are depicted. (B) Pitstop®-2 and Pitstop2-100 efficiently inhibit binding of clathrin terminal domain to amphiphysin in an ELISA based binding assay with IC_{50} values of 7.086 µM and 7.461 µM respectively (SEM, n=4 independent experiments). (C) The panels show transferrin uptake into HeLa cells in presence of DMSO, 30 µM Pitstop®-2 or 30 µM Pitstop2-100. The graph represents the quantification of internalized tf^{488} (SEM, n=3 independent experiments). Scale bar, 10 µm. (Modified from Stahlschmidt et al., 2014)

6.2 Functional Effects of Pitstop®-2 on Clathrin-Mediated Endocytosis

Pitstop®-1 and Pitstop®-2 both efficiently inhibited interactions between the clathrin TD and accessory proteins *in vitro*. To further investigate the functional effects of acute inhibition in cells we analyzed clathrin-mediated endocytosis (CME) in presence of Pitstop®-2 in more detail.

6.2.1 Pitstop®-2 Efficiently Inhibits Transferrin Uptake

The transferrin receptor is, after ligand binding, internalized exclusively via CME. Thus uptake of its fluorescently labeled ligand transferrin (tf) into cells is the standard method to study the functionality of CME.

To investigate the effects of Pitstops on CME transferrin uptake experiments were carried out in collaboration with Lisa von Kleist. Therefore, we preincubated HeLa cells with compound, then incubated with 20 µg / ml tf^{568} (Alexa Fluor 568-conjugated transferrin) for 15 min in presence of compound. Incubation with up to 30 µM Pitstop®-2 decreased tf^{568} uptake compared to 0.1 % DMSO treatment in a dose dependent manner with an IC_{50} value of 10-15 µM. This is in the same range as the inhibition of protein-protein interactions *in vitro*. At a concentration of 30 µM, Pitstop®-2 reduced tf^{568} internalization by 95%. The inhibitory effect was reversed after 1-3 h of washout in serum free medium (Figure 6.2A, B).

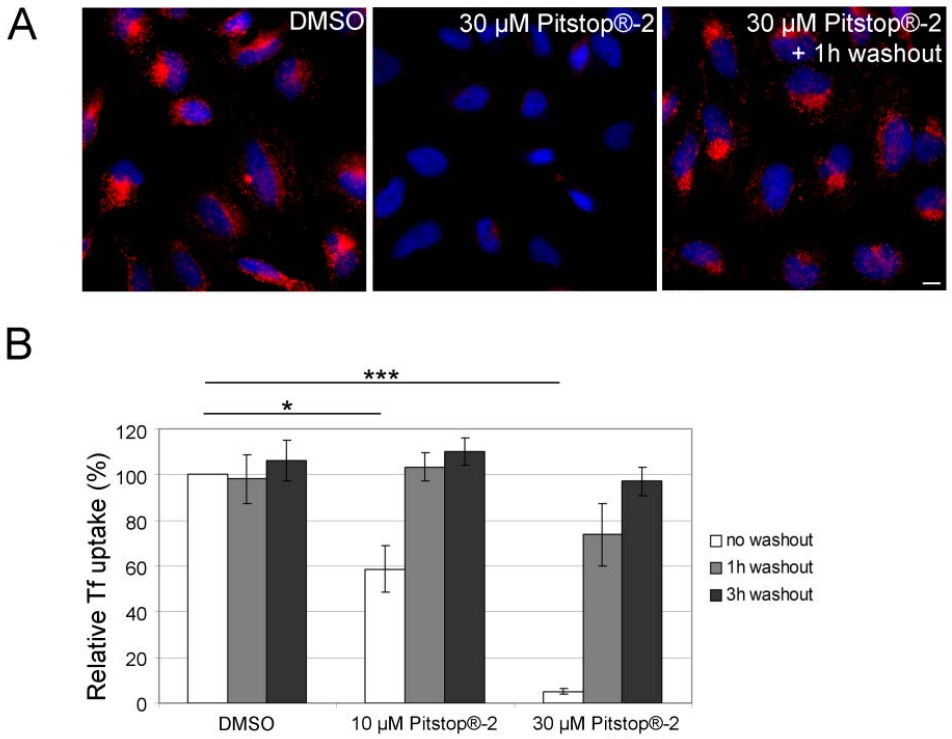

Figure 6.2 Pitstop®-2 reversibly inhibits tf uptake into HeLa cells. (A) HeLa cells were allowed to internalize tf^{568} for 15 min after 15 min preincubation with coumpound. Immunofluorescence images show that uptake of tf^{568} is strongly reduced in presence of Pitstop®-2 compared to 0.1 % DMSO. This effect is reversible after 1-3 h wash out of the drug. Scale bar, 10 µm. (B) Quantification of internalized tf^{568} fluorescence. The graph represents three independent experiments with SEM (* $p < 0.05$; *** $p < 0.0001$). (Modified from von Kleist et al., 2011)

6.2.2 Enrichment of Tf Receptor at the Plasma Membrane after Endocytosis Block

We expected that an endocytosis block would lead to enrichment of non-internalized tf receptor on the cell surface. To investigate this, we incubated COS-7 cells with 0.2 % DMSO or 60 µM Pitstop®-2 for 15 min at 37°C before fixing them and staining with a specific antibody against tf receptor. We could detect an enrichment of tf receptor at the plasma membrane (Figure 6.3A). Quantification of tf receptor fluorescence at the plasma membrane revealed an increase in the relative surface fraction from 11 % in control cells to 20 % in Pitstop®-2 treated cells (Figure 6.3B).

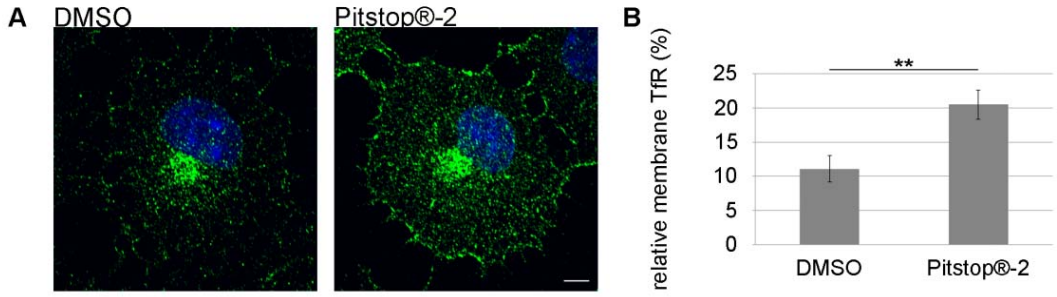

Figure 6.3 Tf receptor accumulates on the plasma membrane in presence of Pitstop®-2. (A) Spinning disc confocal images showed an enrichment of transferrin receptor at the plasma membrane of COS-7 cells after 15 min incubation with 60 µM Pitstop®-2 compared to mock cells (0.2 % DMSO). Scale bar, 10 µm. (B) The graph represents quantifications of the relative membrane localized tf receptor fraction (SEM, ** $p < 0.001$). (Modified from von Kleist et al., 2011)

6.2.3 Cargo Accumulation in Clathrin Coated Pits is not Impaired in Presence of Pitstop®-2

Epidermal growth factor (EGF) receptor is internalized mainly via clathrin-mediated endocytosis upon stimulation with ligand (Goh et al., 2010). After addition of EGF to cells, it binds to the receptor which is then clustered in clathrin coated pits (CCPs) followed by endocytosis. In cells treated with 30 µM Pitstop®-2 internalization of fluorescently labeled EGF is efficiently inhibited (Lisa von Kleist, (von Kleist et al., 2011)). To ensure that Pitstop®-2 does not prevent CME by blocking cargo sequestration into CCPs, we investigated the accumulation of receptor-ligand complexes in CCPs. COS-7 cells were preincubated with 0.1 % DMSO or 30 µM Pitstop®-2 for 15 min at 37°C. Then 100 ng / ml EGF^{488} was added for another 30 min at 8°C. At this temperature, lateral membrane movement but not endocytosis occurs. The cells were fixed and stained with a specific antibody against AP-2 as CCP marker. TIRF images showed that the EGF^{488} and AP-2 fluorescence overlapped in presence of Pitstop®-2 (Figure 6.4A). Quantification using the Pearson's correlation showed a small but significant increase of colocalization (Figure 6.4B). This suggests that inhibited endocytosis in presence of Pitstop®-2 is not due to impaired cargo clustering into CCPs.

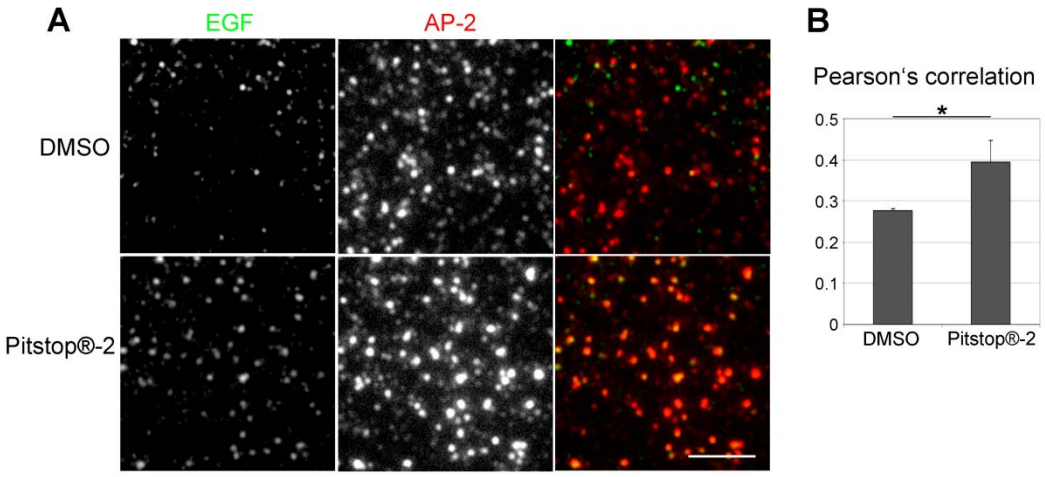

Figure 6.4 Ligand-receptor complex sequestration into clathrin coated pits is not impaired by Pitstop®-2. (A) TIRF microscopy images of COS-7 cells which were incubated with EGF^{488} in presence of 30 µM Pitstop®-2 or 0.1 % DMSO at 8°C. Costaining with the clathrin coated pit marker AP-2 reveals that EGF^{488} and AP-2 localization overlaps. Scale bar, 5 µm. (B) Quantification of the colocalization represented by the Pearson's correlation. An increase in colocalization is detected in presence of Pitstop®-2 (SEM, n=3 independent experiments, * $p < 0.05$). (Modified from von Kleist et al., 2011)

6.2.4 Pitstop®-2 Inhibits Clathrin-Dependent Internalization of MHCI

The specificity of Pitstop®-2 was questioned by findings that the internalization of potentially clathrin-independent cargo, such as MHCI (major histocompatibility complex class I) and CD98, is inhibited in presence of Pitstop®-2 (Dutta et al., 2012). To verify these results, we performed uptake experiments following the same protocol as used in (Dutta et al., 2012). We allowed the internalization of a surface bound antibody against MHCI into HeLa cells for 30 min at 37°C, followed by fixation and staining for internalized antibody using a fluorescently labeled antibody. We observed that the amount of internalized MHCI was decreased to 9.5 % in presence of 30 µM Pitstop®-2 compared to DMSO treated cell (Figure 6.5A, B). To verify specificity we additionally included 30 µM Pitstop2-100 which resulted in a reduction of internalization down to 38.5 %, whereas treatment with the non-clathrin binding control compounds Pitnot-2 and Pitnot-2-100 showed no reduction of MHCI uptake. These results confirmed the inhibitory effect of Pitstop®-2 and Pitstop2-100 on MHCI internalization.

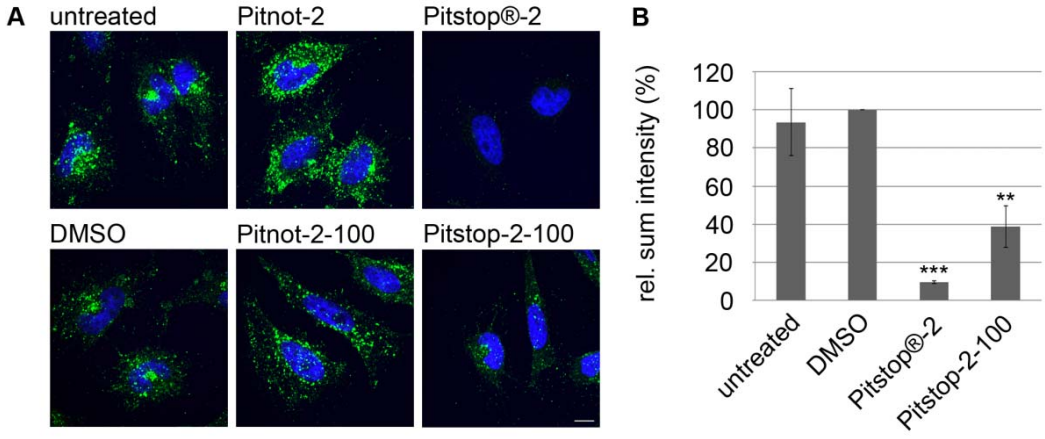

Figure 6.5 MHCI endocytosis is inhibited by Pitstop®-2. (A) MHCI internalization into HeLa cells is inhibited by Pitstop®-2 or the related compound Pitstop2-100 (30 µM) but not by two different non-clathrin binding control compounds. Scale bar, 10 µm. (B) Quantification of data shown in A (n=3 independent experiments). The amount of MHCI internalized into DMSO treated HeLa cells was set to 100 % (n=3 independent experiments; ** $p < 0.005$; *** $p < 0.0005$). (Modified from Stahlschmidt et al., 2014)

The internalization of MHCI was published to be clathrin independent (Eyster et al., 2009; Naslavsky et al., 2003). Alternatively, endocytosis of MHCI might follow a clathrin- / AP-2-dependent mechanism in agreement with several recent studies (Duncan et al., 2006; Goto et al., 2010; Larsen et al., 2004). To verify whether the decrease of internalized MHCI is an unspecific side effect of Pitstop®-2 or Pitstop2-100 on clathrin independent endocytosis we depleted HeLa cells of clathrin heavy chain (HC) and the AP-2 µ2-subunit with two rounds of siRNA knockdown. Immunofluorescence imaging confirmed efficient clathrin HC and AP-2(µ2) depletion by 90-95 % (Figure 6.6D). Allowing uptake of surface bound MHCI antibody for 30 min at 37°C revealed that clathrin and AP-2 knockdown cells failed to internalize MHCI (Figure 6.5A). Meanwhile, MHCI surface levels were not altered (Figure 6.6B). Quantification showed a reduction of MHCI endocytosis after depletion of the AP-2 µ2- subunit or clathrin HC (26.8 % and 23.7 % respectively) comparable to treatment of mock cells with 30 µM Pitstop®-2 (22.4 % internalization). Performing the uptake experiment in clathrin HC or AP-2(µ2) knockdown cells in presence of 30 µM Pitstop®-2 further decreased MHCI uptake into cells by blocking remaining clathrin terminal domains (5.2 % for µ2 knockdown cells, 11.9 % for clathrin HC knockdown cells; Figure 6.6C). Taken together these results indicate that MHCI internalization is clathrin dependent and thus inhibited upon Pitstop®-2 treatment.

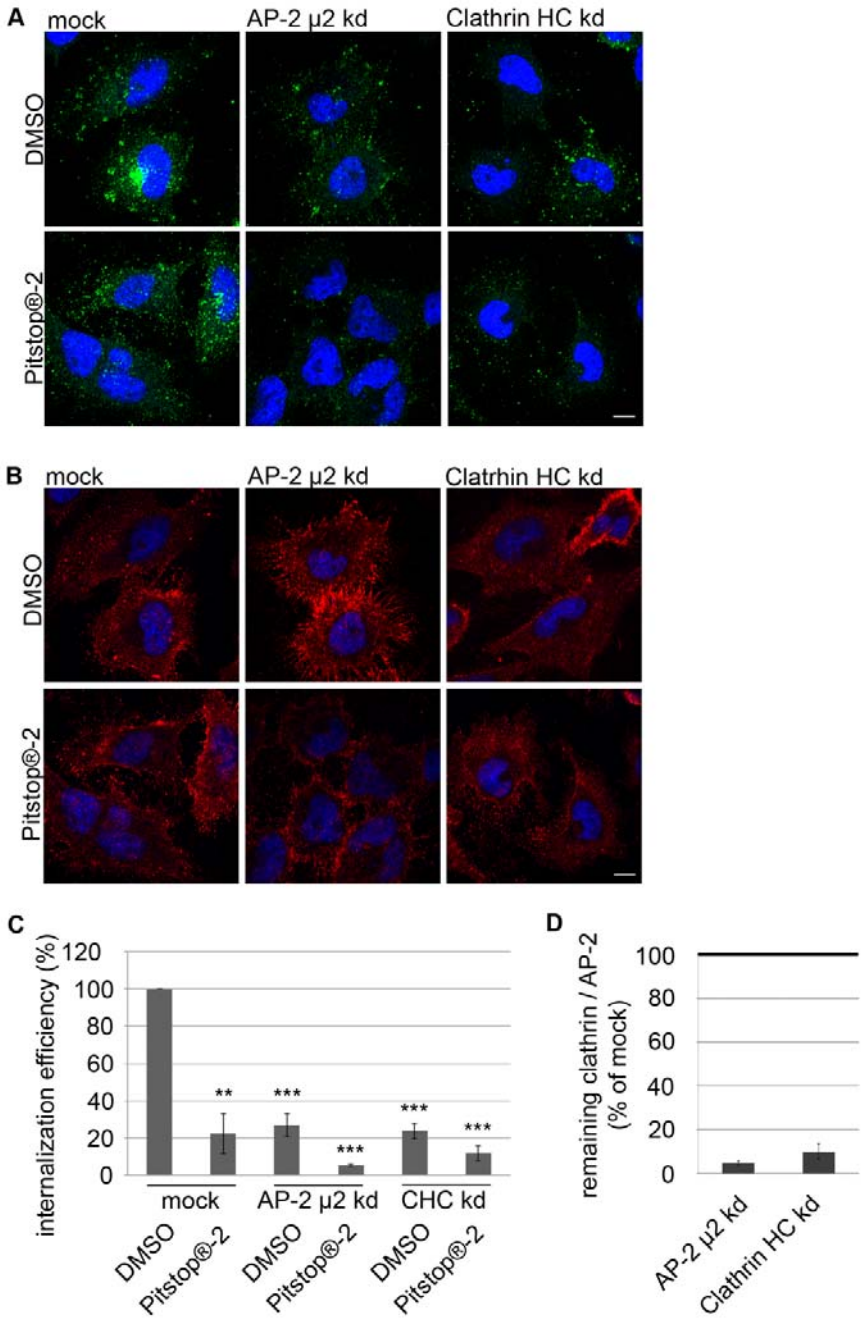

Figure 6.6 MHCI endocytosis is clathrin dependent. (A) Representative images of MHCI internalization into clathrin heavy chain (CHC)- or AP-2 µ2-depleted HeLa cells. Cells were either treated with DMSO or Pitstop®-2. Scale bar, 10 µm. (B) Representative images of MHCI surface levels in knockdown or control cells. Scale bar, 10 µm. (C) Quantification of MHCI internalization into clathrin (CHC k.d.)- or AP-2 µ2-depleted (µ2 k.d.) cells treated with DMSO or Pitstop®-2 as shown in Figure 6.5. The amount of MHC I internalized into DMSO-treated control cells was set to 100 % (n=3 independent experiments). (D) Quantification of clathrin (CHC) and AP-2(α) levels in cells treated with siRNA against AP-2 µ2-subunit or CHC compared to mock-transfected cells (n=3 independent experiments; ** $p < 0.005$; *** $p < 0.0005$). (Modified from Stahlschmidt et al., 2014)

6.3 Protein Recruitment in Presence of Pitstop®-2

6.3.1 Clathrin Recruitment to Membranes

The clathrin terminal domain is a major interaction hub. Thus we initially expected clathrin not to be recruited to membranes in presence of Pitstop®-2. Yet, immunofluorescence staining showed no alterations ins distribution of endogenous clathrin after incubation with 60 µM Pitstop®-2 compared to DMSO (0.2 %) treated cells in either spinning disc confocal microscopy (Figure 6.7A) or TIRF microscopy (Figure 6.7B).

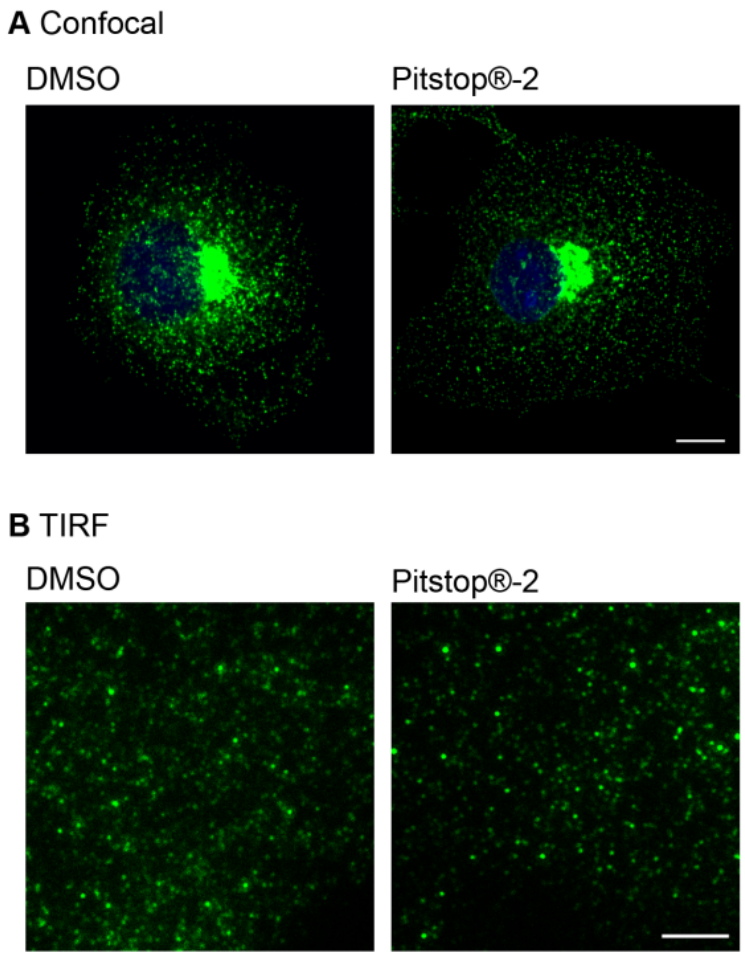

Figure 6.7 Pitstop®-2 does not affect the distribution of endogenous clathrin HC. HeLa cells were incubated with 0.2 % DMSO or 60 µM Pitstop®-2 and then stained with a specific antibody against clathrin HC. Normal distribution of endogenous clathrin was observed in images acquired with spinning disc confocal microscopy (A; scale bar, 10 µm) or TIRF microscopy (B; scale bar, 5 µm).

It was recently suggested that the clathrin terminal domain harbors four interaction sites. Only simultaneous mutation of all four interactions sites resulted in loss of clathrin recruitment (Willox and Royle, 2012). According to X-ray crystallography data, Pitstop®-2 occupies the clathrin box binding site, and there are hints that it might additionally bind with reduced affinity to a second site, the a2L site (Haydar Bulut, not shown). Thus we wanted to investigate whether clathrin TD domain interactions are required for clathrin recruitment to the plasma membrane or the TGN. We depleted COS-7 cells of endogenous clathrin using siRNA designed against clathrin HC. Efficient depletion was confirmed by staining for endogenous clathrin in knockdown cells and knockdown cells overexpressing empty vector. Then we overexpressed vector containing siRNA resistant clathrin HC wildtype (CHC WT), clathrin HC with an inactive clathrin box interaction site (CHC R64A Q89M F91A), or clathrin HC lacking the terminal domain (CHC ΔTD). Immunofluorescence staining of these cells for clathrin HC revealed that clathrin distribution after mutant overexpression was indistinguishable from untreated control cells (Figure 6.8). This indicates that the terminal domain is dispensable for clathrin recruitment.

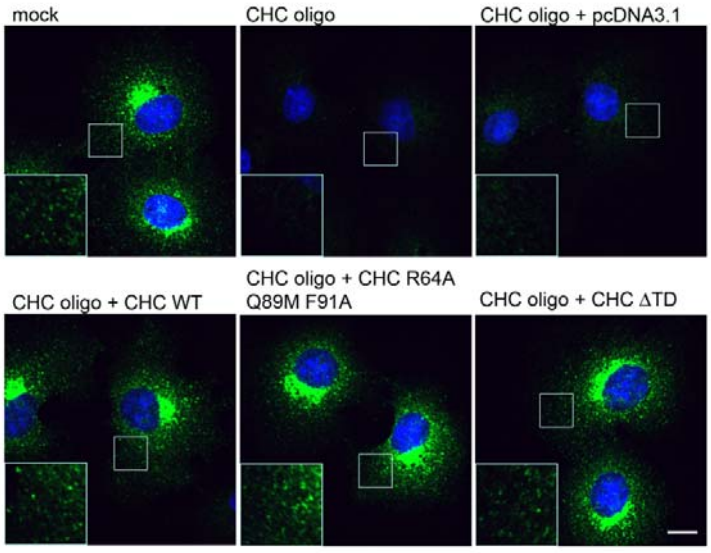

Figure 6.8 The clathrin terminal domain is dispensable for clathrin recruitment. Images represent immunofluorescence staining with clathrin HC antibody in COS-7 cells depleted of endogenous clathrin HC. Clathrin knockdown cells or cells overexpressing empty pcDNA3.1 vector hardly showed clathrin staining. Overexpression of CHC WT, CHC with inactive clathrin box binding site (CHC R64A Q89M F91A) or CHC lacking the terminal domain (CHC ΔTD) resulted in a localization pattern indistinguishable from that of endogenous clathrin. Scale bar, 10 µm. (Modified from von Kleist et al., 2011)

6.3.2 Clathrin is Recruited to the Plasma Membrane in Newly Forming CCPs in Presence of Pitstop®-2

To investigate whether Pitstop®-2 only inhibits exchange of clathrin in pre-existing CCPs we additionally investigated their de novo formation at the plasma membrane. In presence of primary alcohols $PI(4,5)P_2$ synthesis is inhibited resulting in an acute decrease of cellular $PI(4,5)P_2$ levels. This leads to loss of CCPs from the plasma membrane within minutes. Upon removal of the alcohol, CCPs reappear (Boucrot et al., 2006). We incubated cells in presence of 2 % 1-butanol together with 30 µM Pitstop®-2 or 0.1 % DMSO for 5 min. This resulted in a loss of CCPs in both conditions. Then the 1-butanol was removed by exchange of imaging buffer supplemented with DMSO or Pitstop®-2 to allow CCP de novo formation. Three minutes after removal of the alcohol newly formed CCPs could be observed in control cells as well as in presence of inhibitor (Figure 6.9) demonstrating that clathrin terminal domain interactions are not required for CCP de novo formation and clathrin recruitment to the plasma membrane.

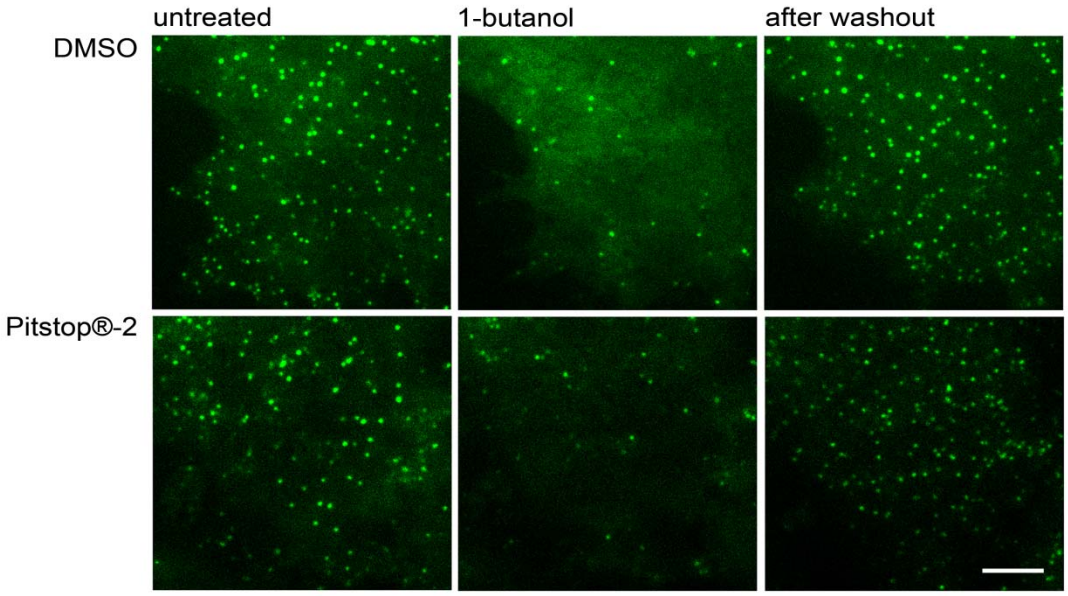

Figure 6.9 Pitstop®-2 does not interfere with de novo clathrin-coated pit formation. TIRF microscopy of COS-7 cells stably expressing clathrin LC-eGFP. Cells were incubated in imaging buffer supplemented with 2 % 1-butanol in presence of 30 µM Pitstop®-2 or 0.1 % DMSO to deplete clathrin coated pits from the plasma membrane. After 5 min the medium was exchanged to remove the 1-butanol. Formation of new clathrin coated pits occurred in presence of DMSO and Pitstop®-2. Scale bar, 2 µm. (Modified from von Kleist et al., 2011)

6.3.3 Distribution of Endocytic Proteins

To investigate the effects of clathrin terminal domain interactions on the recruitment of various CCP components harboring a clathrin box, we incubated COS-7 cells for 15 min with 60 µM Pitstop®-2 and stained them with specific antibodies against AP-2, FCHo, intersectin, and dynamin together with clathrin. TIRF images of the cells reveal that distribution is unchanged for either of the proteins (Figure 6.10A). The colocalization between clathrin and the indicated proteins, quantified using Pearson's correlations is not significantly altered in presence of Pitstop®-2 (Figure 6.10B).

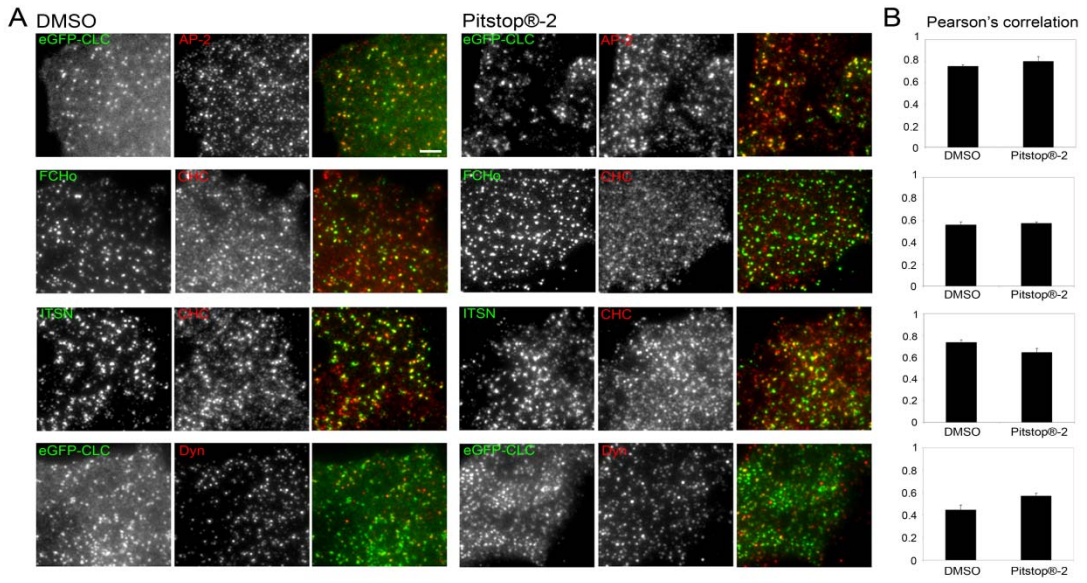

Figure 6.10 Pitstop®-2 does not alter the localization of clathrin-coated pit components. (A) COS-7 cells were treated with 60 µM Pitstop®-2 or 0.2 % DMSO, stained with antibodies against the indicated proteins and imaged using TIRF microscopy. The images reveal no differences in the localization pattern of the indicated proteins. Scale bar, 2 µm. (B) Shown are quantifications of the colocalization between the proteins in (A). The graphs represent the Pearson's correlations (SEM, differences not significant). (Modified from von Kleist et al., 2011)

Only two endocytic proteins tested displayed altered distributions. The BAR protein amphiphysin was partially depleted from the plasma membrane (Lisa von Kleist, (von Kleist et al., 2011)). Meanwhile, immunofluorescence staining of SNX9 revealed that incubation with 60 µM Pitstop®-2 induces cluster formation of SNX9 (Figure 6.11A). Quantitative analysis of the size of SNX9 positive puncta showed an increase in the mean area from 30 px to 67 px (Figure 6.11B). Supersized SNX9 clusters were defined

by an area of at least 90 px which correspond to a threefold increase of cluster area to the average size in control cells. The relative fraction of supersized SNX9 clusters is 5 % of total SNX9 puncta in DMSO treated cells. In presence of Pitstop®-2 the fraction of supersized clusters is increased to 19 % (Figure 6.11C). No significant difference in colocalization quantified by Pearson's correlation could be detected (Figure 6.11D). This is in agreement with a study showing that SNX9 fluorescence at the CCP peaks after scission (Taylor et al., 2011). In presence of Pitstop®-2 scission of the frozen and not maturing CCP is prevented resulting in SNX9 accumulation on the stalled CCP.

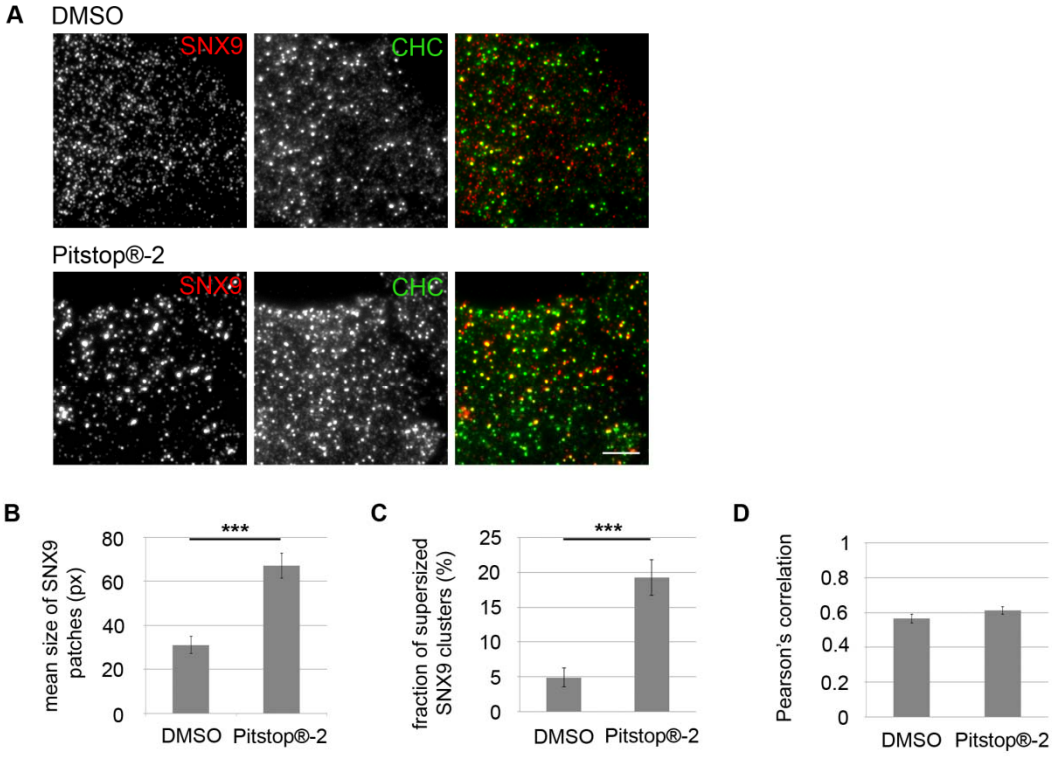

Figure 6.11 Pitstop®-2 induces cluster formation of SNX9. (A) TIRF microscopy of HeLa cells fixed after incubation with 0.2 % DMSO or 60 µM Pitstop®-2 and labeled with antibodies against clathrin HC and SNX9 revealed that SNX9 clusters in presence of Pitstop®-2. Scale bar, 5 µm. (B) Quantification of the size of the patches showed a significant enlargement of the mean area of SNX9 clusters in presence of Pitstop®-2 (SEM, *** $p < 0.0001$). (C) Data are shown as the relative fraction of supersized SNX9 clusters, defined by an area more than threefold above average size. (SEM, *** $p < 0.0001$). (D) Depicted is the Pearson's correlation coefficient between SNX9 and clathrin (SEM, not significant). (Modified from von Kleist et al., 2011)

6.3.4 Distribution of Endosomal and TGN-Localized Proteins

Clathrin is not only involved in CME but also in trafficking from endosomes and the TGN. Therefore we analyzed the effects of inhibition of clathrin terminal domain interactions on the distribution of several endosomal and TGN-localized marker proteins by spinning disc confocal micrsocopy. We incubated COS-7 cells for 15 min with 60 µM Pitstop®-2 or 0.2 % DMSO and subsequently stained them with specific antibodies against the TGN and endosomal marker proteins Gadkin, EEA1, mannose 6-phosphate receptor (MPR), TGN46, AP-1, and CD63. No change of the distribution was detected in presence of Pitstop®-2 (Figure 6.12A). The Pearson's correlations used to quantify the colocalization between indicated proteins were not significantly altered (Figure 6.12B).

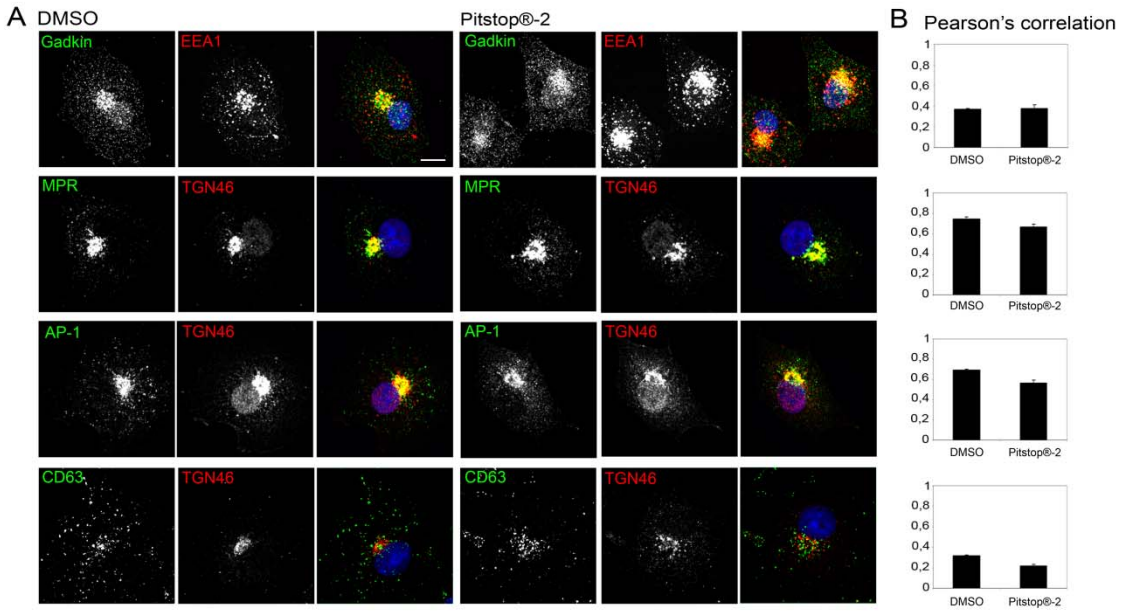

Figure 6.12 Pitstop®-2 does not alter the localization of endosomal and TGN-localized proteins. (A) Immunofluorescence labeling with specific antibodies against the indicated proteins revealed that treatment with 60 µM Pitstop®-2 did not change the localization pattern of intracellular marker proteins compared to 0.2 % DMSO treated cells. Samples were imaged using spinning disc confocal microscopy. Scale bar, 10 µm. (B) Shown are quantifications of the experiments in (A). The graphs represent the colocalization quantified using Pearson's correlations. No significant difference could be observed in presence of Pitstop®-2 compared to DMSO (SEM, differences not significant). (Modified from von Kleist et al., 2011)

6.3.5 Recruitment of Adaptor Proteins to Membranes

With immunofluorescence stainings we did not detect differences in adaptor protein localization in presence of Pitstop®-2. To confirm biochemically, whether adaptor protein recruitment to membranes is affected in presence of inhibitor, we performed a cytosol-membrane fractionation of HeLa cells depleted of endogenous clathrin or treated with Pitstop®-2 for 20 min at 37°C. Next, total cell lysates, lysates of a cytosolic fraction and a membrane fraction were prepared and analyzed in western blot analysis. Total cell lysates (TCL) showed efficient clathrin HC knockdown (Figure 6.13). As expected the distribution of the adaptor proteins AP-1, AP-2, and AP-3 to cytosol or membrane was not altered in absence of clathrin HC or in presence of Pitstop®-2 compared to DMSO treated cells (Figure 6.13). This confirms the immunofluorescence results (Figure 6.10, Figure 6.12) showing that the clathrin TD is not required for recruitment and stabilization of adaptor proteins to membranes.

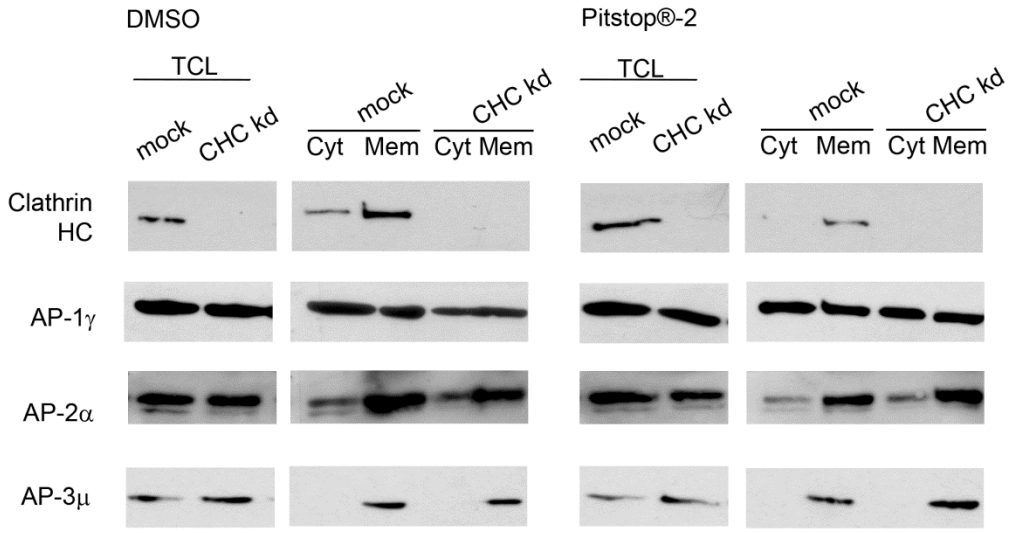

Figure 6.13 Pitstop®-2 has no effect on membrane recruitment of adaptor proteins. Western blots of total cell lysates (TCL), the cytosol and membrane fractions from HeLa cells are shown. There was no difference in membrane recruitment of adaptor proteins in cells depleted of endogenous clathrin HC or control cells (mock). The presence of Pitstop®-2 had no additional effect on protein distribution (n=3 independent experiments). (Modified from Stahlschmidt et al., 2014)

6.4 Clathrin Dynamics

6.4.1 Clathrin-Caoted Pit Dynamics at the Plasma Membrane

Even though clathrin-dependent functions such as CME was inhibited in presence of Pitstop®-2, no effect on distribution of the CME machinery could be detected. Therefore, we studied clathrin dynamics in live COS-7 cells stably expressing clathrin light chain (LC) fused to EGFP (clathrin LC-EGFP). The cells were incubated in presence of 30 µM Pitstop®-2 or 0.1 % DMSO for 5 min, then time lapse movies of 2 min with a framerate of 2 seconds / frame were acquired using TIRF microscopy. In control cells, clathrin LC-EGFP is located in highly dynamic clathrin coated pits, most of them with a liftetime of 26-89 seconds, comparable to previous reports (Ehrlich et al., 2004; Loerke et al., 2009). A smaller fraction of long lived structures which might correspond to clathrin coated plaques exhibited a lifetime of more than 90 s (Saffarian et al., 2009). Pitstop®-2 treatment dramatically increased the lifetime of clathrin coated pits, visualized in kymographs which represent clathrin dynamics over the entire time lapse movie (Figure 6.14A). Quantification of the lifetime of CCPs clearly shows a reduction in the presumably productive fraction (26-89 s) (Loerke et al., 2009) and a strong increase in the fraction of immobile CCPs with a lifetime of 120 s or longer (Figure 6.14B, C). Simultaneously, a lower fluorescence of clathrin LC-EGFP fluorescence was observed, probably due to enhanced bleaching of the stalled clathrin puncta at the plasma membrane (Figure 6.14D). Meanwhile, No increase in clathrin coated plaque number could be observed by electron microscopy (Dmytro Puchkov, (von Kleist et al., 2011)). This confirms that inhibition of clathrin TD-ligand interactions freezes CCPs at their current state and prevents further maturation.

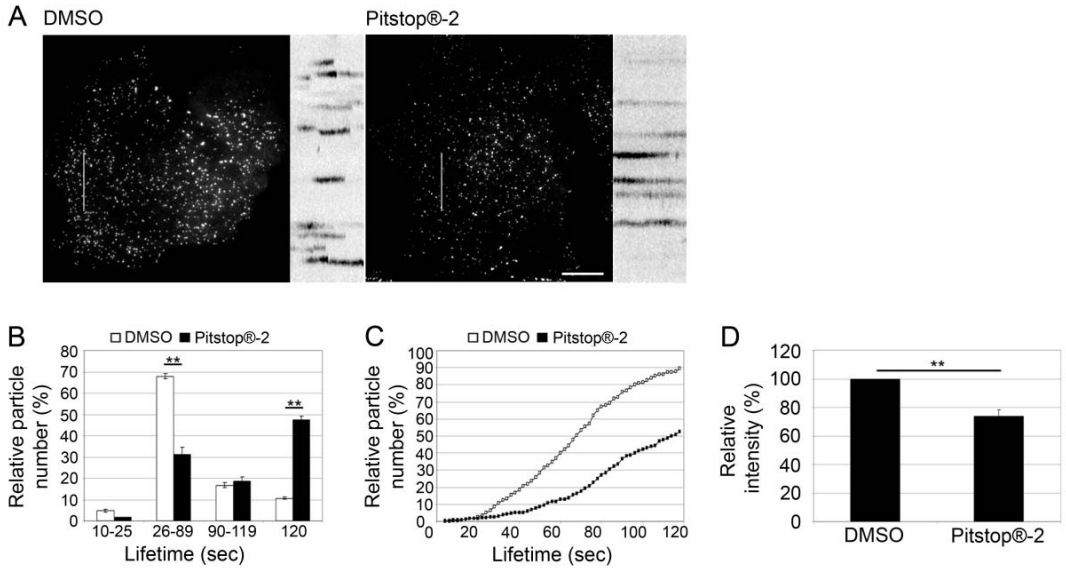

Figure 6.14 Pitstop®-2 freezes the dynamics of clathrin. (A) Live cell TIRF microscopy of COS-7 cells stably expressing LC-eGFP demonstrated that the localization pattern of clathrin is not altered after 5 min preincubation with Pitstop®-2 compared to treatment with DMSO. Kymographs representing the movement of clathrin (2 min, 2 seconds / frame) revealed a decrease in mobility in presence of Pitstop®-2. Scale bar, 10 µm. (B) Shown are the pooled lifetime distributions from the experiments depicted in (A). The values reflect the time between appearance and disappearance of clathrin puncta (n=2 independent experiments, ** $p < 0.001$). (C) Cumulative plot of clathrin lifetime distributions shown in (B). (D) Quantification of the clathrin intensity in presence of Pitstop®-2 normalized to control cells treated with 0.1 % DMSO (n=3 independent experiments, ** $p < 0.001$). (Modified from von Kleist et al., 2011)

6.4.2 Clathrin Exchange in Clathrin-Coated Pits at the Plasma Membrane

In order to investigate whether clathrin LC-EGFP is still exchanged in the immobile CCP, we performed FRAP (fluorescence recovery after photobleaching) experiments using a spinning disc confocal microscope. Live cells stably expressing clathrin LC-EGFP were incubated with 30 µM Pitstop®-2 or 0.1 % DMSO. Clathrin fluorescence was bleached in a region of interest in the cell periphery to mainly bleach CCPs at the plasma membrane but not at the TGN, followed by acquisition for two more minutes (framerate 2 seconds / frame). Control cells showed a fast recovery of fluorescence within two minutes. This is not only due to new formation of CCPs after membrane clearance by internalization but also to exchange of clathrin molecules in existing CCPs. CCPs in Pitstop®-2 treated cells did not recover within two minutes after bleaching demonstrating that clathrin is not exchanged in the frozen CCPs (Figure

6.15A). The quantification of CCP intensities shows that control cells recovered with a half time of approximately 25 seconds, while no recovery was measured in presence of inhibitor (Figure 6.15B). This confirms the role of the clathrin TD in regulating CCP dynamics.

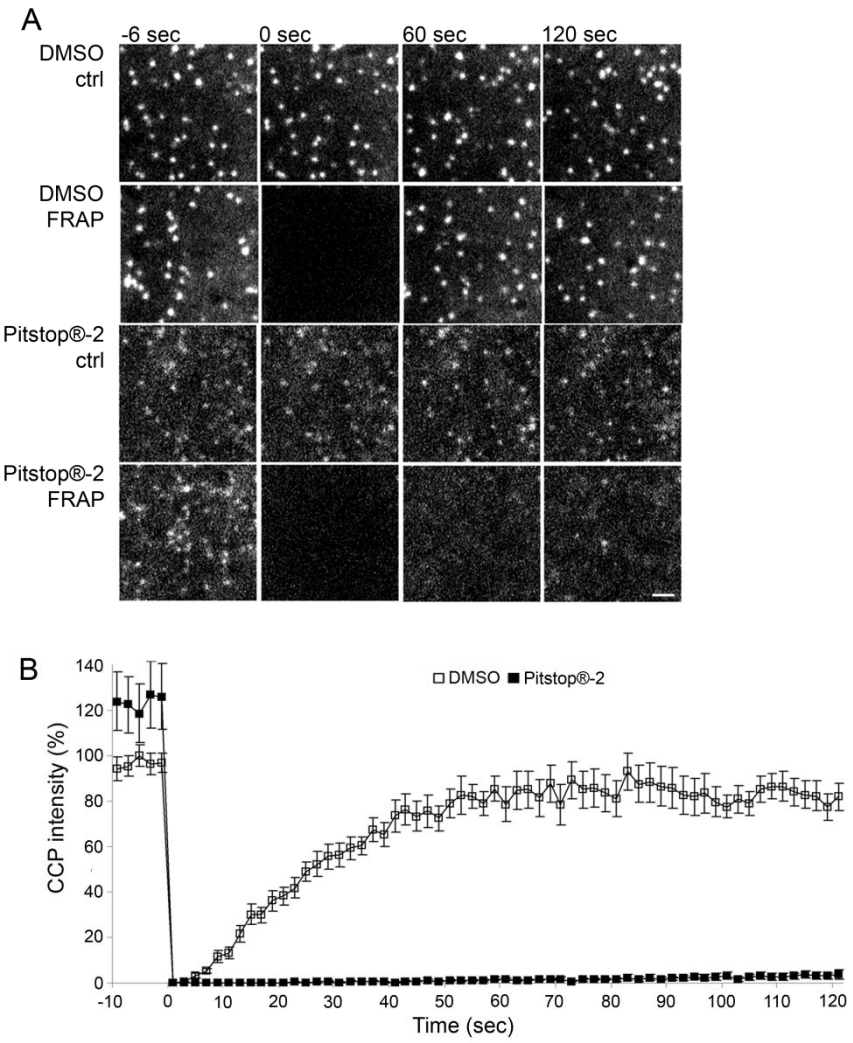

Figure 6.15 Pitstop®-2 inhibits the exchange of clathrin at the plasma membrane. (A) Fluorescence recovery after photobleaching (FRAP) of clathrin LC-eGFP in cells imaged after 5 min preincubation with 30 µM Pitstop®-2 or 0.1 % DMSO. Cells were imaged with a spinning disc confocal microscope at a rate of 2 seconds / frame, starting 10 seconds before bleaching, followed by 2 min acquisition after bleaching. Representative images of the FRAP region and an unbleached control area before bleaching (-6 seconds) and 0 seconds, 60 seconds and 120 seconds after bleaching are shown. Clathrin LC-eGFP fluorescence recovers in control cells, but not in presence of Pitstop®-2. Scale bar, 2 µm. (B) The quantification shows corrected fluorescence intensities in the bleached area over time (SEM, n = 3 independent experiments). (Modified from von Kleist et al., 2011)

6.4.3 Pitstop®-2 Inhibits the Exchange of Intracellular Clathrin Populations

In addition to its role in CME, clathrin can be found on endosomes and at the TGN, where it functions in intracellular trafficking and secretion. To investigate, whether Pitstop®-2 affects the exchange of intracellular clathrin populations as observed at the plasma membrane, we overexpressed clathrin LC fused to the photoswitchable fluorescent protein Kaede in HeLa cells. Exposure of Kaede to UV light (using the 405 nm laser line) causes irreversible photoswitching from green to red fluorescence (Ando et al., 2002). We used this property to specifically convert the fluorescence of the clathrin population located at the TGN. Immediately after photoconversion, intense red fluorescence can be seen in the converted area, while the green fluorescence is strongly reduced in presence of either Pitstop®-2 or DMSO. Green fluorescence was seen to partially recover at the TGN within three minutes after photoconversion in cells treated with DMSO only (Figure 6.16A, C) due to exchange with non-photoconverted clathrin molecules from the surrounding cytosolic area. In Pitstop®-2 treated cells recovery of fluorescence did not occur indicating inhibited exchange of clathrin molecules (Figure 6.16B, C). An exchange of different clathrin populations should result in intermixing of the green and red clathrin populations over time and increase their colocalization. In control cells, colocalization of the different clathrin populations could be observed at the TGN or at endosomes three minutes after photoconversion (Figure 6.16A, arrowheads). Hardly any colocalization was detected in presence of Pitstop®-2 (Figure 6.16B, arrowheads). Determination of the increase of the Pearson's correlations compared to t = 0 min after photoconversion confirms intermixing of the two clathrin populations in cells treated with DMSO or inactive control compound (Pitnot-2). In contrast, Pitstop®-2 treatment shows a significantly reduced increase in colocalization (Figure 6.16D). This demonstrates that Pitstop®-2 freezes the dynamics of clathrin on intracellular membranes to a similar degree as on the plasma membrane, and thus confirms the role of clathrin TD interactions in their dynamic regulation.

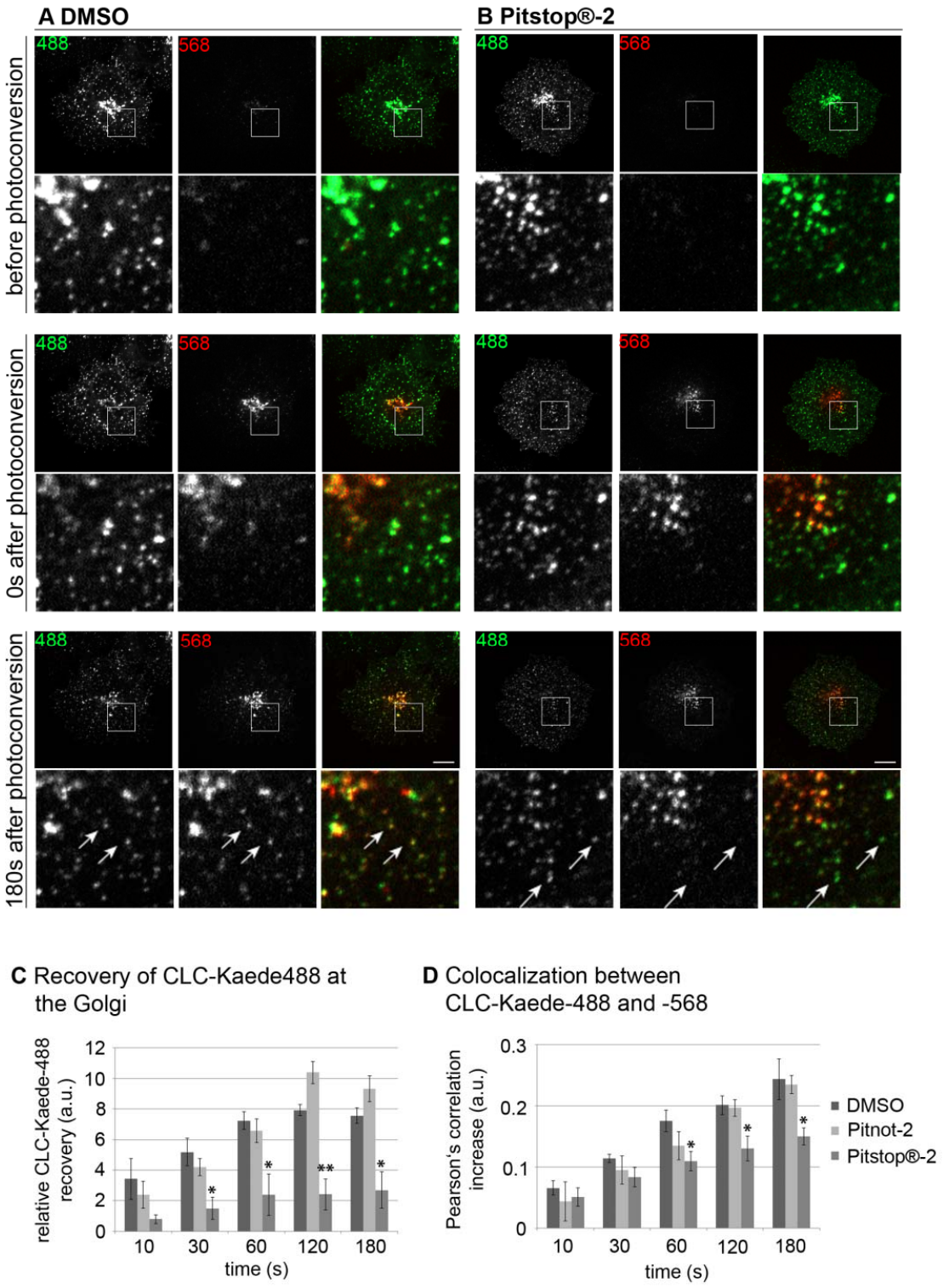

Figure 6.16 Pitstop®-2 inhibits exchange between the TGN and endosomal clathrin populations. (A, B) Before photoconversion Clathrin LC-Kaede overexpressed in HeLa cells is visible in the green channel. Photoconversion of CLC-Kaede in a defined region of interest with the 405 nm laser line leads to fluorescence in the red channel in the converted area. 180 seconds after photoconversion of the TGN a mixing of the two Clathrin LC populations was observed in cells incubated with 0.1% DMSO (A, arrowheads), but not after treatment with 30

μM Pitstop®-2 (B). Scale bar, 10 μm. (C) Quantification of data (n=3 independent experiments) show the relative recovery with t = 0 min set to zero. (D) The increase in colocalization, indicating mixing of the green and the red population, was reduced after addition of Pitstop®-2 compared to cells incubated in DMSO or Pitnot-2. Values show the Pearson's correlation at the according timepoint subtracted by the Pearson's correlation at t = 0 min (n=3 independent experiments; * $p < 0.05$; ** $p < 0.005$). (Modified from Stahlschmidt et al., 2014)

6.5 Dynamics of Adaptor Proteins in Presence of Pitstop®-2

6.5.1 AP-2

After investigation of the effects of Pitstop®-2 on clathrin dynamics, we analyzed the behavior of adaptor proteins. AP-2 recruitment to the plasma membrane is initiated by early-acting CCP components such as FCHo and intersectin which subsequently drives clathrin recruitment (Henne et al., 2010; Pechstein et al., 2010). In order to investigate the effects of inhibition of clathrin TD-ligand interactions on AP-2 dynamics, we preincubated live 3T3 cells stably expressing AP-2 σ2-EGFP with 30 μM Pitstop®-2 or 0.1 % DMSO as a control for 5 min. Then time lapse series were acquired at 37°C for 2 min with a framerate of 2 seconds / frame using a TIRF microscope. In presence of Pitstop®-2 the mobility of σ2-EGFP was decreased, yet not to the degree clathrin LC-eGFP mobility was affected (Figure 6.17A). Quantification reveals that the fraction of σ2-EGFP with a lifetime up to 89 s was reduced while there was an increase in long lived fractions with a lifetime of 90 s or longer (Kira Gromova, Figure 6.17B, C). Depletion of clathrin HC mimics the effect of Pitstop®-2 on σ2-EGFP mobility at the plasma membrane. In presence of Pitstop®-2 σ2-EGFP mobility is not further decreased in clathrin HC knockdown cells (Figure 6.17D).

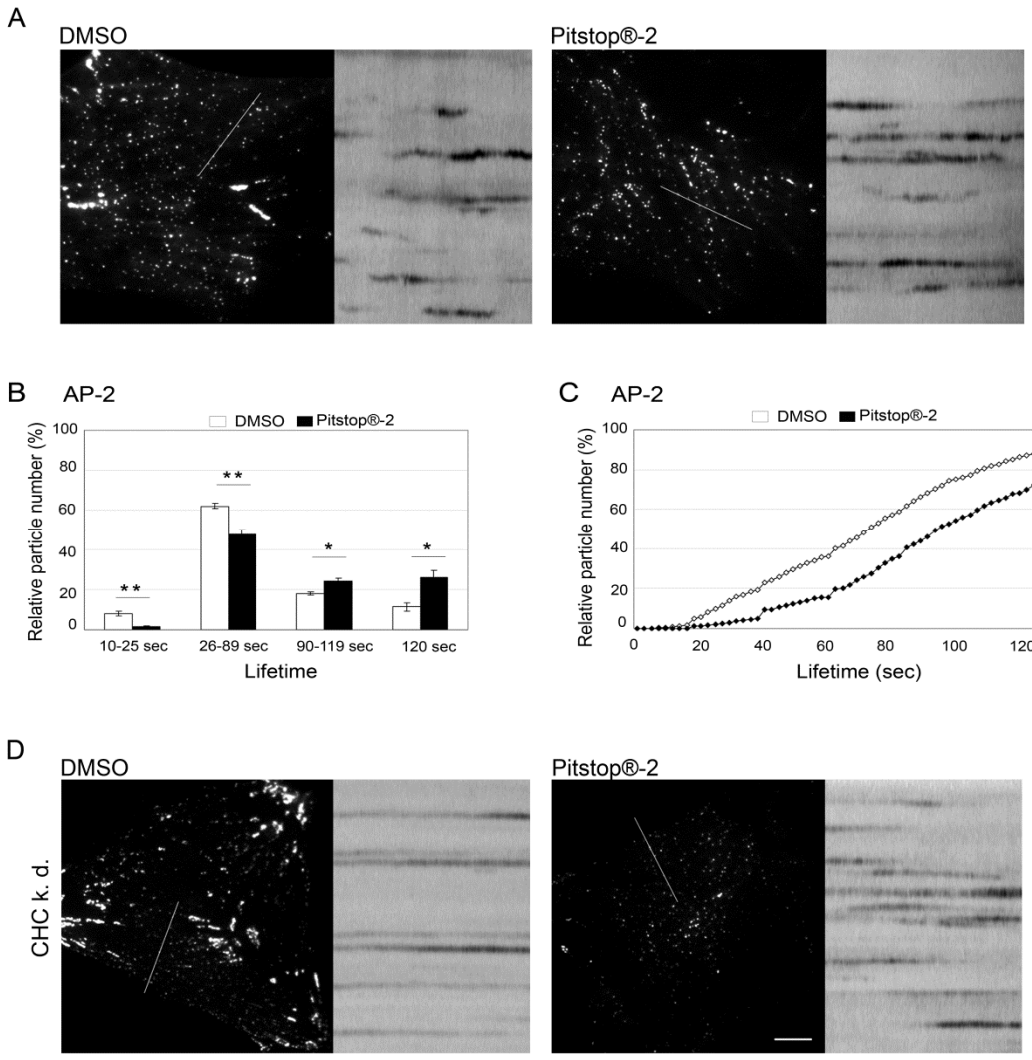

Figure 6.17 Pitstop®-2 decreases AP-2 dynamics. (A) Live cell TIRF microscopy of 3T3 cells stably expressing AP-2 σ2-EGFP demonstrates that incubation with 30 µM Pitstop®-2 decreased AP-2 mobility compared to DMSO (0.1 %) treatment. Kymographs represent the movement of AP-2 (2 min, 2 seconds / frame). Scale bar, 10 µm. (B) Shown are the pooled lifetime distributions of AP-2 in mock (0.1 % DMSO) or Pitstop®-2 treated cells (30 µM). The values reflect the time between appearance and disappearance of AP-2 puncta (SEM, n=3 independent experiments, * $p < 0.05$, ** $p < 0.001$). (C) Cumulative plot of AP-2 lifetime distributions shown in (B). (D) Clathrin HC was depleted in cells stably expressing σ2-EGFP. The kymographs demonstrate that σ2-EGFP dynamics were slowed down in absence of clathrin HC. Additional incubation with 30 µM Pitstop®-2 did not further decrease AP-2 mobility. Scale bar, 10 µm. (Modified from von Kleist et al., 2011)

6.5.2 AP-1

To investigate the effect of Pitstop®-2 on AP-1 dynamics, live BSC-1 cells stably expressing the EGFP tagged AP-1 σ1 subunit (EGFP-σ1) (Anitei et al., 2010) were imaged using spinning disc confocal microscopy. 5 min after addition of 30 µM Pitstop®-2 or 0.1 % DMSO, time lapse series of 2 minutes with a frame rate of 0.5 Hz were acquired. In control cells AP-1 displays a highly dynamic behavior (Kural et al., 2012). Incubation with inhibitor had no obvious effect on AP-1 distribution but freezes the dynamics of EGFP-σ1 positive endosomes (Figure 6.18B) compared to control cells (Figure 6.18A) as displayed in kymographs.

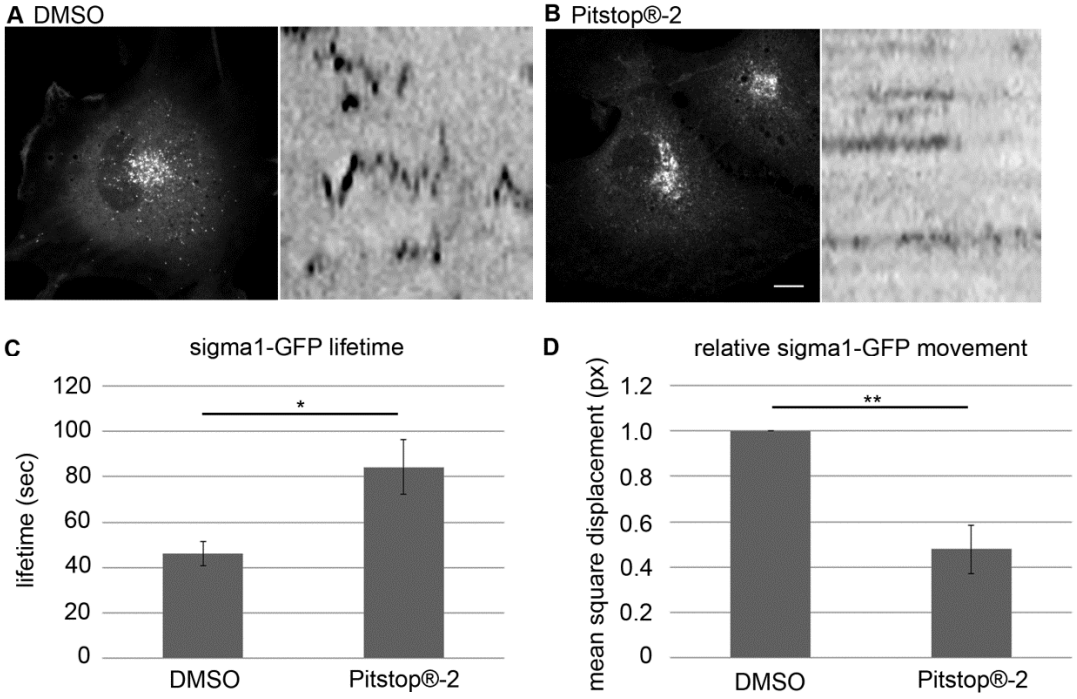

Figure 6.18 Pitstop®-2 reduces AP-1 dynamics. Live-cell confocal imaging acquired in BSC-1 cells stably expressing AP-1 EGFP-σ1 showed that 30 µM Pitstop®-2 (B) addition led to deceleration of AP-1 dynamics compared to treatment with 0.1 % DMSO (A). The kymographs represent the complete time-lapse series obtained with confocal microscopy (2 minutes exposures, 2 seconds per frame). Scale bar 10 µm. (C, D) The plots display the increased lifetime per second (C) and the decreased relative movement per frame (D) of EGFP-σ1 positive structures (SEM, n=3 independent experiments; * $p < 0.05$; ** $p < 0.005$). (Modified from Stahlschmidt et al., 2014)

Quantification of the mean lifetime of EGFP-σ1 positive structures revealed a significant increase from 46 seconds to 84 seconds in presence of Pitstop®-2 (Figure 6.18C). Moreover, the movement reflected by the mean square displacement of the individual σ1-EGFP puncta was reduced from an average of 124 nm per second to 54 nm per second in Pitstop®-2 versus DMSO treated cells, which corresponds to a reduction of velocity to 47.7% compared to control cells (Figure 6.18D).

Additionally we investigated the effect of clathrin HC depletion on EGFP-σ1 mobility. Loss of clathrin leads to a partial redistribution of AP-1 towards the periphery of the cell and an increase in the occurrence of tubule formation from the TGN. Surprisingly the σ1-EGFP puncta were still mobile in knockdown cells (Figure 6.19A left). Western blot analysis of total cell lysates or quantification of immunofluorescence of clathrin knockdown cells (not shown) displayed efficient clathrin depletion with less than 10 % of the remaining protein compared to control cells (Figure 6.19B). We analyzed the distribution of endogenous clathrin and AP-1 by spinning disc confocal microscopy to test whether the remaining amount of clathrin was still associated with AP-1 coated carriers. Even though clathrin expression was strongly reduced in knockdown cells, enhancement of clathrin fluorescence intensity revealed a localization pattern comparable to mock cells (Figure 6.19C). We applied 30 µM Pitstop to clathrin HC knockdown cells to investigate whether the remaining clathrin coated AP-1 carriers remained sensitive to Pitstop®-2. Lifetime and mobility of AP-1 positive puncta was decreased to a degree comparable to Pitstop®-2 addition to mock cells (Figure 6.19A right). Altogether this suggests that only a small amount of clathrin is necessary for AP-1 mobility, but mobility strictly requires a functional clathrin terminal domain.

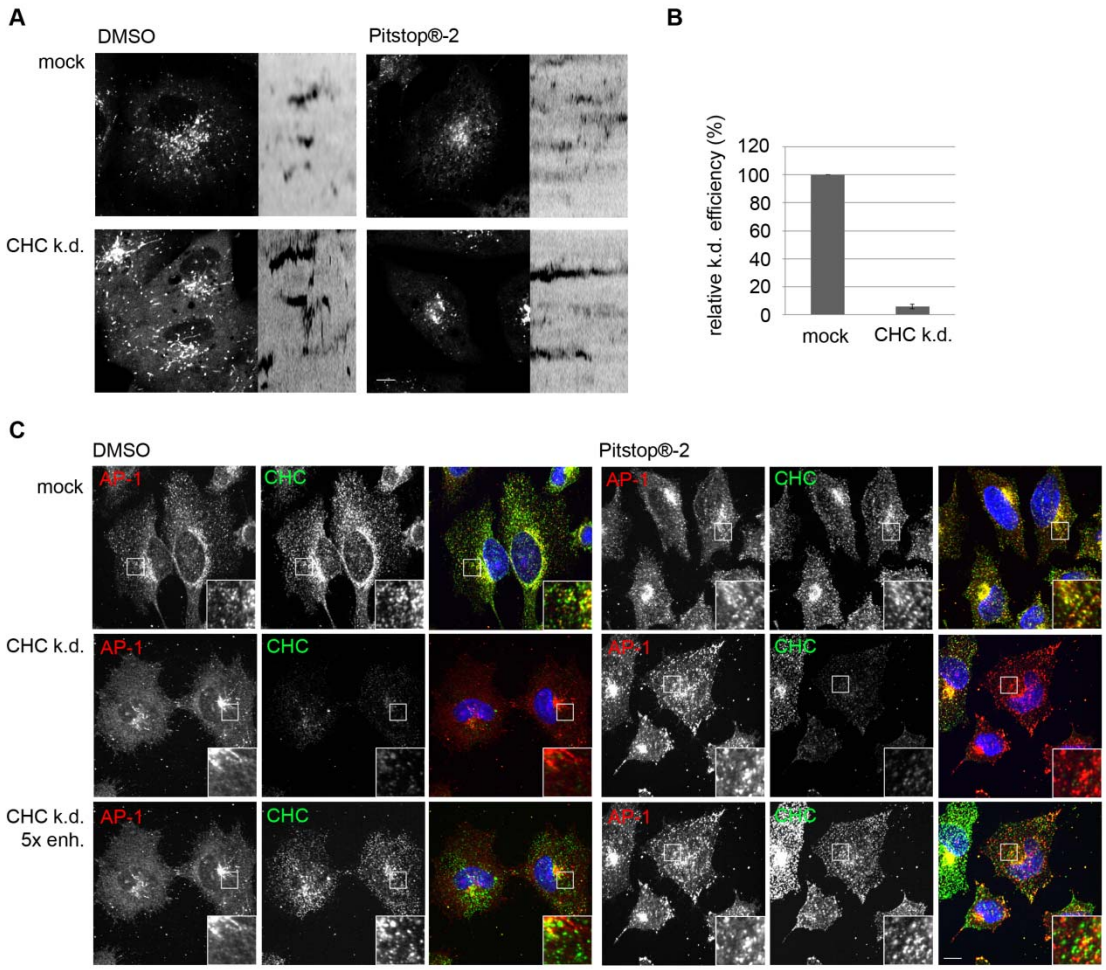

Figure 6.19 Clathrin knockdown cells are still Pitstop®-2 sensitive. (A) Live-cell confocal imaging of BSC-1 cells stably expressing AP-1 EGFP-σ1 was used to acquire time-lapse series of mock cells or after clathrin HC depletion. Images were collected for 2 min at 37°C in the presence of 30 µM Pitstop®-2 or DMSO (0.1 %). Each image corresponds to the first frame of data collection. The kymographs represent the complete time-lapse (2 min exposures, 2 second per frame) and reveal a decrease in EGFP–σ1 mobility. Scale bar, 10 µm. (B) Knockdown efficiency was determined by western blot analysis and quantified using the ImageJ gel analysis tool (n = 3 independent experiments, SEM). (C) siRNA treated and control cells were stained for AP-1(γ) and clathrin HC. The lower panel shows the 5 fold enhanced CHC channel to visualize distribution of the remaining clathrin in knockdown cells which looks unaltered compared to mock cells. Colocalization of AP-1 and clathrin HC is reduced but still visible after image enhancement. Scale bar, 10 µm.

6.5.3 GGAs

The three mammalian GGA proteins are monomeric adaptors, which are additionally to AP-1 associated with clathrin at the TGN and endosomes (reviewed in (Robinson and Bonifacino, 2001)). Therefore we wanted to investigate whether their mobility is affected in presence of Pitstop®-2. We overexpressed GGA1-EGFP, GGA2-EGFP, and GG3-EGFP, respectively in HeLa cells to analyze their mobility by confocal live cell imaging. Kymographs, generated from time lapse series acquired for 2 minutes with a framerate of 0.5 Hz, illustrate that, dynamics of GGA1-EGFP, GGA2-EGFP, or GGA3-EGFP positive structures are decelerated in presence of Pitstop®-2 compared to control cells supplemented with DMSO (Figure 6.20). This demonstrates that a functional clathrin terminal domain is required to regulate the dynamics of GGA proteins similar to AP-1 at endosomes and the TGN.

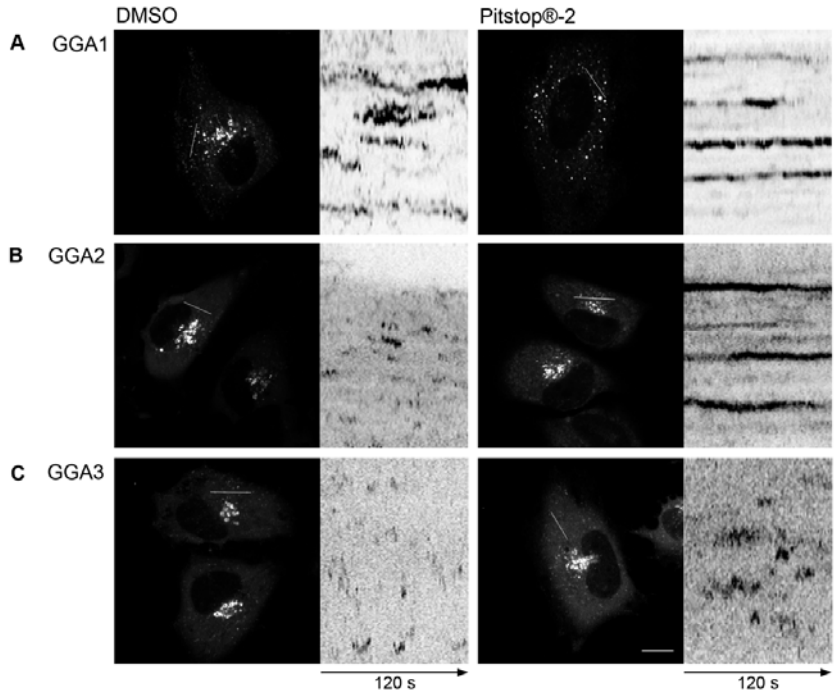

Figure 6.20 Pitstop®-2 decelerates GGA dynamics. Live-cell confocal imaging was acquired of HeLa cells overexpressing GGA1-EGFP, GGA2-EGFP, or GGA3-EGFP, respectively. Time-lapse series were collected for 2 min at 37°C in the presence of 30 µM Pitstop®-2 or DMSO (0.1%). Cellular distribution is not changed after incubation with Pitstop®-2 compared to DMSO treatment, but dynamics of GGA1-EGFP (A), GGA2-EGFP (B), and GGA3-EGFP (C) are strongly decreased in presence of inhibitor. The kymographs represent the complete time-lapse series (2 min exposures, 2 seconds per frame) (scale bar 10 µm, n=3 independent experiments). (Modified from Stahlschmidt et al., 2014)

6.5.4 COP1

So far, it could be shown that Pitstop®-2 decreased the mobility of adaptor proteins interacting with the clathrin terminal domain. To ensure that this is no unspecific effect on dynamics of coated vesicles in general, we investigated the mobility of structurally and functionally related COP1-coated carriers, which traffic between the golgi and the ER. Live cell imaging of the overexpressed COP1 subunit εCOP-EGFP (Ward et al., 2001) was acquired using a confocal microscope with a frame rate of 0.5 Hz. Time lapse series were acquired with a frame rate of 0.5 hertz and the dynamics were compared 5-30 min after addition of 0.1 % DMSO or 30 µM Pitstop®-2. In kymographs, no difference in the mobility of εCOP-EGFP could be observed between cells in presence of DMSO or Pitstop®-2 (Figure 6.21) confirming the specificity of Pitstop®-2 for clathrin dependent trafficking processes.

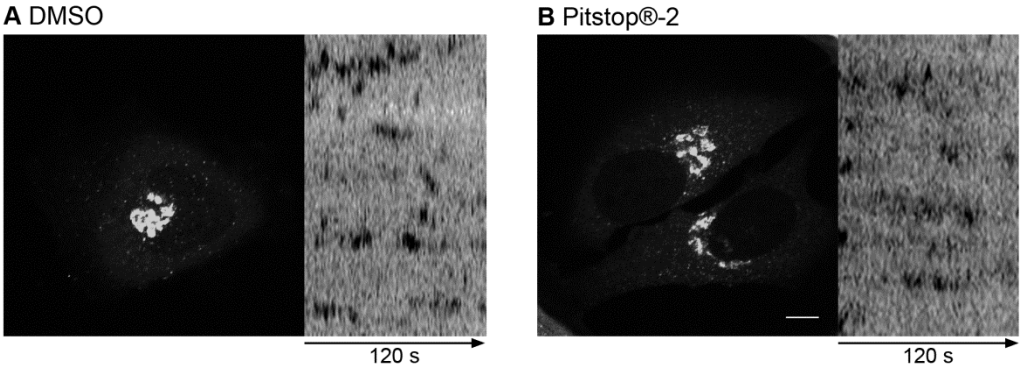

Figure 6.21 Pitstop®-2 has no effect on COP1 dynamics. Live-cell confocal imaging was acquired in HeLa cells overexpressing εCOP-EGFP. Time-lapse series were collected for 2 min at 37°C in the presence of 30 µM Pitstop®-2 (B) or 0.1% DMSO (A). Each image corresponds to the first frame of data collection. The kymographs represent the complete time-lapse series obtained with confocal microscopy (2 min exposures, acquired every second) and reveal that Pitstop®-2 had no effect on COP1 mobility. Scale bar, 10 µm. (Modified from Stahlschmidt et al., 2014)

6.6 Mannose 6-Phosphate Receptor Retrieval to the TGN Requires Clathrin Terminal Domain Function

Mannose 6-phosphate receptor (MPR) sorting of newly synthesized proteins to endosomal and lysosomal compartments is mediated by AP-1 and GGA coated tubular carriers in a clathrin dependent manner (Klumperman et al., 1998; Puertollano et al., 2001; Waguri et al., 2003). Defective retrograde sorting caused by dysfunctional AP-1 results in dispersal of MPRs to the cell periphery (Meyer et al., 2000; Wieffer et al., 2013). We expected acute interference of clathrin terminal domain interactions and thus stalled AP-1 and GGA dynamics to affect MPR sorting in cells. To investigate this we analyzed HeLa cells stably expressing the transmembrane and cytosolic domain of cation independent mannose-6-phosphate receptor fused to GFP (GFP-CI-MPR) (Waguri et al., 2003). Confocal live cell imaging revealed that in control cells GFP-CI-MPR was concentrated in tubular elements at the TGN which frequently detached and moved towards the cell periphery. To investigate the effect of clathrin terminal domain inhibition, we incubated cells with 30 µM Pitstop®-2 and monitored GFP-CI-MPR distribution for up to 90 min. Within 30 min upon Pitstop®-2 addition the GFP-CI-MPR started to lose its integral structure and to disperse to the cell periphery. After 60-90 minutes in presence of inhibitor the former TGN pool of GFP-CI-MPR had scattered into multiple smaller fragments (Figure 6.22A). Quantification shows that interference with clathrin TD function by Pitstop®-2 led to an approximately two-fold increase in the number of GFP-CI-MPR containing fragments within 60-90 min (12.7 ± 1.0 per cell in presence of 0.1 % DMSO, 25.1 ± 2.3 per cell in presence of 30 µM Pitstop®-2; Figure 6.22B). This corresponds to a significant decrease in object size to 40.5% (1.7 ± 0.3 μm^2 in Pitstop®-2- versus 4.2 ± 0.9 μm^2 in DMSO-treated cells; Figure 6.22C).

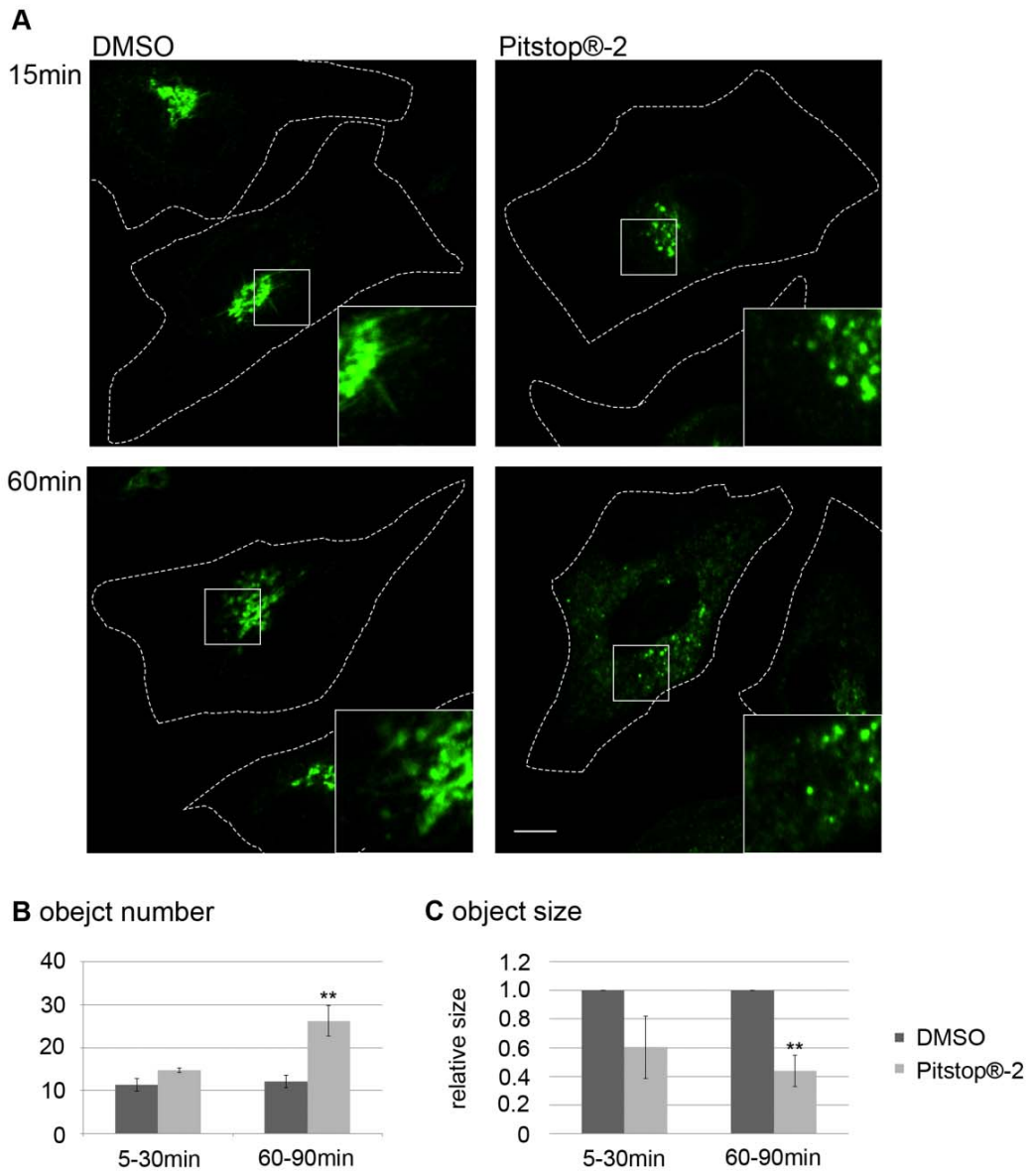

Figure 6.22 Incubation with Pitstop®-2 results in GFP-CI-MPR dispersion. (A) Live cell confocal imaging of HeLa cells stably expressing GFP-CI-MPR revealed GFP-CI-MPR dispersion to endosomal compartments over time after incubation with 30 µM Pitstop®-2, but not in presence of 0.1 % DMSO. Scale bar, 10 µm. (B) The quantifications show a significant increase in the total object number in presence of inhibitor. (C) Accordingly, the size of GFP-CI-MPR positive structures is reduced after Pitstop®-2 treatment. Data is normalized to DMSO (n=3 independent experiments; ** $p < 0.005$). (Modified from Stahlschmidt et al., 2014)

6.7 VSVG Secretion is not Affected in Presence of Pitstop®-2

To exclude unspecific effects of Pitstop®-2 on golgi function resulting in altered GFP-CI-MPR distribution we studied secretion of VSVG (vesicular stomatitis virus G protein) from the golgi complex to the plasma membrane. Therefore we used a temperature sensitive VSVG-SP-GFP fusion protein which was shown to be secreted in a clathrin- and AP-1-independent manner (Hirschberg et al., 1998; Polishchuk et al., 2003). At 39°C VSVG-SP-GFP remains trapped in the ER due to protein misfolding. A temperature drop to 19°C allows correct folding and exit from the ER but retains the protein in the golgi. Finally, a shift to 32°C results in VSVG-SP-GFP exit from the Golgi and secretion to the cell surface in tubular carriers (Hirschberg et al., 1998). After 60 min at 32°C no difference in the distribution pattern could be observed in presence of 30 µM Pitstop®-2 or 0.1 % DMSO (Figure 6.23A). Quantitative analysis of the ratio between VSVG-SP-GFP localized at the TGN and at the plasma membrane showed no significant difference between cells in presence of DMSO and cells incubated with 30 µM Pitnot-2 or 30 µM Pitstop®-2 (Figure 6.23B). This finding confirms that secretion of VSVG is clathrin- and AP-1-independent and thus remains unaffected by Pitstop®-2 treatment, consistent with previous studies (Hirschberg et al., 1998; Polishchuk et al., 2003).

6.8 Transferrin Recycling is Independent of Clathrin Terminal Domain Function

A role for clathrin in endosomal recycling is still debated as clathrin coats have not only been observed at the TGN and the plasma membrane but also on endosomes (Stoorvogel et al., 1996; van Dam and Stoorvogel, 2002). Clathrin is suggested to be involved in polarized sorting to the basolateral surface in epithelial cells (Deborde et al., 2008). Furthermore gyrating clathrin (G-clathrin), a highly dynamic endosomal form of clathrin, has been reported to regulate rapid recycling of transferrin (Zhao and Keen, 2008). Other data suggest that transferrin is localized in EHD1 associated endosomal tubules lacking apparent clathrin coats (Grant and Donaldson, 2009; Jovic et al., 2009). The role of clathrin in transferrin recycling cannot be studied efficiently using genetic approaches or siRNA knockdown as its internalization is strictly clathrin dependent. Therefore Pitstop®-2 can be used as a tool to study recycling of transferrin by acutely blocking clathrin TD-ligand interactions right after transferrin internalization. We loaded HeLa cells with transferrin fluorescently labeled with Alexa488 (tf^{488}) for 30 min,

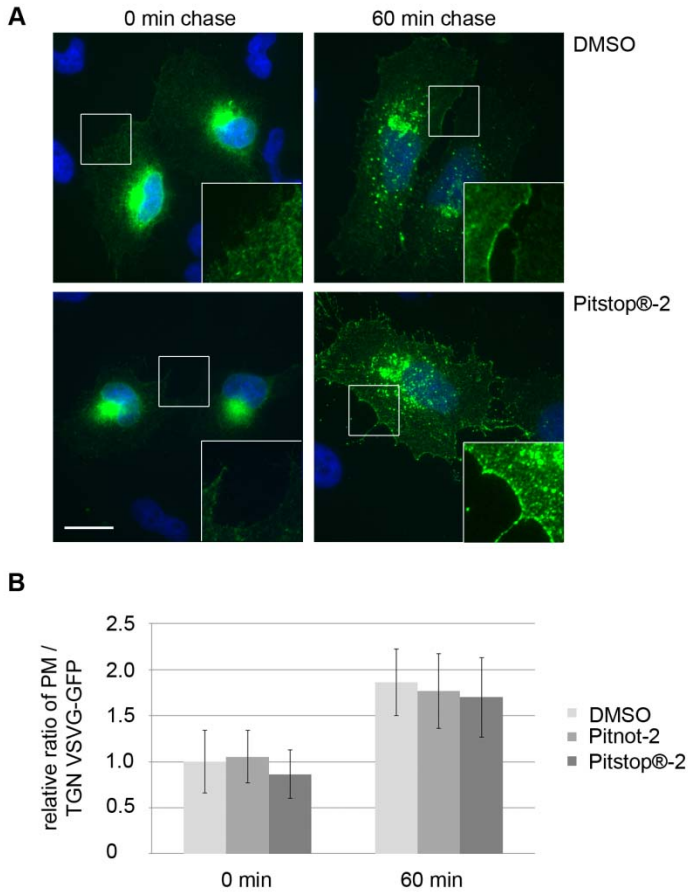

Figure 6.23 VSVG-SP-GFP secretion to the plasma membrane is unaffected by Pitstop®-2. (A) After 60 min incubation at 19°C, VSVG-SP-GFP accumulates in the Golgi. 60 min chase of VSVG-SP-GFP at 32°C leads to secretion to the plasma membrane. No obvious differences of fluorescence distribution can be detected in cells treated with DMSO or Pitstop®-2. Scale bar, 10 µm. Fluorescence intensity in the blow ups were enhanced for better visualization of VSVG-SP-GFP at the plasma membrane. (B) Quantification of the ratio of surface to plasma membrane localized VSVG-SP-GFP reveals that the distribution was not altered in cells treated with DMSO, Pitstop®-2, or Pitnot-2 (n=3 independent experiments, SEM, differences not significant). (Modified from Stahlschmidt et al., 2014)

subsequently allowed tf^{488} recycling in presence of 0.1 % DMSO, 30 µM Pitstop®-2, or 30 µM Pitnot-2, respectively at 37°C. No difference in tf^{488} fluorescence intensity could be observed in cells with or without compound after 0, 7.5, and 15 minutes of recycling (Figure 6.24A). Quantification shows that tf^{488} recycling proceeded unperturbed as fluorescence intensity decreased to the same degree in all conditions (Figure 6.24B). This suggests that clathrin TD domain function is not required for endosomal recycling of transferrin back to the cell surface.

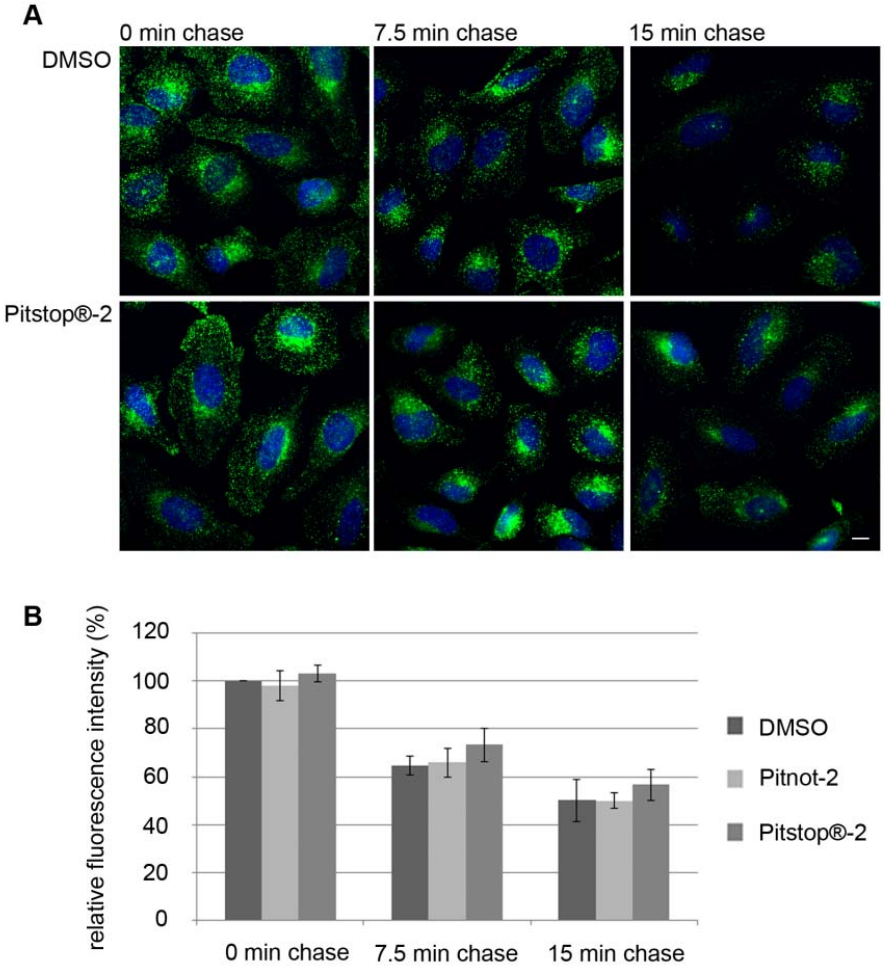

Figure 6.24 Pitstop®-2 does not affect transferrin recycling. (A) After 30 min transferrin uptake, HeLa cells were allowed to recycle tf^{488} for 0 min, 7.5 min, and 15 min at 37°C. Addition of 30 µM Pitstop®-2 or 30 µM Pitnot-2 did not affect transferrin recycling compared to control cells treated with 0.1 % DMSO. Scale bar, 10 µm. (B) The graph shows the quantification of tf^{488} fluorescence intensity after recycling from three independent experiments normalized to the amount of fluorescence in DMSO treated cells after 0 min chase (SEM, differences not significant). (Modified from Stahlschmidt et al., 2014)

6.9 EGFR Degradation is Unaffected in Presence of Pitstop®-2

To further ensure specificity of Pitstop®-2 we investigated whether lysosomal transport, acidification of lysosomes and thus degradation of EGFR might be perturbed in presence of Pitstop®-2. Cells were stimulated with unlabeled EGF 30 minutes prior to the addition of 30 µM Pitstop®-2, 30 µM Pitnot-2 or 0.1 % DMSO. Western Blot analysis reveals that the degradation of EGF receptor proceeds unperturbed in presence of Pitstop®-2 or Pitnot-2 compared to DMSO treated controls (Figure 6.25A, B).

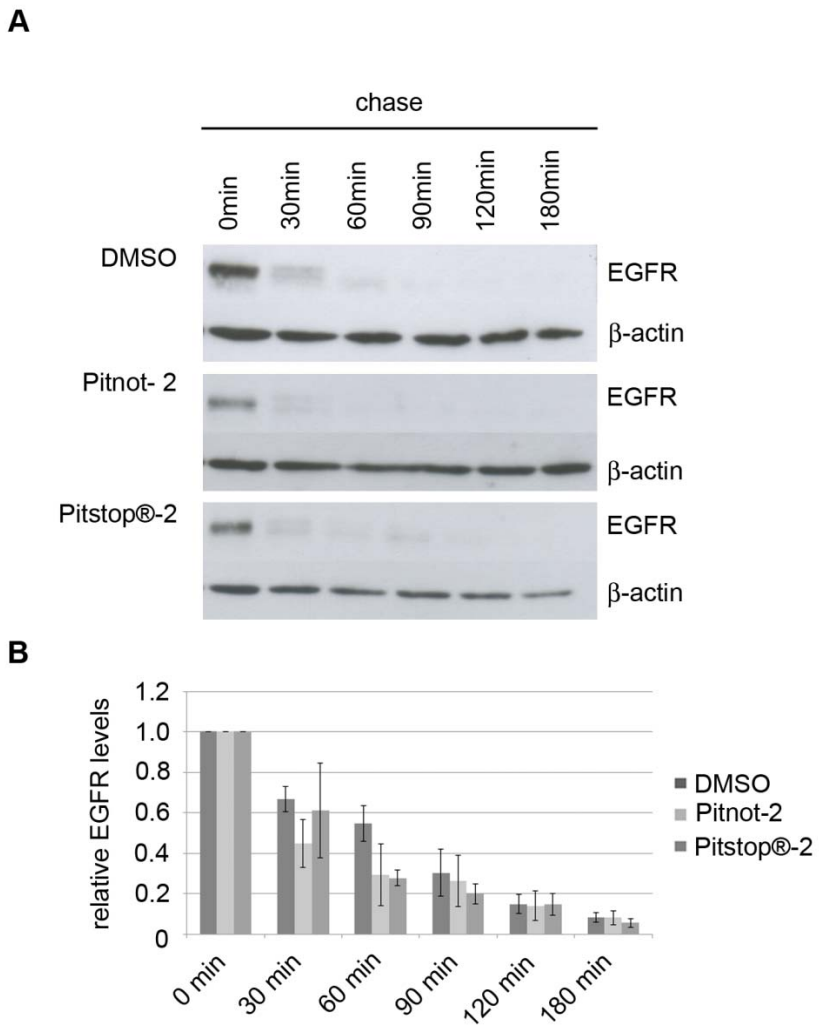

Figure 6.25 EGFR degradation is not affected by Pitstop®-2. (A) 30 µM Pitstop®-2, 30 µM Pitnot-2, or 0.1 % DMSO were added to HeLa cells 30 min after stimulation with 500 ng / ml unlabeled EGF, chased for the indicated timepoints and analyzed in western blot. Compound treatment did not affect EGFR degradation. (B) Three independent experiments were quantified using the ImageJ gel analysis tool (SEM, differences not significant). (Modified from Stahlschmidt et al., 2014)

Likewise, degradation of fluorescently labelled EGF^{647} is not affected in presence of Pitstop®-2 (Figure 6.25C, D). This demonstrates that clathrin TD function is dispensable for degradation of internalized EGFRs or its ligand (Figure 6.26).

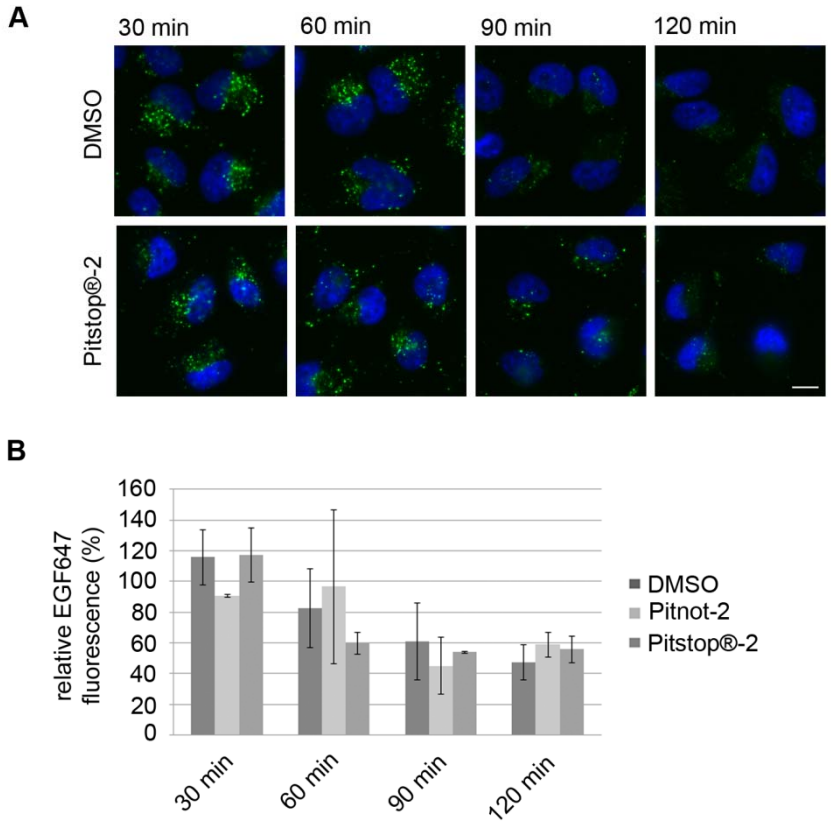

Figure 6.26 Degradation of fluorescently labelled EGF^{647} is not affected by Pitstop®-2. (A) HeLa cells loaded for 20 min with Alexa647-labeled EGF (EGF^{647}) were treated with DMSO or 30 µM Pitstop®-2 and allowed to degrade EGF^{647} for the indicated times. Scale bar, 10 µm. (B) Quantification of the data shown in A (n=2 independent experiments, differences not significant). Data were normalized to the amount of EGF^{647} present in DMSO-treated cells at 0 min chase. (Modified from Stahlschmidt et al., 2014)

6.10 Plasma Membrane Mobility

To analyze a possible perturbance of plasma membrane mobility by Pitstop®-2, we investigated the mobility of overexpressed GFP fused to a GPI anchor (GPI-GFP) using fluorescence recovery after photobleaching (FRAP). After bleaching a region of interest, only minor differences in fluorescence recovery of GPI-GFP could be

observed in the presence of 30 µM Pitstop®-2 compared to control cells treated with 0.1 % DMSO (Figure 6.27A).

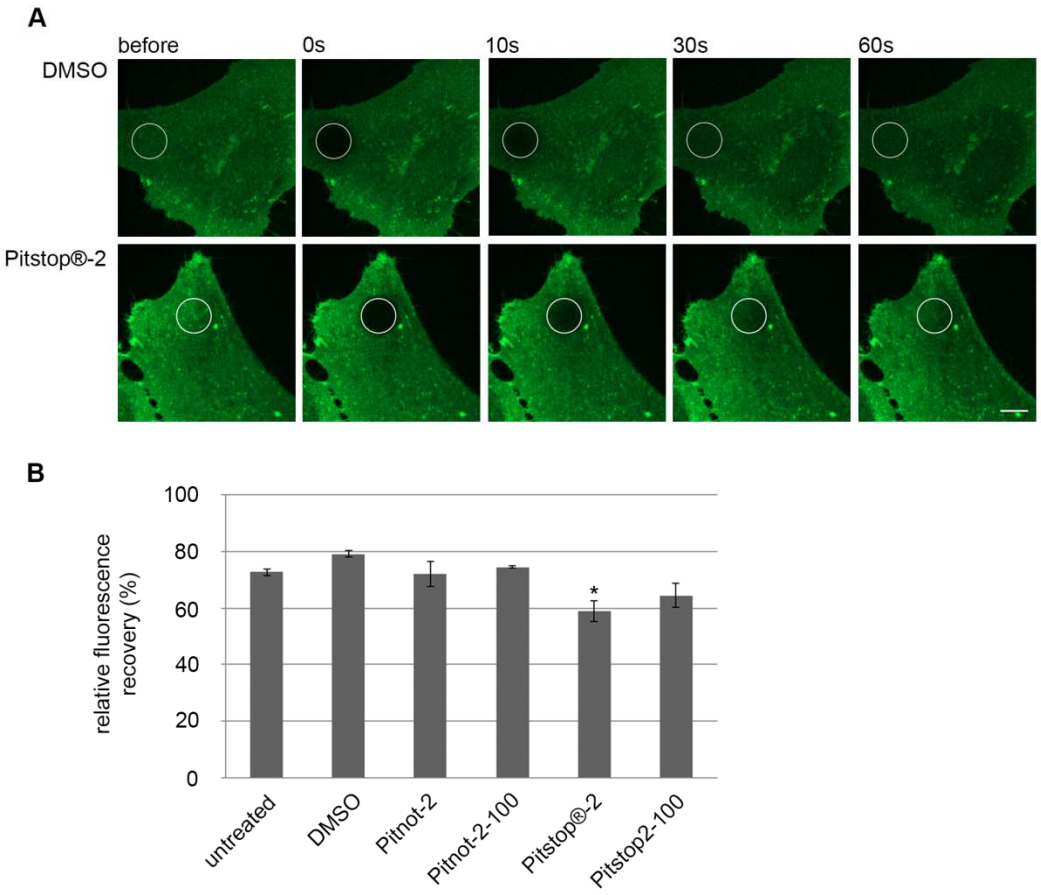

Figure 6.27 Pitstop®-2 has no unspecific effect on membrane mobility. (B) FRAP experiments were acquired in HeLa cells overexpressing GPI-GFP as a plasma membrane marker. Time lapse series were collected without compound, in presence of 0.1 % DMSO or 30 µM compound (Pitstop®-2, Pitstop2-100, Pitnot-2, or Pitnot-2-100). Panels show images before, 0 s, 10 s, 30 s and 60 s after bleaching. The circle indicates the bleached area. Scale bar, 10 µm. (C) Quantification reveals a slight but significant decrease of fluorescence recovery after addition of Pitstop®-2 or Pitstop2-100 compared to untreated cells or incubation with control compounds. The graph represents the relative fluorescence recovery normalized to the fluorescent intensity before bleaching (SEM, n=3 independent experiments; * $p < 0.05$). (Modified from Stahlschmidt et al., 2014)

Quantification of the fluorescence intensity of the bleached area for 60 seconds after bleaching showed that the slight reduction in recovery observed in presence of Pitstop®-2 or Pitstop2-100 is small but significant. Control cells, which were untreated or incubated with DMSO, 30 µM Pitnot-2 or Pitnot-2-100, respectively, displayed recovery of 72 % to 79 % compared to the pre-bleached state. In presence of 30 µM Pitstop®-2 or Pitstop2-100, the fluorescence recovers to 58 % (Pitstop®-2) or 64 % (Pitstop2-100) compared to before bleaching (Figure 6.27B). This indicates that Pitstop®-2 indeed slightly decreases the mobility of proteins diffusing freely in the plasma membrane. This is probably due to stalled CCPs which may lead to restricted diffusion of plasma membrane proteins being unable to enter CCPs.

7 Discussion

In this study, we have demonstrated the requirement for clathrin TD / ligand interactions for CME and intracellular traffic between endosomes and the TGN using small molecule inhibitors termed Pitstops (Figure 6.1A).

In vitro, Pitstops competitively interfere with the association of endocytic clathrin box ligands. Structural data based on X-ray crystallography confirmed their association with the clathrin box interaction site on the clathrin TD (von Kleist et al., 2011). Effects of Pitstop®-2 and structurally related Pitstop-2-100 are evident within a few minutes of cell treatment, presumably only being limited by the rate of drug diffusion across the cell membrane. We observe reversible inhibition of CME at concentrations closely matching the IC_{50} values of the *in vitro* binding experiments. Additionally, MPR sorting is perturbed after inhibition of clathrin TD domain interactions leading to dispersion of MPRs. The functional defects are caused by inhibition of the exchange of clathrin molecules at the plasma membrane as well as on intracellular membranes. Adaptors necessary for CCP formation at the cell surface, on endosomes and at the TGN are recruited but display decreased mobility in presence of Pitstop®-2. To confirm specificity we included two inactive control compounds, Pitnot-2 and Pitnot-2-100, which showed no effects on cell physiology.

Together, the data demonstrate the importance of clathrin TD interactions with clathrin box containing accessory proteins during maturation of the CCP rather than in its generation.

7.1 Role of the Clathrin TD in Protein Recruitment

We showed that clathrin TD interactions are not required for its recruitment to membranes. In presence of Pitstops, endogenous as well as overexpressed clathrin localized normally in cells (Figure 6.8). Also, de novo formation of CCPs, which can be observed after treatment of cells with primary alcohols, was not impaired in presence of Pitstop®-2 (Figure 6.9). Additionally, clathrin mutants lacking the TD (CHC ΔTD) or having a mutated clathrin box interaction site (CHC R64A Q89M F91A) showed normal distribution (Figure 6.8), thus confirming that clathrin recruitment is not mediated by clathrin TD interactions. Clathrin recruitment to CCPs after blocking clathrin box interactions or in absence of the TD could be mediated by an additional binding site located on the ankle of the clathrin heavy chain (Knuehl et al., 2006). This site interacts

with appendages of AP-2β, AP-1γ, and the GGA-GAE domain, thereby competing with accessory proteins required for regulation of CCP maturation. Our results suggest that binding between the CHC ankle and adaptor appendages is sufficient to keep clathrin associated with membranes and for its recruitment to membranes of newly forming CCPs in presence of Pitstop®-2 while further CCP progression is stalled.

Next, we analyzed membrane recruitment of adaptor proteins and various accessory proteins in presence of Pitstop®-2. Biochemical analysis, confirmed by immunofluorescence and live cell imaging, revealed that membrane recruitment of the adaptor proteins AP-1, AP-2, and AP-3 is not dependent on clathrin (Figure 6.13). This was to be expected as it is known that they directly interact with membrane phosphoinositides and cargo before recruiting clathrin to CCPs (Owen et al., 2004). In addition to adaptor proteins, we investigated the localization of a plethora of accessory proteins by immunofluorescence and live cell imaging. The recruitment of most of the proteins analyzed was not affected in presence of Pitstop®-2. Most CLASPs interact not only with clathrin via their clathrin box but also with adaptor proteins and membrane lipids (Schmid and McMahon, 2007; Wieffer et al., 2009). Therefore, inhibition of the interaction with clathrin in presence of Pitstops is not sufficient to displace them from CCPs.

Only two proteins showed an altered distribution in presence of Pitstop®-2. SNX9 accumulated in supersized puncta (Figure 6.11), while amphiphysin was partially lost from membranes (not shown, (von Kleist et al., 2011)). Both are BAR domain containing proteins required for curvature generation in late stages of CCP maturation. They interact with the clathrin TD and AP-2 (Lundmark and Carlsson, 2009; Slepnev et al., 2000) and operate at consecutive steps during CME (Taylor et al., 2011). These findings propose that clathrin TD interactions may coordinate turnover of endocytic proteins at nascent CCPs.

Yet, Pitstop treatment does not lead to accumulation of CCPs at late stages just before fission like it was observed in cells overexpressing the dominant negative dynamin K44A mutant. Equally, it does not increase the number of clathrin coated placques at membranes. Ultrastructural analysis indicates a normal distribution of CCP intermediates in presence of inhibitor (Dmytro Puchkov, (von Kleist et al., 2011)). This indicates that it is not interference with one particular interaction which stops CCP maturation at a certain stage but rather a general freezing of CCPs in their current state as soon as Pitstops interfere with clathrin TD / ligand interactions. To further investigate

the effects of clathrin TD inhibition we analyzed dynamics of clathrin and adaptor proteins.

7.2 Effect of Clathrin TD Inhibition on Clathrin and Adaptor Protein Dynamics

After observing no effect on clathrin recruitment or distribution it was of great interest to investigate the effects of Pitstop®-2 on clathrin dynamics in living cells. Therefore, we used a cell line stably expressing clathrin LC tagged with EGFP. Live imaging of clathrin reveals that application of Pitstop®-2 causes a profound arrest in its dynamics resulting in frozen clathrin coated pits at the plasma membrane (Figure 6.14). This is in line with data showing decreased mobility for clathrin with a mutated CBM box in yeast (Collette et al., 2009). FRAP analysis revealed that clathrin triskelia are not exchanged anymore after incubation with compound (Figure 6.15, Figure 6.16). Dynamics were equally stalled for the endocytic adaptor AP-2 (Figure 6.17), as well as for AP-1 (Figure 6.18) and GGA1-3 (Figure 6.20) located on endosomal membranes and the TGN, respectively. The data clearly demonstrates that inhibition of clathrin TD interactions stalls the maturation and fission of CCPs resulting in freezing of clathrin mediated transport processes, thereby emphasizing a role for the clathrin TD in regulation of CCP maturation (see also 7.4). Proteins harboring clathrin box motifs, such as adaptor proteins, membrane deforming proteins, or uncoating factors, fulfill a variety of functions at all stages of CCP progression (Taylor et al., 2011). This variability in function of clathrin TD ligands may be the cause for Pitstop-induced inhibition of CME at multiple stages.

We demonstrated that Pitstop®-2 as well as the structurally related Pitstop-2-100 efficiently inhibits CME of transferrin receptor (Figure 6.2) and EGF (Lisa von Kleist, (von Kleist et al., 2011)), while clathrin independent endocytosis of Shiga toxin proceeds unperturbed (Lisa von Kleist, (von Kleist et al., 2011)). Pitstops inhibit CME with an IC_{50} value comparable to the IC_{50}s inhibiting clathrin TD / ligand interactions *in vitro*. It would be expected that inhibition in cells is reduced compared to *in vitro* application. This underscores that Pitstop®-2 efficiently traverses membranes. Presumably, most clathrin TDs bind to Pitstops rapidly once the compound has reached the cytosol. Alternatively a partial block of clathrin TD / ligand interactions might already be sufficient for efficient inhibition of CME. Inhibition is accompanied by enrichment of cargo at the plasma membrane in presence of Pitstops due to lack of internalization (Figure 6.3). Yet, cargo is still sequestered into CCPs normally (Figure

6.4), confirming that cargo recruitment to the nascent CCP takes place prior to clathrin recruitment and that clathrin is not involved in this step (Traub, 2009).

Analysis of AP-1 and AP-2 dynamics in cells depleted of the clathrin HC revealed that the effect of Pitstop®-2 is only partially phenocopied. Knockdown in cells stably expressing AP-2 σ2-EGFP mimics the effect of Pitstop®-2 induced decrease of dynamics. Additional treatment with the compound in knockdown cells does not result in further deceleration (Figure 6.17). In contrast, AP-1 EGFP-σ1 mobility was not perturbed after clathrin HC depletion, yet still sensitive to Pitstop®-2 treatment (Figure 6.19). This can be explained by incomplete clathrin knockdown. The remaining clathrin still colocalizes with AP-1 and presumably is sufficient to enable CCV formation. Addition of Pitstop®-2 interferes with the remaining clathrin TD interactions at these sites thereby resulting in decreased dynamics. A possible explanation for the differences between AP-2 and AP-1 dynamics after clathrin HC depletion might be that clathrin is preferentially incorporated into intracellular transport vesicles. Specific accessory proteins could drive recruitment of the remaining clathrin to these sites with increased affinity. Therefore, strongly reduced amounts of clathrin might still be sufficient to sustain intracellular transport but not CME. In contrast, Pitstops equally interfere with all available clathrin triskelia, regardless of their location in the cell, thereby inhibiting all clathrin dependent processes. However, the precise mechanisms causing this difference still have to be elucidated.

The specificity of these phenotypes is underscored by the observation that, in spite of its profound block of AP-1 and GGA dynamics, Pitstop®-2 had no effect on the mobility or function of COPI-coated carriers, formed at the Golgi complex and required for intra-Golgi traffic and retrograde traffic from the Golgi back to the ER (Figure 6.21). Equally, general mobility of plasma membrane proteins, which has been shown to be strongly reduced in presence of Pitstop®-2 in another study (Dutta et al., 2012), was only slightly decreased in our hands (Figure 6.27). The minor reduction in mobility we have observed is presumably caused by stalled CCPs interfering with general diffusion of membrane proteins.

7.3 Effects of Pitstop®-2 on Traffic between Endosomes and the TGN

Next, we dissected the role of clathrin and its TD in AP-1- and GGA-mediated sorting of MPRs, a well characterized cargo for clathrin dependent intracellular traffic, between

the TGN and endosomes. Changes in adaptor protein dynamics are accompanied by the progressive dispersion of MPRs to peripheral endosomal puncta (Figure 6.22), a phenotype mimicking AP-1 deficiency in cells and *in vivo* (Meyer et al., 2000). Our data therefore confirm and extend previous work on the role of the clathrin-associated adaptors AP-1 and GGAs in TGN/ endosomal sorting of MPRs and, thus, in the delivery of lysosomal hydrolases (Ghosh and Kornfeld, 2003). While it is well established that MPRs exit the TGN via clathrin-coated buds (Geuze et al., 1985; Ghosh and Kornfeld, 2003), it is still debated how endosomal sorting of MPRs is exactly achieved. Multiple retrograde transport machineries have been implied in MPR retrieval from endosomes, including endosomal AP-1 (Meyer et al., 2000), the AP-1 adaptor phosphofurin acidic cluster-sorting protein-1 (PACS-1) (Crump et al., 2001), the late endosomal Rab9 together with the tail-interacting protein of 47 kD (TIP47) (Barbero et al., 2002; Diaz et al., 1997), the t-SNARE syntaxin 16 (Amessou et al., 2007), the clathrin-interacting protein EpsinR (Saint-Pol et al., 2004) and the retromer complex (Arighi et al., 2004). A role for clathrin has only been shown for traffic mediated by AP-1, PACS-1, EpsinR, and potentially retromer. Yet our data suggest a scenario where clathrin is more important in MPR retrieval from endosomes than in its secretion from the TGN as we observe accumulation in endosomes after inhibition. However, an alternative explanation for MPR peripheral dispersion in presence of Pitstop®-2 could be a role for clathrin together with AP-1 as a segregation factor at the TGN (Bonifacino, 2014). Clathrin might be important for retention of cargo at the TGN to exclude it from transport carriers to the cell periphery (Bonifacino, 2014). Thus, inhibition of clathrin TD ligand interactions could result in defective retention and potentially increased secretion from the TGN which then leads to MPR dispersion to endosomal compartments. Yet, the precise mechanisms which underlie MPR accumulation in endosomes after inhibition of clathrin TD interactions remain to be elucidated.

Interestingly, the multi-ligand receptor sortilin has been shown to colocalize with MPRs at the TGN and on endosomes and to share identical intracellular trafficking pathways (Mari et al., 2008). Future studies will show whether the phenotype observed for MPRs in presence of Pitstop®-2 will also apply to sortilin.

To ensure specificity of the phenotype we also investigated secretion of constitutive cargo such as VSVG from the Golgi to the plasma membrane. Normal traffic of VSVG was observed in presence of Pitstop®-2 (Figure 6.23), in agreement with recent data suggesting a clathrin independent secretion mechanism for VSVG (Hirschberg et al., 1998; Polishchuk et al., 2003). Constitutive secretion of VSVG thus appears to be

distinct from post-Golgi delivery of regulated secretory cargo which has been reported to involve components of the endocytic machinery including clathrin (Jaiswal et al., 2009).

An additional role for clathrin was also suggested in endosomal recycling. So far, investigation of this was difficult, as interference with clathrin function often resulted in inhibition of endocytosis of the cargo to be recycled. Using Pitstop®-2 as an acute inhibitor we could investigate the effects of the clathrin TD on recycling of just internalized cargo. Our work revealed that transferrin recycling proceeds unperturbed in presence of Pitstop®-2 (Figure 6.24). This indicates that clathrin TD / ligand interactions are apparently dispensable for the recycling of internalized transferrin from perinuclear endosomes. These results correlate well with observations obtained from live imaging and electron microscopy experiments. Recycling transferrin is present in endosomal EHD-coated tubules emanating from perinuclear sites devoid of discernable clathrin coats (Grant and Donaldson, 2009; Jovic et al., 2009; Sharma et al., 2009). Additionally, inducible overexpression of the clathrin hub domain or ligand-induced crosslinking of clathrin LCs does not affect transferrin recycling (Bennett et al., 2001; Moskowitz et al., 2003). However, our recycling assay has experimental limitations: it is based on the prior accumulation of transferrin in perinuclear endosomes. Thus, we cannot rule out the possibility that clathrin and its partners play a role in rapid recycling from early sorting endosomes, a pathway shown to depend on the small GTPases Rab35 and Arf6 (Chaineau et al., 2013), the actin cytoskeleton, and possibly clathrin (Luo et al., 2013).

On endosomes, restricted flat Hrs / clathrin coats were suggested to function in retention and concentration of cargo, such as the EGF receptor, destined for lysosomal degradation to prevent their recycling back to the plasma membrane. Clathrin and Hrs dissociate after recruitment of the ESCRT machinery which mediates invagination of the endosome membrane into MVBs (Raiborg et al., 2002; Raiborg et al., 2006; Sachse et al., 2002). Yet, our data reveal that clathrin TD interactions are not required for correct EGF receptor sorting as their ligand induced degradation is not affected in presence of Pitstop®-2 (Figure 6.25, Figure 6.26). This could be explained by a different mode of action for flat endosomal clathrin coats: unlike at the plasma membrane, flat clathrin lattices do not mature and generate membrane curvature in a mode comparable to CCPs and therefore, do not require transient TD / ligand interactions for their function. Yet, clathrin and Hrs are both exchanged rapidly on these structures with halflifetimes comparable to those at the plasma membrane (Raiborg et al., 2006). It will be interesting to investigate whether dynamics of endosomal clathrin

are equally affected by inhibition of TD / ligand interactions and how precisely this affects endosomal sorting.

The results described here confirm that clathrin TD association with its ligands not only regulates CCP dynamics at the cell surface but also at the TGN / endosomal boundary. Putative CLASPs interacting with the clathrin TD at the TGN comprise a plethora of proteins. Future work will need to address precisely which of these interactions underlie the stalled dynamics of AP-1-, and GGA-containing clathrin carriers observed in Pitstop®-2 treated cells. Presumably, clathrin TD / ligand interactions regulate CCP formation and maturation at multiple stages within their life cycle at the TGN in a mode comparable to their role in CME.

7.4 Specificity of Pitstops

As with all drugs and small molecules, activities as well as potential side-effects caused by the chemical scaffold of the drug itself should be monitored carefully. It is essential not to depend on one small molecule inhibitor solely, but to confirm results using different approaches and controls.

Recently, off-target effects for the dynamin inhibitors Dynasore (Macia et al., 2006) and Dyngo-4a (Harper et al., 2011) were shown in dynamin triple knockout cells (Park et al., 2013). The small molecules inhibit GTPase activity of dynamin. In dynamin triple knockout cells they also block membrane ruffling and inhibit fluid phase endocytosis (Park et al., 2013), potential unspecific effects, as the cells are devoid of any dynamin isoform. However, the inhibitors might act on other members of the dynamin superfamily of GTPases (Faelber et al., 2011; Ferguson and De Camilli, 2012) or show off-target effects due to GTPase independent actions. Meanwhile, the knockdown of target proteins can have side effects as well due to compensatory effects after depletion of the protein or even unspecific siRNA binding to off-target sequences. An alternative to small molecule inhibitors for immediate inhibition of protein function is acute crosslinking of two FKBP domains fused to a protein of interest by a dimerizer. For example, crosslinking of FKBP-clathrin chimera resulted in inhibition of clathrin function, evident by disruption of clathrin lattices on membranes and reduced CME (Moskowitz et al., 2003). To remove clathrin from its original membranes one could use a knocksideways approach, targeting the protein of interest to a compartment of choice, such as mitochondria (Robinson et al., 2010). But also this approach, even

though inhibition occurs after acute treatment only, requires transfection of cells with tagged proteins which might induce compensatory effects.

In this study, we ensured specificity of Pitstops by including additional compounds which are structurally related to Pitstop®-2 in some of the experiments. Pitstop-2-100 inhibits clathrin TD / ligand interactions as well as transferrin uptake with an IC_{50} comparable to Pitstop®-2, thus serving as an active control compound. Whenever assayed in parallel to Pitstop®-2 the observed effects of Pitstop-2-100 are comparable to effects of Pitstop®-2 treatment. We also included the inactive control compounds Pitnot-2 and Pitnot-2-100. Neither of them showed effects on clathrin dependent processes in cells, although we can be sure that they are internalized into cells, as Pitnot-2 has a bright yellow color which results in a slight increase in green fluorescence in presence of the compound (not shown). In our experiments we did not see effects on clathrin independent processes caused by the inhibitors, either.

In conclusion, within the scope of our experiments Pitstops turned out to be specific inhibitors for clathrin TD / ligand interactions with a broad spectrum of potential applications for future research.

7.4.1 Binding of Pitstops to the Clathrin Terminal Domain

Recently the specificity of Pitstop® binding to the clathrin box motif (CBM) interaction site on the clathrin terminal domain was doubted by Willox and colleagues (Willox et al., 2014). It has been suggested that the clathrin TD has four interaction sites, each of them with redundant function. To interfere with transferrin endocytosis, all four interaction sites have to be mutated (Willox and Royle, 2012). X-ray crystallography data demonstrate that Pitstops bind to the CBM interaction site on the clathrin TD. Therefore, the authors questioned the specificity of Pitstop®-2 as interference with one interaction site only should not be enough to successfully inhibit CME. To confirm this they tested the ability of the mutants described in (Willox and Royle, 2012) for endocytosis in presence of the compound (Willox et al., 2014). They claimed that Pitstop®-2 inhibits CME of transferrin regardless of the clathrin TD mutant. Also the mutant lacking the CBM interaction site showed reduced internalization in presence of Pitstop®-2 (Willox et al., 2014). This was interpreted as an indicator for unspecificity as Pitstops were initially shown to bind to the clathrin TD at the CBM site. However it cannot be excluded that Pitstops also interact with other sites on the clathrin TD. There are hints that Pitstops also bind to the a2L site with reduced affinity (Haydar Bulut, unpublished observation). Additionally, Pitstop binding to the clathrin TD induces

conformational changes (von Kleist et al., 2011). These changes might interfere with ligand binding at other interaction sites. To define this in more detail, an in vitro binding assay between Pitstops and the clathrin TD mutants used in (Willox and Royle, 2012) would be a more straight forward experiment, which allows to quantitatively analyze the amount of each clathrin mutant bound to the compound.

Alternatively, the observations that Pitstop®-2 still inhibits CME of transferrin after mutation of the CBM site can be explained by inefficient clathrin knockdown. After clathrin knockdown, Willox and colleagues still see approximately 30-50% transferrin uptake compared to control cells. However, the achieved knockdown efficiency was not shown (Willox and Royle, 2012; Willox et al., 2014) and it cannot be excluded that the remaining clathrin is able to partially internalize transferrin. Overexpressed clathrin TD mutants lacking up to three of their interaction sites might still be able to interact with the remaining endogenous clathrin TDs, thereby compensate for loss of function in the mutant clathrin and rescue the endocytosis phenotype.

7.4.2 Endocytosis of MHCI

Another study recently questioned the specificity of Pitstop®-2 showing inhibition of internalization of presumably clathrin independent cargo such as MHCI (Dutta et al., 2012). MHCI was previously suggested to be internalized in a clathrin independent manner based on the fact that MHCI lacks internalization sequences for AP-2 or clathrin and that cargo internalized via this route does not colocalize with classical cargo for CME such as the transferrin receptor shortly after internalization (Naslavsky et al., 2003). Furthermore, it was claimed that overexpression of a constitutively active Arf6 mutant defective in GTP hydrolysis enhances internalization of clathrin independent cargo indicating an Arf6-specific clathrin independent endocytosis pathway (Naslavsky et al., 2004).

We have demonstrated that internalization of MHCI is indeed efficiently blocked by Pitstops while the two structurally similar inactive control compounds had no effect (Figure 6.5). Depletion of clathrin HC or AP-2(μ) with siRNA confirmed a requirement for clathrin and AP-2 in MHCI endocytosis while MHCI surface expression levels were unchanged (Figure 6.6). These results are in agreement with data from several other groups suggesting epsin 1 being the endocytic adaptor for MHCI internalization (Duncan et al., 2006; Goto et al., 2010). Additionally, it could be shown that MHCI internalization proceeds unaffected after knockdown of Arf6 or overexpression of an Arf6 mutant defective in GDP to GTP exchange (Arf6T27N) contradicting a role for Arf6

in internalization (Larsen et al., 2004). The phenotypes caused by overexpression of dominant-negative Arf6 may have resulted from general perturbations of the endosomal system due to an enormous increase in $PI(4,5)P_2$ levels and subsequent massive membrane internalization.

Together, these results confirm the specificity of Pitstops as inhibitors of clathrin mediated endocytosis while demonstrating the importance of using multiple approaches to prove obtained results.

7.5 Model of Clathrin Function in Cellular Traffic

Two potential models of clathrin function can be envisioned (Figure 7.1). It was long believed that CCP maturation would follow a step-wise multivalent assembly. First, adaptor proteins bind to membranes where they drive recruitment of accessory proteins. Next, clathrin TD interactions with its endocytic ligands, i.e. adaptor proteins and accessory proteins, facilitate local enrichment of endocytic proteins and clathrin coat generation (Figure 7.1A).

However, the data obtained in this study rather support a model of dynamic exchange of endocytic proteins eventually resulting in the formation of a clathrin-coated vesicle (Figure 7.1B). The dynamic exchange model suggests that the clathrin TD supports the maturation of CCPs at multiple stages. The functional diversity of clathrin TD ligands allows transient binding of regulatory proteins to drive CCP progression. Most endocytic proteins lack stable tertiary structures or contain segments of natively unfolded polypeptide chains. In contrast, clathrin triskelia are stable entities with a defined arrangement, distance and geometry between their terminal domains (Brodsky, 2012). Therefore, clathrin is one of a few molecules within the endocytic network with the ability to spatiotemporally regulate vesicle formation and disassembly after fission. Hence, we favor a model where clathrin serves as an organizing scaffold after assembly at nascent endocytic sites which regulates CCP dynamics by providing spatially defined binding sites on its TD for accessory proteins. These accessory proteins then drive CCP maturation and disassembly (Figure 7.1B). After inhibition of clathrin TD / ligand interactions productive maturation of CCPs is prevented. This is presumably caused by interference with the dynamic exchange of key endocytic factors essential for regulation of CCP maturation. The specific mechanisms by which the clathrin TD controls such transitions within an assembling or disassembling CCP have yet to be identified.

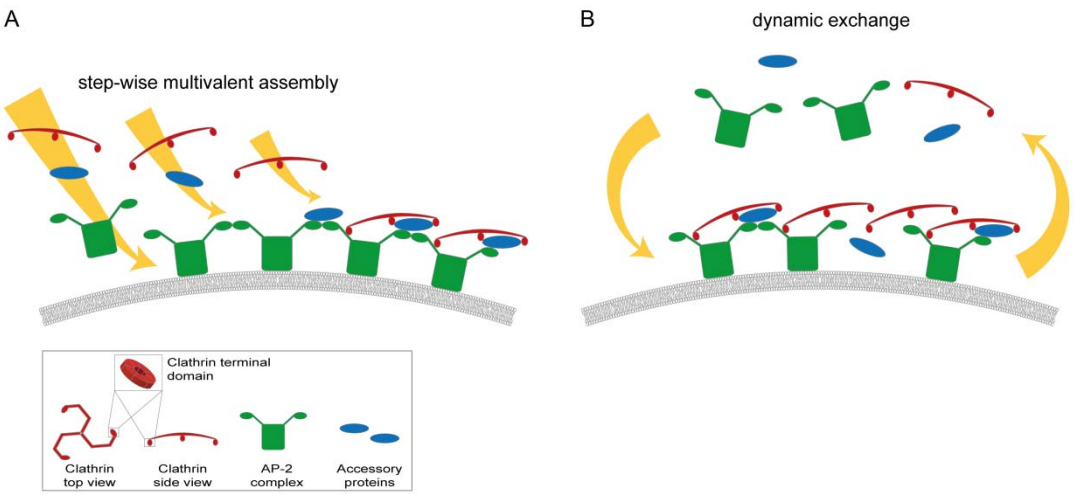

Figure 7.1 Hypothetical models illustrating the potential roles of clathrin TD-ligand association in endocytosis. (A) Multiple redundant interactions of the clathrin TD with its endocytic ligands (blue) may serve to stably recruit clathrin to membranes, thereby facilitating assembly through local enrichment. (B) Alternatively, clathrin assembled at endocytic sites could serve as an organizing scaffold that regulates CCP dynamics by providing spatially defined binding sites on its TD for accessory proteins that drive CCP maturation and disassembly. (Modified from von Kleist et al., 2011)

8 Conclusion and Outlook

Taken together, in this study the effects of Pitstops, new small molecule inhibitors of clathrin function, were investigated in detail. We could show that Pitstops specifically inhibit CME as well as clathrin dependent intracellular traffic while having no effect on clathrin independent endocytosis, transferrin recycling or EGF degradation. Evidently, as with all small molecule inhibitors one has to carefully observe potential side-effects and include controls. Therefore, we assayed structurally related control compounds in parallel. The specificity of Pitstop®-2 was confirmed by the use of the active control Pitstop-2-100 and the inactive control compounds Pitnot-2 and Pitnot-2-100 which did not interfere with any of the investigated processes.

Since their first publication (von Kleist et al., 2011) Pitstops have served as a valuable tool to further elucidate clathrin function in cell physiology. For instance, our data strongly support the hypothesis that HIV enters cells largely via CME (Daecke et al., 2005; Miyauchi et al., 2009). Also for other viruses, such as Crimean-Congo hemorrhagic fever virus, it could be shown using Pitstop®-2 that its internalization is clathrin dependent (Garrison et al., 2013). Additionally, Pitstop®-2 was shown to impair clathrin function in mitosis by trapping cells in metaphase and disrupting mitosis of cancer cells (Smith et al., 2013).

This confirms the need for specific inhibitors to investigate clathrin's role in cell physiology and disease after acute interference. To further improve Pitstops, future compound derivates based on the crystal structures of the compounds in complex with the clathrin TD will be generated. Their increased affinity and specificity will allow Pitstops to be used at lower concentrations, thereby minimizing potential, unspecific side effects. Additionally, the generation of new chemical scaffolds will facilitate selective targeting of specific tissues or cell types thereby enabling more specific applications and providing the potential for future therapeutics. A photo-activatable Pitstop compound could be used to inhibit clathrin function at defined time-points and sites in the cell to compare the effects with an untreated control region within one cell, such as synapses in neurons.

Already, drugs are prescribed to patients which target CME, e.g. chlorpromazine (Wang et al., 1993) or arbidol (Blaising et al., 2013). Yet, they do not target clathrin solely, thereby lacking specificity. Thus, in addition to their use as a tool in basic research, Pitstops might serve as lead compounds for the development of potential medication against a number of diseases which are related to a misregulated or mis-

used clathrin machinery, such as cancer, neurological and psychotic disorders, or viral infections.

9 Bibliography

Ait-Slimane, T., Galmes, R., Trugnan, G., and Maurice, M. (2009). Basolateral internalization of GPI-anchored proteins occurs via a clathrin-independent flotillin-dependent pathway in polarized hepatic cells. Molecular biology of the cell *20*, 3792-3800.

Altankov, G., and Grinnell, F. (1993). Depletion of intracellular potassium disrupts coated pits and reversibly inhibits cell polarization during fibroblast spreading. The Journal of cell biology *120*, 1449-1459.

Amessou, M., Fradagrada, A., Falguieres, T., Lord, J.M., Smith, D.C., Roberts, L.M., Lamaze, C., and Johannes, L. (2007). Syntaxin 16 and syntaxin 5 are required for efficient retrograde transport of several exogenous and endogenous cargo proteins. Journal of cell science *120*, 1457-1468.

Ando, R., Hama, H., Yamamoto-Hino, M., Mizuno, H., and Miyawaki, A. (2002). An optical marker based on the UV-induced green-to-red photoconversion of a fluorescent protein. Proceedings of the National Academy of Sciences of the United States of America *99*, 12651-12656.

Anitei, M., Stange, C., Parshina, I., Baust, T., Schenck, A., Raposo, G., Kirchhausen, T., and Hoflack, B. (2010). Protein complexes containing CYFIP/Sra/PIR121 coordinate Arf1 and Rac1 signalling during clathrin-AP-1-coated carrier biogenesis at the TGN. Nature cell biology *12*, 330-340.

Argani, P., Lui, M.Y., Couturier, J., Bouvier, R., Fournet, J.C., and Ladanyi, M. (2003). A novel CLTC-TFE3 gene fusion in pediatric renal adenocarcinoma with t(X;17)(p11.2;q23). Oncogene *22*, 5374-5378.

Arighi, C.N., Hartnell, L.M., Aguilar, R.C., Haft, C.R., and Bonifacino, J.S. (2004). Role of the mammalian retromer in sorting of the cation-independent mannose 6-phosphate receptor. The Journal of cell biology *165*, 123-133.

Barbero, P., Bittova, L., and Pfeffer, S.R. (2002). Visualization of Rab9-mediated vesicle transport from endosomes to the trans-Golgi in living cells. The Journal of cell biology *156*, 511-518.

Barlowe, C., Orci, L., Yeung, T., Hosobuchi, M., Hamamoto, S., Salama, N., Rexach, M.F., Ravazzola, M., Amherdt, M., and Schekman, R. (1994). COPII: a membrane coat formed by Sec proteins that drive vesicle budding from the endoplasmic reticulum. Cell *77*, 895-907.

Barr, A.R., and Gergely, F. (2008). MCAK-independent functions of ch-Tog/XMAP215 in microtubule plus-end dynamics. Molecular and cellular biology *28*, 7199-7211.

Bashkirov, P.V., Akimov, S.A., Evseev, A.I., Schmid, S.L., Zimmerberg, J., and Frolov, V.A. (2008). GTPase cycle of dynamin is coupled to membrane squeeze and release, leading to spontaneous fission. Cell *135*, 1276-1286.

Beaulieu, J.M., Marion, S., Rodriguiz, R.M., Medvedev, I.O., Sotnikova, T.D., Ghisi, V., Wetsel, W.C., Lefkowitz, R.J., Gainetdinov, R.R., and Caron, M.G. (2008). A beta-arrestin 2 signaling complex mediates lithium action on behavior. Cell *132*, 125-136.

Benmerah, A., Bayrou, M., Cerf-Bensussan, N., and Dautry-Varsat, A. (1999). Inhibition of clathrin-coated pit assembly by an Eps15 mutant. Journal of cell science *112 (Pt 9)*, 1303-1311.

Bennett, E.M., Lin, S.X., Towler, M.C., Maxfield, F.R., and Brodsky, F.M. (2001). Clathrin hub expression affects early endosome distribution with minimal impact on receptor sorting and recycling. Molecular biology of the cell *12*, 2790-2799.

Bhattacharyya, S., Warfield, K.L., Ruthel, G., Bavari, S., Aman, M.J., and Hope, T.J. (2010). Ebola virus uses clathrin-mediated endocytosis as an entry pathway. Virology *401*, 18-28.

Blaising, J., Levy, P.L., Polyak, S.J., Stanifer, M., Boulant, S., and Pecheur, E.I. (2013). Arbidol inhibits viral entry by interfering with clathrin-dependent trafficking. Antiviral research.

Blanchard, E., Belouzard, S., Goueslain, L., Wakita, T., Dubuisson, J., Wychowski, C., and Rouille, Y. (2006). Hepatitis C virus entry depends on clathrin-mediated endocytosis. Journal of virology *80*, 6964-6972.

Bocking, T., Aguet, F., Harrison, S.C., and Kirchhausen, T. (2011). Single-molecule analysis of a molecular disassemblase reveals the mechanism of Hsc70-driven clathrin uncoating. Nature structural & molecular biology *18*, 295-301.

Bonifacino, J.S. (2004). The GGA proteins: adaptors on the move. Nature reviews Molecular cell biology *5*, 23-32.

Bonifacino, J.S. (2014). Adaptor proteins involved in polarized sorting. The Journal of cell biology *204*, 7-17.

Bonifacino, J.S., and Glick, B.S. (2004). The mechanisms of vesicle budding and fusion. Cell *116*, 153-166.

Bonifacino, J.S., and Lippincott-Schwartz, J. (2003). Coat proteins: shaping membrane transport. Nature reviews Molecular cell biology *4*, 409-414.

Booth, D.G., Hood, F.E., Prior, I.A., and Royle, S.J. (2011). A TACC3/ch-TOG/clathrin complex stabilises kinetochore fibres by inter-microtubule bridging. The EMBO journal *30*, 906-919.

Boucrot, E., Saffarian, S., Massol, R., Kirchhausen, T., and Ehrlich, M. (2006). Role of lipids and actin in the formation of clathrin-coated pits. Experimental cell research *312*, 4036-4048.

Boumil, R.M., Letts, V.A., Roberts, M.C., Lenz, C., Mahaffey, C.L., Zhang, Z.W., Moser, T., and Frankel, W.N. (2010). A missense mutation in a highly conserved alternate exon of dynamin-1 causes epilepsy in fitful mice. PLoS genetics *6*.

Braell, W.A., Schlossman, D.M., Schmid, S.L., and Rothman, J.E. (1984). Dissociation of clathrin coats coupled to the hydrolysis of ATP: role of an uncoating ATPase. The Journal of cell biology *99*, 734-741.

Bridge, J.A., Kanamori, M., Ma, Z., Pickering, D., Hill, D.A., Lydiatt, W., Lui, M.Y., Colleoni, G.W., Antonescu, C.R., Ladanyi, M.*, et al.* (2001). Fusion of the ALK gene to the clathrin heavy chain gene, CLTC, in inflammatory myofibroblastic tumor. The American journal of pathology *159*, 411-415.

Brodsky, F.M. (2012). Diversity of clathrin function: new tricks for an old protein. Annual review of cell and developmental biology *28*, 309-336.

Cao, H., Chen, J., Awoniyi, M., Henley, J.R., and McNiven, M.A. (2007). Dynamin 2 mediates fluid-phase micropinocytosis in epithelial cells. Journal of cell science *120*, 4167-4177.

Carpentier, J.L., Sawano, F., Geiger, D., Gorden, P., Perrelet, A., and Orci, L. (1989). Potassium depletion and hypertonic medium reduce "non-coated" and clathrin-coated

pit formation, as well as endocytosis through these two gates. Journal of cellular physiology *138*, 519-526.

Chadda, R., Howes, M.T., Plowman, S.J., Hancock, J.F., Parton, R.G., and Mayor, S. (2007). Cholesterol-sensitive Cdc42 activation regulates actin polymerization for endocytosis via the GEEC pathway. Traffic *8*, 702-717.

Chaineau, M., Ioannou, M.S., and McPherson, P.S. (2013). Rab35: GEFs, GAPs and effectors. Traffic *14*, 1109-1117.

Chardin, P., and McCormick, F. (1999). Brefeldin A: the advantage of being uncompetitive. Cell *97*, 153-155.

Cheeseman, L.P., Booth, D.G., Hood, F.E., Prior, I.A., and Royle, S.J. (2011). Aurora A kinase activity is required for localization of TACC3/ch-TOG/clathrin inter-microtubule bridges. Communicative & integrative biology *4*, 409-412.

Cocucci, E., Aguet, F., Boulant, S., and Kirchhausen, T. (2012). The first five seconds in the life of a clathrin-coated pit. Cell *150*, 495-507.

Collette, J.R., Chi, R.J., Boettner, D.R., Fernandez-Golbano, I.M., Plemel, R., Merz, A.J., Geli, M.I., Traub, L.M., and Lemmon, S.K. (2009). Clathrin functions in the absence of the terminal domain binding site for adaptor-associated clathrin-box motifs. Molecular biology of the cell *20*, 3401-3413.

Collins, B.M., McCoy, A.J., Kent, H.M., Evans, P.R., and Owen, D.J. (2002). Molecular architecture and functional model of the endocytic AP2 complex. Cell *109*, 523-535.

Cosson, P., de Curtis, I., Pouyssegur, J., Griffiths, G., and Davoust, J. (1989). Low cytoplasmic pH inhibits endocytosis and transport from the trans-Golgi network to the cell surface. The Journal of cell biology *108*, 377-387.

Cremona, O., Di Paolo, G., Wenk, M.R., Luthi, A., Kim, W.T., Takei, K., Daniell, L., Nemoto, Y., Shears, S.B., Flavell, R.A*., et al.* (1999). Essential role of phosphoinositide metabolism in synaptic vesicle recycling. Cell *99*, 179-188.

Crump, C.M., Xiang, Y., Thomas, L., Gu, F., Austin, C., Tooze, S.A., and Thomas, G. (2001). PACS-1 binding to adaptors is required for acidic cluster motif-mediated protein traffic. The EMBO journal *20*, 2191-2201.

Daboussi, L., Costaguta, G., and Payne, G.S. (2012). Phosphoinositide-mediated clathrin adaptor progression at the trans-Golgi network. Nature cell biology *14*, 239-248.

Daecke, J., Fackler, O.T., Dittmar, M.T., and Krausslich, H.G. (2005). Involvement of clathrin-mediated endocytosis in human immunodeficiency virus type 1 entry. Journal of virology *79*, 1581-1594.

Dai, J., Li, J., Bos, E., Porcionatto, M., Premont, R.T., Bourgoin, S., Peters, P.J., and Hsu, V.W. (2004). ACAP1 promotes endocytic recycling by recognizing recycling sorting signals. Developmental cell *7*, 771-776.

Damke, H., Baba, T., Warnock, D.E., and Schmid, S.L. (1994). Induction of mutant dynamin specifically blocks endocytic coated vesicle formation. The Journal of cell biology *127*, 915-934.

Damm, E.M., Pelkmans, L., Kartenbeck, J., Mezzacasa, A., Kurzchalia, T., and Helenius, A. (2005). Clathrin- and caveolin-1-independent endocytosis: entry of simian virus 40 into cells devoid of caveolae. The Journal of cell biology *168*, 477-488.

Dannhauser, P.N., and Ungewickell, E.J. (2012). Reconstitution of clathrin-coated bud and vesicle formation with minimal components. Nature cell biology *14*, 634-639.

Daukas, G., and Zigmond, S.H. (1985). Inhibition of receptor-mediated but not fluid-phase endocytosis in polymorphonuclear leukocytes. The Journal of cell biology *101*, 1673-1679.

De Paepe, P., Baens, M., van Krieken, H., Verhasselt, B., Stul, M., Simons, A., Poppe, B., Laureys, G., Brons, P., Vandenberghe, P.*, et al.* (2003). ALK activation by the CLTC-ALK fusion is a recurrent event in large B-cell lymphoma. Blood *102*, 2638-2641.

Deborde, S., Perret, E., Gravotta, D., Deora, A., Salvarezza, S., Schreiner, R., and Rodriguez-Boulan, E. (2008). Clathrin is a key regulator of basolateral polarity. Nature *452*, 719-723.

Dell'Angelica, E.C., Puertollano, R., Mullins, C., Aguilar, R.C., Vargas, J.D., Hartnell, L.M., and Bonifacino, J.S. (2000). GGAs: a family of ADP ribosylation factor-binding proteins related to adaptors and associated with the Golgi complex. The Journal of cell biology *149*, 81-94.

Di Paolo, G., and De Camilli, P. (2006). Phosphoinositides in cell regulation and membrane dynamics. Nature *443*, 651-657.

Di Paolo, G., Sankaranarayanan, S., Wenk, M.R., Daniell, L., Perucco, E., Caldarone, B.J., Flavell, R., Picciotto, M.R., Ryan, T.A., Cremona, O.*, et al.* (2002). Decreased synaptic vesicle recycling efficiency and cognitive deficits in amphiphysin 1 knockout mice. Neuron *33*, 789-804.

Diaz, E., Schimmoller, F., and Pfeffer, S.R. (1997). A novel Rab9 effector required for endosome-to-TGN transport. The Journal of cell biology *138*, 283-290.

Diril, M.K., Wienisch, M., Jung, N., Klingauf, J., and Haucke, V. (2006). Stonin 2 is an AP-2-dependent endocytic sorting adaptor for synaptotagmin internalization and recycling. Developmental cell *10*, 233-244.

Doherty, G.J., and McMahon, H.T. (2009). Mechanisms of endocytosis. Annual review of biochemistry *78*, 857-902.

Donaldson, J.G., and Jackson, C.L. (2011). ARF family G proteins and their regulators: roles in membrane transport, development and disease. Nature reviews Molecular cell biology *12*, 362-375.

Donaldson, J.G., Porat-Shliom, N., and Cohen, L.A. (2009). Clathrin-independent endocytosis: a unique platform for cell signaling and PM remodeling. Cellular signalling *21*, 1-6.

Doray, B., Ghosh, P., Griffith, J., Geuze, H.J., and Kornfeld, S. (2002). Cooperation of GGAs and AP-1 in packaging MPRs at the trans-Golgi network. Science *297*, 1700-1703.

Duncan, L.M., Piper, S., Dodd, R.B., Saville, M.K., Sanderson, C.M., Luzio, J.P., and Lehner, P.J. (2006). Lysine-63-linked ubiquitination is required for endolysosomal degradation of class I molecules. The EMBO journal *25*, 1635-1645.

Dutta, D., Williamson, C.D., Cole, N.B., and Donaldson, J.G. (2012). Pitstop 2 is a potent inhibitor of clathrin-independent endocytosis. PloS one *7*, e45799.

Edeling, M.A., Mishra, S.K., Keyel, P.A., Steinhauser, A.L., Collins, B.M., Roth, R., Heuser, J.E., Owen, D.J., and Traub, L.M. (2006). Molecular switches involving the AP-2 beta2 appendage regulate endocytic cargo selection and clathrin coat assembly. Developmental cell *10*, 329-342.

Ehrlich, M., Boll, W., Van Oijen, A., Hariharan, R., Chandran, K., Nibert, M.L., and Kirchhausen, T. (2004). Endocytosis by random initiation and stabilization of clathrin-coated pits. Cell *118*, 591-605.

Elferink, J.G. (1979). Chlorpromazine inhibits phagocytosis and exocytosis in rabbit polymorphonuclear leukocytes. Biochemical pharmacology *28*, 965-968.

English, J.A., Dicker, P., Focking, M., Dunn, M.J., and Cotter, D.R. (2009). 2-D DIGE analysis implicates cytoskeletal abnormalities in psychiatric disease. Proteomics *9*, 3368-3382.

Esk, C., Chen, C.Y., Johannes, L., and Brodsky, F.M. (2010). The clathrin heavy chain isoform CHC22 functions in a novel endosomal sorting step. The Journal of cell biology *188*, 131-144.

Eyster, C.A., Higginson, J.D., Huebner, R., Porat-Shliom, N., Weigert, R., Wu, W.W., Shen, R.F., and Donaldson, J.G. (2009). Discovery of new cargo proteins that enter cells through clathrin-independent endocytosis. Traffic *10*, 590-599.

Faelber, K., Posor, Y., Gao, S., Held, M., Roske, Y., Schulze, D., Haucke, V., Noe, F., and Daumke, O. (2011). Crystal structure of nucleotide-free dynamin. Nature *477*, 556-560.

Fazili, Z., Sun, W., Mittelstaedt, S., Cohen, C., and Xu, X.X. (1999). Disabled-2 inactivation is an early step in ovarian tumorigenicity. Oncogene *18*, 3104-3113.

Feng, Y., Jadhav, A.P., Rodighiero, C., Fujinaga, Y., Kirchhausen, T., and Lencer, W.I. (2004). Retrograde transport of cholera toxin from the plasma membrane to the endoplasmic reticulum requires the trans-Golgi network but not the Golgi apparatus in Exo2-treated cells. EMBO reports *5*, 596-601.

Feng, Y., Yu, S., Lasell, T.K., Jadhav, A.P., Macia, E., Chardin, P., Melancon, P., Roth, M., Mitchison, T., and Kirchhausen, T. (2003). Exo1: a new chemical inhibitor of the exocytic pathway. Proceedings of the National Academy of Sciences of the United States of America *100*, 6469-6474.

Ferguson, S.M., and De Camilli, P. (2012). Dynamin, a membrane-remodelling GTPase. Nature reviews Molecular cell biology *13*, 75-88.

Ferguson, S.M., Raimondi, A., Paradise, S., Shen, H., Mesaki, K., Ferguson, A., Destaing, O., Ko, G., Takasaki, J., Cremona, O.*, et al.* (2009). Coordinated actions of actin and BAR proteins upstream of dynamin at endocytic clathrin-coated pits. Developmental cell *17*, 811-822.

Focking, M., Dicker, P., English, J.A., Schubert, K.O., Dunn, M.J., and Cotter, D.R. (2011). Common proteomic changes in the hippocampus in schizophrenia and bipolar disorder and particular evidence for involvement of cornu ammonis regions 2 and 3. Archives of general psychiatry *68*, 477-488.

Folsch, H., Ohno, H., Bonifacino, J.S., and Mellman, I. (1999). A novel clathrin adaptor complex mediates basolateral targeting in polarized epithelial cells. Cell *99*, 189-198.

Folsch, H., Pypaert, M., Maday, S., Pelletier, L., and Mellman, I. (2003). The AP-1A and AP-1B clathrin adaptor complexes define biochemically and functionally distinct membrane domains. The Journal of cell biology *163*, 351-362.

Ford, M.G., Mills, I.G., Peter, B.J., Vallis, Y., Praefcke, G.J., Evans, P.R., and McMahon, H.T. (2002). Curvature of clathrin-coated pits driven by epsin. Nature *419*, 361-366.

Ford, M.G., Pearse, B.M., Higgins, M.K., Vallis, Y., Owen, D.J., Gibson, A., Hopkins, C.R., Evans, P.R., and McMahon, H.T. (2001). Simultaneous binding of PtdIns(4,5)P2 and clathrin by AP180 in the nucleation of clathrin lattices on membranes. Science *291*, 1051-1055.

Fotin, A., Cheng, Y., Grigorieff, N., Walz, T., Harrison, S.C., and Kirchhausen, T. (2004). Structure of an auxilin-bound clathrin coat and its implications for the mechanism of uncoating. Nature *432*, 649-653.

Frick, M., Bright, N.A., Riento, K., Bray, A., Merrified, C., and Nichols, B.J. (2007). Coassembly of flotillins induces formation of membrane microdomains, membrane curvature, and vesicle budding. Current biology : CB *17*, 1151-1156.

Fu, W., Tao, W., Zheng, P., Fu, J., Bian, M., Jiang, Q., Clarke, P.R., and Zhang, C. (2010). Clathrin recruits phosphorylated TACC3 to spindle poles for bipolar spindle assembly and chromosome alignment. Journal of cell science *123*, 3645-3651.

Fukumatsu, M., Ogawa, M., Arakawa, S., Suzuki, M., Nakayama, K., Shimizu, S., Kim, M., Mimuro, H., and Sasakawa, C. (2012). Shigella targets epithelial tricellular junctions and uses a noncanonical clathrin-dependent endocytic pathway to spread between cells. Cell host & microbe *11*, 325-336.

Garrison, A.R., Radoshitzky, S.R., Kota, K.P., Pegoraro, G., Ruthel, G., Kuhn, J.H., Altamura, L.A., Kwilas, S.A., Bavari, S., Haucke, V.*, et al.* (2013). Crimean-Congo hemorrhagic fever virus utilizes a clathrin- and early endosome-dependent entry pathway. Virology *444*, 45-54.

Gergely, F., Draviam, V.M., and Raff, J.W. (2003). The ch-TOG/XMAP215 protein is essential for spindle pole organization in human somatic cells. Genes & development *17*, 336-341.

Geuze, H.J., Slot, J.W., Strous, G.J., Hasilik, A., and von Figura, K. (1985). Possible pathways for lysosomal enzyme delivery. The Journal of cell biology *101*, 2253-2262.

Ghosh, P., and Kornfeld, S. (2003). Phosphorylation-induced conformational changes regulate GGAs 1 and 3 function at the trans-Golgi network. The Journal of biological chemistry *278*, 14543-14549.

Glebov, O.O., Bright, N.A., and Nichols, B.J. (2006). Flotillin-1 defines a clathrin-independent endocytic pathway in mammalian cells. Nature cell biology *8*, 46-54.

Goh, L.K., Huang, F., Kim, W., Gygi, S., and Sorkin, A. (2010). Multiple mechanisms collectively regulate clathrin-mediated endocytosis of the epidermal growth factor receptor. The Journal of cell biology *189*, 871-883.

Goto, E., Yamanaka, Y., Ishikawa, A., Aoki-Kawasumi, M., Mito-Yoshida, M., Ohmura-Hoshino, M., Matsuki, Y., Kajikawa, M., Hirano, H., and Ishido, S. (2010). Contribution of lysine 11-linked ubiquitination to MIR2-mediated major histocompatibility complex class I internalization. The Journal of biological chemistry *285*, 35311-35319.

Gourlaouen, M., Welti, J.C., Vasudev, N.S., and Reynolds, A.R. (2013). Essential role for endocytosis in the growth factor-stimulated activation of ERK1/2 in endothelial cells. The Journal of biological chemistry *288*, 7467-7480.

Govero, J., Doray, B., Bai, H., and Kornfeld, S. (2012). Analysis of Gga null mice demonstrates a non-redundant role for mammalian GGA2 during development. PloS one *7*, e30184.

Grant, B.D., and Donaldson, J.G. (2009). Pathways and mechanisms of endocytic recycling. Nature reviews Molecular cell biology *10*, 597-608.

Harel, A., Mattson, M.P., and Yao, P.J. (2011). CALM, a clathrin assembly protein, influences cell surface GluR2 abundance. Neuromolecular medicine *13*, 88-90.

Harper, C.B., Martin, S., Nguyen, T.H., Daniels, S.J., Lavidis, N.A., Popoff, M.R., Hadzic, G., Mariana, A., Chau, N., McCluskey, A.*, et al.* (2011). Dynamin inhibition blocks botulinum neurotoxin type A endocytosis in neurons and delays botulism. The Journal of biological chemistry *286*, 35966-35976.

Helle, F., and Dubuisson, J. (2008). Hepatitis C virus entry into host cells. Cellular and molecular life sciences : CMLS *65*, 100-112.

Henley, J.R., Krueger, E.W., Oswald, B.J., and McNiven, M.A. (1998). Dynamin-mediated internalization of caveolae. The Journal of cell biology *141*, 85-99.

Henne, W.M., Boucrot, E., Meinecke, M., Evergren, E., Vallis, Y., Mittal, R., and McMahon, H.T. (2010). FCHo proteins are nucleators of clathrin-mediated endocytosis. Science *328*, 1281-1284.

Hernandez-Deviez, D.J., Howes, M.T., Laval, S.H., Bushby, K., Hancock, J.F., and Parton, R.G. (2008). Caveolin regulates endocytosis of the muscle repair protein, dysferlin. The Journal of biological chemistry *283*, 6476-6488.

Heuser, J. (1989). Effects of cytoplasmic acidification on clathrin lattice morphology. The Journal of cell biology *108*, 401-411.

Heuser, J.E., and Anderson, R.G. (1989). Hypertonic media inhibit receptor-mediated endocytosis by blocking clathrin-coated pit formation. The Journal of cell biology *108*, 389-400.

Hinrichsen, L., Harborth, J., Andrees, L., Weber, K., and Ungewickell, E.J. (2003). Effect of clathrin heavy chain- and alpha-adaptin-specific small inhibitory RNAs on endocytic accessory proteins and receptor trafficking in HeLa cells. The Journal of biological chemistry *278*, 45160-45170.

Hinrichsen, L., Meyerholz, A., Groos, S., and Ungewickell, E.J. (2006). Bending a membrane: how clathrin affects budding. Proceedings of the National Academy of Sciences of the United States of America *103*, 8715-8720.

Hinshaw, J.E., and Schmid, S.L. (1995). Dynamin self-assembles into rings suggesting a mechanism for coated vesicle budding. Nature *374*, 190-192.

Hirschberg, K., Miller, C.M., Ellenberg, J., Presley, J.F., Siggia, E.D., Phair, R.D., and Lippincott-Schwartz, J. (1998). Kinetic analysis of secretory protein traffic and characterization of golgi to plasma membrane transport intermediates in living cells. The Journal of cell biology *143*, 1485-1503.

Hirst, J., Borner, G.H., Antrobus, R., Peden, A.A., Hodson, N.A., Sahlender, D.A., and Robinson, M.S. (2012). Distinct and overlapping roles for AP-1 and GGAs revealed by the "knocksideways" system. Current biology : CB *22*, 1711-1716.

Hirst, J., Lui, W.W., Bright, N.A., Totty, N., Seaman, M.N., and Robinson, M.S. (2000). A family of proteins with gamma-adaptin and VHS domains that facilitate trafficking between the trans-Golgi network and the vacuole/lysosome. The Journal of cell biology *149*, 67-80.

Hirst, J., Motley, A., Harasaki, K., Peak Chew, S.Y., and Robinson, M.S. (2003). EpsinR: an ENTH domain-containing protein that interacts with AP-1. Molecular biology of the cell *14*, 625-641.

Holstein, S.E., Ungewickell, H., and Ungewickell, E. (1996). Mechanism of clathrin basket dissociation: separate functions of protein domains of the DnaJ homologue auxilin. The Journal of cell biology *135*, 925-937.

Honing, S., Ricotta, D., Krauss, M., Spate, K., Spolaore, B., Motley, A., Robinson, M., Robinson, C., Haucke, V., and Owen, D.J. (2005). Phosphatidylinositol-(4,5)-bisphosphate regulates sorting signal recognition by the clathrin-associated adaptor complex AP2. Molecular cell *18*, 519-531.

Howes, M.T., Kirkham, M., Riches, J., Cortese, K., Walser, P.J., Simpson, F., Hill, M.M., Jones, A., Lundmark, R., Lindsay, M.R.*, et al.* (2010). Clathrin-independent

carriers form a high capacity endocytic sorting system at the leading edge of migrating cells. The Journal of cell biology *190*, 675-691.

Hubner, N.C., Bird, A.W., Cox, J., Splettstoesser, B., Bandilla, P., Poser, I., Hyman, A., and Mann, M. (2010). Quantitative proteomics combined with BAC TransgeneOmics reveals in vivo protein interactions. The Journal of cell biology *189*, 739-754.

Huser, S., Suri, G., Crottet, P., and Spiess, M. (2013). Interaction of amphiphysins with AP-1 clathrin adaptors at the membrane. The Biochemical journal *450*, 73-83.

Jaiswal, J.K., Rivera, V.M., and Simon, S.M. (2009). Exocytosis of post-Golgi vesicles is regulated by components of the endocytic machinery. Cell *137*, 1308-1319.

Janvier, K., Kato, Y., Boehm, M., Rose, J.R., Martina, J.A., Kim, B.Y., Venkatesan, S., and Bonifacino, J.S. (2003). Recognition of dileucine-based sorting signals from HIV-1 Nef and LIMP-II by the AP-1 gamma-sigma1 and AP-3 delta-sigma3 hemicomplexes. The Journal of cell biology *163*, 1281-1290.

Johannes, L., and Popoff, V. (2008). Tracing the retrograde route in protein trafficking. Cell *135*, 1175-1187.

Jovic, M., Kieken, F., Naslavsky, N., Sorgen, P.L., and Caplan, S. (2009). Eps15 homology domain 1-associated tubules contain phosphatidylinositol-4-phosphate and phosphatidylinositol-(4,5)-bisphosphate and are required for efficient recycling. Molecular biology of the cell *20*, 2731-2743.

Kan, Z., Jaiswal, B.S., Stinson, J., Janakiraman, V., Bhatt, D., Stern, H.M., Yue, P., Haverty, P.M., Bourgon, R., Zheng, J.*, et al.* (2010). Diverse somatic mutation patterns and pathway alterations in human cancers. Nature *466*, 869-873.

Kang, D.S., Kern, R.C., Puthenveedu, M.A., von Zastrow, M., Williams, J.C., and Benovic, J.L. (2009). Structure of an arrestin2-clathrin complex reveals a novel clathrin binding domain that modulates receptor trafficking. The Journal of biological chemistry *284*, 29860-29872.

Karam, J.A., Shariat, S.F., Huang, H.Y., Pong, R.C., Ashfaq, R., Shapiro, E., Lotan, Y., Sagalowsky, A.I., Wu, X.R., and Hsieh, J.T. (2007). Decreased DOC-2/DAB2 expression in urothelial carcinoma of the bladder. Clinical cancer research : an official journal of the American Association for Cancer Research *13*, 4400-4406.

Kelly, B.T., McCoy, A.J., Spate, K., Miller, S.E., Evans, P.R., Honing, S., and Owen, D.J. (2008). A structural explanation for the binding of endocytic dileucine motifs by the AP2 complex. Nature *456*, 976-979.

Kent, H.M., McMahon, H.T., Evans, P.R., Benmerah, A., and Owen, D.J. (2002). Gamma-adaptin appendage domain: structure and binding site for Eps15 and gamma-synergin. Structure *10*, 1139-1148.

Kim, O.J., Gardner, B.R., Williams, D.B., Marinec, P.S., Cabrera, D.M., Peters, J.D., Mak, C.C., Kim, K.M., and Sibley, D.R. (2004). The role of phosphorylation in D1 dopamine receptor desensitization: evidence for a novel mechanism of arrestin association. The Journal of biological chemistry *279*, 7999-8010.

Kinoshita, K., Noetzel, T.L., Pelletier, L., Mechtler, K., Drechsel, D.N., Schwager, A., Lee, M., Raff, J.W., and Hyman, A.A. (2005). Aurora A phosphorylation of TACC3/maskin is required for centrosome-dependent microtubule assembly in mitosis. The Journal of cell biology *170*, 1047-1055.

Kirchhausen, T. (2000). Three ways to make a vesicle. Nature reviews Molecular cell biology *1*, 187-198.

Kirkham, M., Fujita, A., Chadda, R., Nixon, S.J., Kurzchalia, T.V., Sharma, D.K., Pagano, R.E., Hancock, J.F., Mayor, S., and Parton, R.G. (2005). Ultrastructural

identification of uncoated caveolin-independent early endocytic vehicles. The Journal of cell biology *168*, 465-476.

Kittler, J.T., Delmas, P., Jovanovic, J.N., Brown, D.A., Smart, T.G., and Moss, S.J. (2000). Constitutive endocytosis of GABAA receptors by an association with the adaptin AP2 complex modulates inhibitory synaptic currents in hippocampal neurons. The Journal of neuroscience : the official journal of the Society for Neuroscience *20*, 7972-7977.

Klausner, R.D., Donaldson, J.G., and Lippincott-Schwartz, J. (1992). Brefeldin A: insights into the control of membrane traffic and organelle structure. The Journal of cell biology *116*, 1071-1080.

Klumperman, J., Kuliawat, R., Griffith, J.M., Geuze, H.J., and Arvan, P. (1998). Mannose 6-phosphate receptors are sorted from immature secretory granules via adaptor protein AP-1, clathrin, and syntaxin 6-positive vesicles. The Journal of cell biology *141*, 359-371.

Knuehl, C., Chen, C.Y., Manalo, V., Hwang, P.K., Ota, N., and Brodsky, F.M. (2006). Novel binding sites on clathrin and adaptors regulate distinct aspects of coat assembly. Traffic *7*, 1688-1700.

Koch, S., and Claesson-Welsh, L. (2012). Signal transduction by vascular endothelial growth factor receptors. Cold Spring Harbor perspectives in medicine *2*, a006502.

Koo, S.J., Markovic, S., Puchkov, D., Mahrenholz, C.C., Beceren-Braun, F., Maritzen, T., Dernedde, J., Volkmer, R., Oschkinat, H., and Haucke, V. (2011). SNARE motif-mediated sorting of synaptobrevin by the endocytic adaptors clathrin assembly lymphoid myeloid leukemia (CALM) and AP180 at synapses. Proceedings of the National Academy of Sciences of the United States of America *108*, 13540-13545.

Kumari, S., Mg, S., and Mayor, S. (2010). Endocytosis unplugged: multiple ways to enter the cell. Cell research *20*, 256-275.

Kural, C., Tacheva-Grigorova, S.K., Boulant, S., Cocucci, E., Baust, T., Duarte, D., and Kirchhausen, T. (2012). Dynamics of intracellular clathrin/AP1- and clathrin/AP3-containing carriers. Cell reports *2*, 1111-1119.

Lampugnani, M.G., Orsenigo, F., Gagliani, M.C., Tacchetti, C., and Dejana, E. (2006). Vascular endothelial cadherin controls VEGFR-2 internalization and signaling from intracellular compartments. The Journal of cell biology *174*, 593-604.

Larkin, J.M., Brown, M.S., Goldstein, J.L., and Anderson, R.G. (1983). Depletion of intracellular potassium arrests coated pit formation and receptor-mediated endocytosis in fibroblasts. Cell *33*, 273-285.

Larsen, J.E., Massol, R.H., Nieland, T.J., and Kirchhausen, T. (2004). HIV Nef-mediated major histocompatibility complex class I down-modulation is independent of Arf6 activity. Molecular biology of the cell *15*, 323-331.

Lau, C.G., and Zukin, R.S. (2007). NMDA receptor trafficking in synaptic plasticity and neuropsychiatric disorders. Nature reviews Neuroscience *8*, 413-426.

Lee, M.J., Gergely, F., Jeffers, K., Peak-Chew, S.Y., and Raff, J.W. (2001). Msps/XMAP215 interacts with the centrosomal protein D-TACC to regulate microtubule behaviour. Nature cell biology *3*, 643-649.

LeRoy, P.J., Hunter, J.J., Hoar, K.M., Burke, K.E., Shinde, V., Ruan, J., Bowman, D., Galvin, K., and Ecsedy, J.A. (2007). Localization of human TACC3 to mitotic spindles is mediated by phosphorylation on Ser558 by Aurora A: a novel pharmacodynamic method for measuring Aurora A activity. Cancer research *67*, 5362-5370.

Letourneur, F., Gaynor, E.C., Hennecke, S., Demolliere, C., Duden, R., Emr, S.D., Riezman, H., and Cosson, P. (1994). Coatomer is essential for retrieval of dilysine-tagged proteins to the endoplasmic reticulum. Cell *79*, 1199-1207.

Li, J., Peters, P.J., Bai, M., Dai, J., Bos, E., Kirchhausen, T., Kandror, K.V., and Hsu, V.W. (2007). An ACAP1-containing clathrin coat complex for endocytic recycling. The Journal of cell biology *178*, 453-464.

Lin, C.H., Hu, C.K., and Shih, H.M. (2010). Clathrin heavy chain mediates TACC3 targeting to mitotic spindles to ensure spindle stability. The Journal of cell biology *189*, 1097-1105.

Lippincott-Schwartz, J., Yuan, L.C., Bonifacino, J.S., and Klausner, R.D. (1989). Rapid redistribution of Golgi proteins into the ER in cells treated with brefeldin A: evidence for membrane cycling from Golgi to ER. Cell *56*, 801-813.

Liu, S.H., Wong, M.L., Craik, C.S., and Brodsky, F.M. (1995). Regulation of clathrin assembly and trimerization defined using recombinant triskelion hubs. Cell *83*, 257-267.

Loerke, D., Mettlen, M., Yarar, D., Jaqaman, K., Jaqaman, H., Danuser, G., and Schmid, S.L. (2009). Cargo and dynamin regulate clathrin-coated pit maturation. PLoS biology *7*, e57.

Lu, L., Hannoush, R.N., Goess, B.C., Varadarajan, S., Shair, M.D., and Kirchhausen, T. (2013). The small molecule dispergo tubulates the endoplasmic reticulum and inhibits export. Molecular biology of the cell *24*, 1020-1029.

Luan, Z., Zhang, Y., Lu, T., Ruan, Y., Zhang, H., Yan, J., Li, L., Sun, W., Wang, L., Yue, W., *et al.* (2011). Positive association of the human STON2 gene with schizophrenia. Neuroreport *22*, 288-293.

Lundmark, R., and Carlsson, S.R. (2009). SNX9 - a prelude to vesicle release. Journal of cell science *122*, 5-11.

Luo, Y., Zhan, Y., and Keen, J.H. (2013). Arf6 regulation of Gyrating-clathrin. Traffic *14*, 97-106.

Macia, E., Ehrlich, M., Massol, R., Boucrot, E., Brunner, C., and Kirchhausen, T. (2006). Dynasore, a cell-permeable inhibitor of dynamin. Developmental cell *10*, 839-850.

Manning, A.L., and Compton, D.A. (2008). Structural and regulatory roles of nonmotor spindle proteins. Current opinion in cell biology *20*, 101-106.

Margarucci, L., Monti, M.C., Fontanella, B., Riccio, R., and Casapullo, A. (2011). Chemical proteomics reveals bolinaquinone as a clathrin-mediated endocytosis inhibitor. Molecular bioSystems *7*, 480-485.

Mari, M., Bujny, M.V., Zeuschner, D., Geerts, W.J., Griffith, J., Petersen, C.M., Cullen, P.J., Klumperman, J., and Geuze, H.J. (2008). SNX1 defines an early endosomal recycling exit for sortilin and mannose 6-phosphate receptors. Traffic *9*, 380-393.

Maritzen, T., Schmidt, M.R., Kukhtina, V., Higman, V.A., Strauss, H., Volkmer, R., Oschkinat, H., Dotti, C.G., and Haucke, V. (2010). A novel subtype of AP-1-binding motif within the palmitoylated trans-Golgi network/endosomal accessory protein Gadkin/gamma-BAR. The Journal of biological chemistry *285*, 4074-4086.

Maro, B., Johnson, M.H., Pickering, S.J., and Louvard, D. (1985). Changes in the distribution of membranous organelles during mouse early development. Journal of embryology and experimental morphology *90*, 287-309.

Masri, B., Salahpour, A., Didriksen, M., Ghisi, V., Beaulieu, J.M., Gainetdinov, R.R., and Caron, M.G. (2008). Antagonism of dopamine D2 receptor/beta-arrestin 2 interaction is a common property of clinically effective antipsychotics. Proceedings of the National Academy of Sciences of the United States of America *105*, 13656-13661.

Massol, R.H., Boll, W., Griffin, A.M., and Kirchhausen, T. (2006). A burst of auxilin recruitment determines the onset of clathrin-coated vesicle uncoating. Proceedings of the National Academy of Sciences of the United States of America *103*, 10265-10270.

McCluskey, A., Daniel, J.A., Hadzic, G., Chau, N., Clayton, E.L., Mariana, A., Whiting, A., Gorgani, N., Lloyd, J., Quan, A.*, et al.* (2013). Building a Better Dynasore: The Dyngo Compounds Potently Inhibit Dynamin and Endocytosis. Traffic.

McMahon, H.T., and Boucrot, E. (2011). Molecular mechanism and physiological functions of clathrin-mediated endocytosis. Nature reviews Molecular cell biology *12*, 517-533.

McMahon, H.T., and Boucrot, E. (2012). Molecular mechanism and physiological functions of clathrin-mediated endocytosis. Nat Rev Mol Cell Biol *12*, 517-533.

McMahon, H.T., and Gallop, J.L. (2005). Membrane curvature and mechanisms of dynamic cell membrane remodelling. Nature *438*, 590-596.

Meertens, L., Bertaux, C., and Dragic, T. (2006). Hepatitis C virus entry requires a critical postinternalization step and delivery to early endosomes via clathrin-coated vesicles. Journal of virology *80*, 11571-11578.

Mercer, J., Schelhaas, M., and Helenius, A. (2010). Virus entry by endocytosis. Annual review of biochemistry *79*, 803-833.

Meyer, C., Zizioli, D., Lausmann, S., Eskelinen, E.L., Hamann, J., Saftig, P., von Figura, K., and Schu, P. (2000). mu1A-adaptin-deficient mice: lethality, loss of AP-1 binding and rerouting of mannose 6-phosphate receptors. The EMBO journal *19*, 2193-2203.

Miele, A.E., Watson, P.J., Evans, P.R., Traub, L.M., and Owen, D.J. (2004). Two distinct interaction motifs in amphiphysin bind two independent sites on the clathrin terminal domain beta-propeller. Nature structural & molecular biology *11*, 242-248.

Mills, I.G., Praefcke, G.J., Vallis, Y., Peter, B.J., Olesen, L.E., Gallop, J.L., Butler, P.J., Evans, P.R., and McMahon, H.T. (2003). EpsinR: an AP1/clathrin interacting protein involved in vesicle trafficking. The Journal of cell biology *160*, 213-222.

Milosevic, I., Giovedi, S., Lou, X., Raimondi, A., Collesi, C., Shen, H., Paradise, S., O'Toole, E., Ferguson, S., Cremona, O.*, et al.* (2011). Recruitment of endophilin to clathrin-coated pit necks is required for efficient vesicle uncoating after fission. Neuron *72*, 587-601.

Mitsunari, T., Nakatsu, F., Shioda, N., Love, P.E., Grinberg, A., Bonifacino, J.S., and Ohno, H. (2005). Clathrin adaptor AP-2 is essential for early embryonal development. Molecular and cellular biology *25*, 9318-9323.

Miyauchi, K., Kim, Y., Latinovic, O., Morozov, V., and Melikyan, G.B. (2009). HIV enters cells via endocytosis and dynamin-dependent fusion with endosomes. Cell *137*, 433-444.

Mok, S.C., Chan, W.Y., Wong, K.K., Cheung, K.K., Lau, C.C., Ng, S.W., Baldini, A., Colitti, C.V., Rock, C.O., and Berkowitz, R.S. (1998). DOC-2, a candidate tumor suppressor gene in human epithelial ovarian cancer. Oncogene *16*, 2381-2387.

Moskowitz, H.S., Heuser, J., McGraw, T.E., and Ryan, T.A. (2003). Targeted chemical disruption of clathrin function in living cells. Molecular biology of the cell *14*, 4437-4447.

Motley, A., Bright, N.A., Seaman, M.N., and Robinson, M.S. (2003). Clathrin-mediated endocytosis in AP-2-depleted cells. The Journal of cell biology *162*, 909-918.

Nakatsu, F., Okada, M., Mori, F., Kumazawa, N., Iwasa, H., Zhu, G., Kasagi, Y., Kamiya, H., Harada, A., Nishimura, K.*, et al.* (2004). Defective function of GABA-containing synaptic vesicles in mice lacking the AP-3B clathrin adaptor. The Journal of cell biology *167*, 293-302.

Naslavsky, N., Weigert, R., and Donaldson, J.G. (2003). Convergence of non-clathrin- and clathrin-derived endosomes involves Arf6 inactivation and changes in phosphoinositides. Molecular biology of the cell *14*, 417-431.

Naslavsky, N., Weigert, R., and Donaldson, J.G. (2004). Characterization of a nonclathrin endocytic pathway: membrane cargo and lipid requirements. Molecular biology of the cell *15*, 3542-3552.

Nichols, B.J., Kenworthy, A.K., Polishchuk, R.S., Lodge, R., Roberts, T.H., Hirschberg, K., Phair, R.D., and Lippincott-Schwartz, J. (2001). Rapid cycling of lipid raft markers between the cell surface and Golgi complex. The Journal of cell biology *153*, 529-541.

Ogiso, T., Iwaki, M., and Mori, K. (1981). Fluidity of human erythrocyte membrane and effect of chlorpromazine on fluidity and phase separation of membrane. Biochimica et biophysica acta *649*, 325-335.

Ohno, H., Aguilar, R.C., Yeh, D., Taura, D., Saito, T., and Bonifacino, J.S. (1998). The medium subunits of adaptor complexes recognize distinct but overlapping sets of tyrosine-based sorting signals. The Journal of biological chemistry *273*, 25915-25921.

Ohno, H., Stewart, J., Fournier, M.C., Bosshart, H., Rhee, I., Miyatake, S., Saito, T., Gallusser, A., Kirchhausen, T., and Bonifacino, J.S. (1995). Interaction of tyrosine-based sorting signals with clathrin-associated proteins. Science *269*, 1872-1875.

Ohno, H., Tomemori, T., Nakatsu, F., Okazaki, Y., Aguilar, R.C., Foelsch, H., Mellman, I., Saito, T., Shirasawa, T., and Bonifacino, J.S. (1999). Mu1B, a novel adaptor medium chain expressed in polarized epithelial cells. FEBS letters *449*, 215-220.

Okamoto, C.T., McKinney, J., and Jeng, Y.Y. (2000). Clathrin in mitotic spindles. American journal of physiology Cell physiology *279*, C369-374.

Owen, D.J., Collins, B.M., and Evans, P.R. (2004). Adaptors for clathrin coats: structure and function. Annual review of cell and developmental biology *20*, 153-191.

Page, L.J., Sowerby, P.J., Lui, W.W., and Robinson, M.S. (1999). Gamma-synergin: an EH domain-containing protein that interacts with gamma-adaptin. The Journal of cell biology *146*, 993-1004.

Park, R., Shen, H., Liu, L., Liu, X., Ferguson, S.M., and De Camilli, P. (2013). Dynamin triple knockout cells reveal off target effects of commonly used dynamin inhibitors. Journal of cell science.

Paspalas, C.D., Rakic, P., and Goldman-Rakic, P.S. (2006). Internalization of D2 dopamine receptors is clathrin-dependent and select to dendro-axonic appositions in primate prefrontal cortex. The European journal of neuroscience *24*, 1395-1403.

Payne, C.K., Jones, S.A., Chen, C., and Zhuang, X. (2007). Internalization and trafficking of cell surface proteoglycans and proteoglycan-binding ligands. Traffic *8*, 389-401.

Pece, S., Serresi, M., Santolini, E., Capra, M., Hulleman, E., Galimberti, V., Zurrida, S., Maisonneuve, P., Viale, G., and Di Fiore, P.P. (2004). Loss of negative regulation by Numb over Notch is relevant to human breast carcinogenesis. The Journal of cell biology *167*, 215-221.

Pechstein, A., Bacetic, J., Vahedi-Faridi, A., Gromova, K., Sundborger, A., Tomlin, N., Krainer, G., Vorontsova, O., Schafer, J.G., Owe, S.G.*, et al.* (2010). Regulation of synaptic vesicle recycling by complex formation between intersectin 1 and the clathrin adaptor complex AP2. Proceedings of the National Academy of Sciences of the United States of America *107*, 4206-4211.

Pelish, H.E., Peterson, J.R., Salvarezza, S.B., Rodriguez-Boulan, E., Chen, J.L., Stamnes, M., Macia, E., Feng, Y., Shair, M.D., and Kirchhausen, T. (2006). Secramine inhibits Cdc42-dependent functions in cells and Cdc42 activation in vitro. Nature chemical biology *2*, 39-46.

Pelkmans, L., Puntener, D., and Helenius, A. (2002). Local actin polymerization and dynamin recruitment in SV40-induced internalization of caveolae. Science *296*, 535-539.

Peter, B.J., Kent, H.M., Mills, I.G., Vallis, Y., Butler, P.J., Evans, P.R., and McMahon, H.T. (2004). BAR domains as sensors of membrane curvature: the amphiphysin BAR structure. Science *303*, 495-499.

Polishchuk, E.V., Di Pentima, A., Luini, A., and Polishchuk, R.S. (2003). Mechanism of constitutive export from the golgi: bulk flow via the formation, protrusion, and en bloc cleavage of large trans-golgi network tubular domains. Molecular biology of the cell *14*, 4470-4485.

Porpaczy, E., Bilban, M., Heinze, G., Gruber, M., Vanura, K., Schwarzinger, I., Stilgenbauer, S., Streubel, B., Fonatsch, C., and Jaeger, U. (2009). Gene expression signature of chronic lymphocytic leukaemia with Trisomy 12. European journal of clinical investigation *39*, 568-575.

Posor, Y., Eichhorn-Gruenig, M., Puchkov, D., Schoneberg, J., Ullrich, A., Lampe, A., Muller, R., Zarbakhsh, S., Gulluni, F., Hirsch, E.*, et al.* (2013). Spatiotemporal control of endocytosis by phosphatidylinositol-3,4-bisphosphate. Nature *499*, 233-237.

Presley, J.F., Cole, N.B., Schroer, T.A., Hirschberg, K., Zaal, K.J., and Lippincott-Schwartz, J. (1997). ER-to-Golgi transport visualized in living cells. Nature *389*, 81-85.

Puertollano, R., Aguilar, R.C., Gorshkova, I., Crouch, R.J., and Bonifacino, J.S. (2001). Sorting of mannose 6-phosphate receptors mediated by the GGAs. Science *292*, 1712-1716.

Radhakrishna, H., and Donaldson, J.G. (1997). ADP-ribosylation factor 6 regulates a novel plasma membrane recycling pathway. The Journal of cell biology *139*, 49-61.

Raiborg, C., Bache, K.G., Gillooly, D.J., Madshus, I.H., Stang, E., and Stenmark, H. (2002). Hrs sorts ubiquitinated proteins into clathrin-coated microdomains of early endosomes. Nature cell biology *4*, 394-398.

Raiborg, C., Wesche, J., Malerod, L., and Stenmark, H. (2006). Flat clathrin coats on endosomes mediate degradative protein sorting by scaffolding Hrs in dynamic microdomains. Journal of cell science *119*, 2414-2424.

Rapoport, I., Boll, W., Yu, A., Bocking, T., and Kirchhausen, T. (2008). A motif in the clathrin heavy chain required for the Hsc70/auxilin uncoating reaction. Molecular biology of the cell *19*, 405-413.

Razani, B., Engelman, J.A., Wang, X.B., Schubert, W., Zhang, X.L., Marks, C.B., Macaluso, F., Russell, R.G., Li, M., Pestell, R.G.*, et al.* (2001). Caveolin-1 null mice are viable but show evidence of hyperproliferative and vascular abnormalities. The Journal of biological chemistry *276*, 38121-38138.

Ren, X., Farias, G.G., Canagarajah, B.J., Bonifacino, J.S., and Hurley, J.H. (2013). Structural basis for recruitment and activation of the AP-1 clathrin adaptor complex by Arf1. Cell *152*, 755-767.

Robinson, M.S. (2004). Adaptable adaptors for coated vesicles. Trends in cell biology *14*, 167-174.

Robinson, M.S., and Bonifacino, J.S. (2001). Adaptor-related proteins. Current opinion in cell biology *13*, 444-453.

Robinson, M.S., Sahlender, D.A., and Foster, S.D. (2010). Rapid inactivation of proteins by rapamycin-induced rerouting to mitochondria. Developmental cell *18*, 324-331.

Rothberg, K.G., Heuser, J.E., Donzell, W.C., Ying, Y.S., Glenney, J.R., and Anderson, R.G. (1992). Caveolin, a protein component of caveolae membrane coats. Cell *68*, 673-682.

Rothnie, A., Clarke, A.R., Kuzmic, P., Cameron, A., and Smith, C.J. (2011). A sequential mechanism for clathrin cage disassembly by 70-kDa heat-shock cognate protein (Hsc70) and auxilin. Proceedings of the National Academy of Sciences of the United States of America *108*, 6927-6932.

Roux, A., Uyhazi, K., Frost, A., and De Camilli, P. (2006). GTP-dependent twisting of dynamin implicates constriction and tension in membrane fission. Nature *441*, 528-531.

Royle, S.J. (2012). The role of clathrin in mitotic spindle organisation. Journal of cell science *125*, 19-28.

Royle, S.J., Bright, N.A., and Lagnado, L. (2005). Clathrin is required for the function of the mitotic spindle. Nature *434*, 1152-1157.

Sabharanjak, S., Sharma, P., Parton, R.G., and Mayor, S. (2002). GPI-anchored proteins are delivered to recycling endosomes via a distinct cdc42-regulated, clathrin-independent pinocytic pathway. Developmental cell *2*, 411-423.

Sachse, M., Urbe, S., Oorschot, V., Strous, G.J., and Klumperman, J. (2002). Bilayered clathrin coats on endosomal vacuoles are involved in protein sorting toward lysosomes. Molecular biology of the cell *13*, 1313-1328.

Saffarian, S., Cocucci, E., and Kirchhausen, T. (2009). Distinct dynamics of endocytic clathrin-coated pits and coated plaques. PLoS biology *7*, e1000191.

Saint-Pol, A., Yelamos, B., Amessou, M., Mills, I.G., Dugast, M., Tenza, D., Schu, P., Antony, C., McMahon, H.T., Lamaze, C.*, et al.* (2004). Clathrin adaptor epsinR is required for retrograde sorting on early endosomal membranes. Developmental cell *6*, 525-538.

Sandvig, K., Olsnes, S., Petersen, O.W., and van Deurs, B. (1987). Acidification of the cytosol inhibits endocytosis from coated pits. The Journal of cell biology *105*, 679-689.

Sandvig, K., Pust, S., Skotland, T., and van Deurs, B. (2011). Clathrin-independent endocytosis: mechanisms and function. Current opinion in cell biology *23*, 413-420.

Schlossman, D.M., Schmid, S.L., Braell, W.A., and Rothman, J.E. (1984). An enzyme that removes clathrin coats: purification of an uncoating ATPase. The Journal of cell biology *99*, 723-733.

Schmid, E.M., and McMahon, H.T. (2007). Integrating molecular and network biology to decode endocytosis. Nature *448*, 883-888.

Schmidt, M.R., Maritzen, T., Kukhtina, V., Higman, V.A., Doglio, L., Barak, N.N., Strauss, H., Oschkinat, H., Dotti, C.G., and Haucke, V. (2009). Regulation of

endosomal membrane traffic by a Gadkin/AP-1/kinesin KIF5 complex. Proceedings of the National Academy of Sciences of the United States of America *106*, 15344-15349.

Schubert, K.O., Focking, M., Prehn, J.H., and Cotter, D.R. (2012). Hypothesis review: are clathrin-mediated endocytosis and clathrin-dependent membrane and protein trafficking core pathophysiological processes in schizophrenia and bipolar disorder? Molecular psychiatry *17*, 669-681.

Semerdjieva, S., Shortt, B., Maxwell, E., Singh, S., Fonarev, P., Hansen, J., Schiavo, G., Grant, B.D., and Smythe, E. (2008). Coordinated regulation of AP2 uncoating from clathrin-coated vesicles by rab5 and hRME-6. The Journal of cell biology *183*, 499-511.

Sharma, M., Giridharan, S.S., Rahajeng, J., Naslavsky, N., and Caplan, S. (2009). MICAL-L1 links EHD1 to tubular recycling endosomes and regulates receptor recycling. Molecular biology of the cell *20*, 5181-5194.

Sinha, B., Koster, D., Ruez, R., Gonnord, P., Bastiani, M., Abankwa, D., Stan, R.V., Butler-Browne, G., Vedie, B., Johannes, L.*, et al.* (2011). Cells respond to mechanical stress by rapid disassembly of caveolae. Cell *144*, 402-413.

Slepnev, V.I., Ochoa, G.C., Butler, M.H., and De Camilli, P. (2000). Tandem arrangement of the clathrin and AP-2 binding domains in amphiphysin 1 and disruption of clathrin coat function by amphiphysin fragments comprising these sites. The Journal of biological chemistry *275*, 17583-17589.

Smith, C.M., and Chircop, M. (2012). Clathrin-mediated endocytic proteins are involved in regulating mitotic progression and completion. Traffic *13*, 1628-1641.

Smith, C.M., Haucke, V., McCluskey, A., Robinson, P.J., and Chircop, M. (2013). Inhibition of clathrin by pitstop 2 activates the spindle assembly checkpoint and induces cell death in dividing HeLa cancer cells. Molecular cancer *12*, 4.

Spencer, D.M., Wandless, T.J., Schreiber, S.L., and Crabtree, G.R. (1993). Controlling signal transduction with synthetic ligands. Science *262*, 1019-1024.

Stoorvogel, W., Oorschot, V., and Geuze, H.J. (1996). A novel class of clathrin-coated vesicles budding from endosomes. The Journal of cell biology *132*, 21-33.

Stowell, M.H., Marks, B., Wigge, P., and McMahon, H.T. (1999). Nucleotide-dependent conformational changes in dynamin: evidence for a mechanochemical molecular spring. Nature cell biology *1*, 27-32.

Sun, X., and Whittaker, G.R. (2013). Entry of influenza virus. Advances in experimental medicine and biology *790*, 72-82.

Sundborger, A., Soderblom, C., Vorontsova, O., Evergren, E., Hinshaw, J.E., and Shupliakov, O. (2011). An endophilin-dynamin complex promotes budding of clathrin-coated vesicles during synaptic vesicle recycling. Journal of cell science *124*, 133-143.

Sweitzer, S.M., and Hinshaw, J.E. (1998). Dynamin undergoes a GTP-dependent conformational change causing vesiculation. Cell *93*, 1021-1029.

Tam, C., Idone, V., Devlin, C., Fernandes, M.C., Flannery, A., He, X., Schuchman, E., Tabas, I., and Andrews, N.W. (2010). Exocytosis of acid sphingomyelinase by wounded cells promotes endocytosis and plasma membrane repair. The Journal of cell biology *189*, 1027-1038.

Taylor, M.J., Perrais, D., and Merrifield, C.J. (2011). A high precision survey of the molecular dynamics of mammalian clathrin-mediated endocytosis. PLoS biology *9*, e1000604.

Tebar, F., Sorkina, T., Sorkin, A., Ericsson, M., and Kirchhausen, T. (1996). Eps15 is a component of clathrin-coated pits and vesicles and is located at the rim of coated pits. The Journal of biological chemistry *271*, 28727-28730.

ter Haar, E., Harrison, S.C., and Kirchhausen, T. (2000). Peptide-in-groove interactions link target proteins to the beta-propeller of clathrin. Proceedings of the National Academy of Sciences of the United States of America *97*, 1096-1100.

Thompson, D., and Whistler, J.L. (2011). Trafficking properties of the D5 dopamine receptor. Traffic *12*, 644-656.

Thomsen, P., Roepstorff, K., Stahlhut, M., and van Deurs, B. (2002). Caveolae are highly immobile plasma membrane microdomains, which are not involved in constitutive endocytic trafficking. Molecular biology of the cell *13*, 238-250.

Traub, L.M. (2005). Common principles in clathrin-mediated sorting at the Golgi and the plasma membrane. Biochimica et biophysica acta *1744*, 415-437.

Traub, L.M. (2009). Tickets to ride: selecting cargo for clathrin-regulated internalization. Nature reviews Molecular cell biology *10*, 583-596.

Ungewickell, E., Ungewickell, H., Holstein, S.E., Lindner, R., Prasad, K., Barouch, W., Martin, B., Greene, L.E., and Eisenberg, E. (1995). Role of auxilin in uncoating clathrin-coated vesicles. Nature *378*, 632-635.

van Dam, E.M., and Stoorvogel, W. (2002). Dynamin-dependent transferrin receptor recycling by endosome-derived clathrin-coated vesicles. Molecular biology of the cell *13*, 169-182.

van der Schaar, H.M., Rust, M.J., Chen, C., van der Ende-Metselaar, H., Wilschut, J., Zhuang, X., and Smit, J.M. (2008). Dissecting the cell entry pathway of dengue virus by single-particle tracking in living cells. PLoS pathogens *4*, e1000244.

Veiga, E., Guttman, J.A., Bonazzi, M., Boucrot, E., Toledo-Arana, A., Lin, A.E., Enninga, J., Pizarro-Cerda, J., Finlay, B.B., Kirchhausen, T.*, et al.* (2007). Invasive and adherent bacterial pathogens co-Opt host clathrin for infection. Cell host & microbe *2*, 340-351.

von Kleist, L., and Haucke, V. (2012). At the crossroads of chemistry and cell biology: inhibiting membrane traffic by small molecules. Traffic *13*, 495-504.

von Kleist, L., Stahlschmidt, W., Bulut, H., Gromova, K., Puchkov, D., Robertson, M.J., MacGregor, K.A., Tomilin, N., Pechstein, A., Chau, N.*, et al.* (2011). Role of the clathrin terminal domain in regulating coated pit dynamics revealed by small molecule inhibition. Cell *146*, 471-484.

Waguri, S., Dewitte, F., Le Borgne, R., Rouille, Y., Uchiyama, Y., Dubremetz, J.F., and Hoflack, B. (2003). Visualization of TGN to endosome trafficking through fluorescently labeled MPR and AP-1 in living cells. Molecular biology of the cell *14*, 142-155.

Wang, J., Sun, H.Q., Macia, E., Kirchhausen, T., Watson, H., Bonifacino, J.S., and Yin, H.L. (2007). PI4P promotes the recruitment of the GGA adaptor proteins to the trans-Golgi network and regulates their recognition of the ubiquitin sorting signal. Molecular biology of the cell *18*, 2646-2655.

Wang, L.H., Rothberg, K.G., and Anderson, R.G. (1993). Mis-assembly of clathrin lattices on endosomes reveals a regulatory switch for coated pit formation. The Journal of cell biology *123*, 1107-1117.

Wang, Y.J., Wang, J., Sun, H.Q., Martinez, M., Sun, Y.X., Macia, E., Kirchhausen, T., Albanesi, J.P., Roth, M.G., and Yin, H.L. (2003). Phosphatidylinositol 4 phosphate regulates targeting of clathrin adaptor AP-1 complexes to the Golgi. Cell *114*, 299-310.

Ward, T.H., Polishchuk, R.S., Caplan, S., Hirschberg, K., and Lippincott-Schwartz, J. (2001). Maintenance of Golgi structure and function depends on the integrity of ER export. The Journal of cell biology *155*, 557-570.

Wasiak, S., Denisov, A.Y., Han, Z., Leventis, P.A., de Heuvel, E., Boulianne, G.L., Kay, B.K., Gehring, K., and McPherson, P.S. (2003). Characterization of a gamma-adaptin ear-binding motif in enthoprotin. FEBS letters *555*, 437-442.

Wasiak, S., Legendre-Guillemin, V., Puertollano, R., Blondeau, F., Girard, M., de Heuvel, E., Boismenu, D., Bell, A.W., Bonifacino, J.S., and McPherson, P.S. (2002). Enthoprotin: a novel clathrin-associated protein identified through subcellular proteomics. The Journal of cell biology *158*, 855-862.

Wieffer, M., Cibrián Uhalte, E., Posor, Y., Otten, C., Branz, K., Schütz, I., Mössinger, J., Schu, P., Abdelilah-Seyfried, S., Krauß, M*., et al.* (2013). PI4K2²/AP-1-Based TGN-Endosomal Sorting Regulates Wnt Signaling. Current biology : CB *23*, 2185-2190.

Wieffer, M., Maritzen, T., and Haucke, V. (2009). SnapShot: endocytic trafficking. Cell *137*, 382 e381-383.

Wigge, P., Kohler, K., Vallis, Y., Doyle, C.A., Owen, D., Hunt, S.P., and McMahon, H.T. (1997). Amphiphysin heterodimers: potential role in clathrin-mediated endocytosis. Molecular biology of the cell *8*, 2003-2015.

Willox, A.K., and Royle, S.J. (2012). Functional analysis of interaction sites on the N-terminal domain of clathrin heavy chain. Traffic *13*, 70-81.

Willox, A.K., Sahraoui, Y.M.E., and Royle, S.J. (2014). Non-specificity of Pitstop 2 in clathrin-mediated endocytosis. bioRxiv.

Wu, M., Huang, B., Graham, M., Raimondi, A., Heuser, J.E., Zhuang, X., and De Camilli, P. (2010). Coupling between clathrin-dependent endocytic budding and F-BAR-dependent tubulation in a cell-free system. Nature cell biology *12*, 902-908.

Xing, Y., Bocking, T., Wolf, M., Grigorieff, N., Kirchhausen, T., and Harrison, S.C. (2010). Structure of clathrin coat with bound Hsc70 and auxilin: mechanism of Hsc70-facilitated disassembly. The EMBO journal *29*, 655-665.

Ybe, J.A., Brodsky, F.M., Hofmann, K., Lin, K., Liu, S.H., Chen, L., Earnest, T.N., Fletterick, R.J., and Hwang, P.K. (1999). Clathrin self-assembly is mediated by a tandemly repeated superhelix. Nature *399*, 371-375.

Yu, A., Rual, J.F., Tamai, K., Harada, Y., Vidal, M., He, X., and Kirchhausen, T. (2007). Association of Dishevelled with the clathrin AP-2 adaptor is required for Frizzled endocytosis and planar cell polarity signaling. Developmental cell *12*, 129-141.

Zhao, X., Greener, T., Al-Hasani, H., Cushman, S.W., Eisenberg, E., and Greene, L.E. (2001). Expression of auxilin or AP180 inhibits endocytosis by mislocalizing clathrin: evidence for formation of nascent pits containing AP1 or AP2 but not clathrin. Journal of cell science *114*, 353-365.

Zhao, Y., and Keen, J.H. (2008). Gyrating clathrin: highly dynamic clathrin structures involved in rapid receptor recycling. Traffic *9*, 2253-2264.

Zhu, Y., Traub, L.M., and Kornfeld, S. (1998). ADP-ribosylation factor 1 transiently activates high-affinity adaptor protein complex AP-1 binding sites on Golgi membranes. Molecular biology of the cell *9*, 1323-1337.

10 Appendix

10.1 Abbreviations

ACAP1	(ARFGAP with coiled coil, ANK repeat, and pleckstrin homology domains)
AP	adaptor protein
Arf1	ADP-ribosylation factor 1
ARF6	ADP-ribosylation factor 6
BAR domain	Bin–Amphiphysin–Rvs
BFA	brefeldin A
CIP	Calf intestinal phosphatase
Cdc42	Cell division control protein
CHCR	CHC repeat
CTxB	cholera toxin B subunit
CLASP	clathrin associated protein
CBM	clathrin box motif
CCP	clathrin coated pit
CHC	clathrin heavy chain
CLIC	clathrin indepedent carrier
CLC	clathrin light chain
CME	clathrin mediated endocytosis
COP	coat protein complex
ch-TOG	colonic hepatic tumour overexpressed gene
ctrl	control
CCHFV	Crimean-Congo hemorrhagic fever virus
DTT	Dithiothreitol
dko	double knockout
Eps15	EGFR pathway substrate 15
EM	electron microscopy
ER	endoplasmic reticulum
eGFP	enhanced green fluorescent protein
ELISA	Enzyme Linked Immunosorbent Assay
EGF	epidermal growth factor
ENTH	epsin N-terminal homology

ERGIC	ER-Golgi intermediate compartment
E. coli	Escherichia coli
ERK1/2	extracellular related kinases 1/2
FCHo	Fer/Cip4 homology domain domain-only
FKBP	FK506 binding protein 12
GAE	g-adaptin ear
$GABA_AR$	gamma-aminobutyric acid A receptor
GAT	GGA and TOM1
GPI	Glycosylphosphatidylinositol
GGA	Golgi-localized, gamma-ear containing, ADP- ribosylation factor- binding proteins
GEEC	GPI-anchored protein enriched endosomal compartment
GFP	green fluorescent protein
GTP	guanosine triphosphate
HSC70	heat shock cognate 70
HC	heavy chain
Hrs	hepatocyte growth factor-regulated tyrosine kinase substrate
Hz	Hertz
HRP	horseradish peroxidase
IPTG	Isopropyl-b-D-thioglactopyranoside
k-fibres	kinetochor fibres
kd	knockdown
ko	knockout
LC	light chain
LDL	low density lipoprotein
MHCI	major histocompatibility complex class I
MPR	Mannose 6-phophate receptor
MT	microtubule
MVB	mulivesicular bodies
PMSF	phenylmethylsulfonylfluoride
$PI(4,5)P_2$	phosphatidylinositol 4,5-bisphosphate
PCR	Polymerase chain reaction
SV40	simian virus 40
siRNA	small interfereing RNA
TIP47	tail-interacting protein of 47 kD
TD	terminal domain

TGN	trans golgi network
tf	transferrin
TACC3	Transforming acidic coiled-coil-containing protein 3
tko	triple knockout
VEGF	vascular endothelial growth factor
VEGFR2	vascular endothelial growth factor receptor 2
VSVG	vesicular stomatitis virus G protein
VHS	VPS-27, Hrs, and STAM
WT	wild type

10.2 List of figures

10.3 Publications

Stahlschmidt W., Robertson M. J., Robinson P. J., McCluskey A., Haucke V.: Clathrin terminal domain-ligand interactions regulate sorting of mannose 6-phosphatereceptors mediated by AP-1 and GGA adaptors. Journal of Biological Chemistry, 2014 289(8), 4906-18.

Macgregor K. A., Robertson M. J., Young K. A., von Kleist L., **Stahlschmidt W**., Whiting A., Chau N., Robinson P. J., Haucke V., McCluskey A.: Development of 1,8-Naphthalimides as Clathrin Inhibitors. Journal of Medicinal Chemistry, 2014, 57(1), 131-43.

von Kleist L., **Stahlschmidt W.**, Bulut H., Gromova K., Puchkov D., Robertson M. J., MacGregor K. A., Tomilin N., Pechstein A., Chau N., Chircop M., Sakoff J., von Kries J. P., Saenger W., Kräusslich H. G., Shupliakov O., Robinson P. J., McCluskey A., Haucke V.: Role of the clathrin terminal domain in regulating coated pit dynamics revealed by small molecule inhibition. Cell, 2011, 146(3), 471-84.